University of Alberta

Improved Stability of Adsorbed Ion-Exchange Sites on Silica-based Columns for Ion Chromatography

by

Karen Marie Glenn

A thesis submitted to the Faculty of Graduate Studies and Research
in partial fulfillment of the requirements for the degree of

Master of Science

Department of Chemistry

Edmonton, Alberta
Spring 2008

Library and Archives Canada

Published Heritage Branch

395 Wellington Street
Ottawa ON K1A 0N4
Canada

Bibliothèque et Archives Canada

Direction du Patrimoine de l'édition

395, rue Wellington
Ottawa ON K1A 0N4
Canada

Your file Votre référence
ISBN: 978-0-494-45813-6
Our file Notre référence
ISBN: 978-0-494-45813-6

NOTICE:
The author has granted a non-exclusive license allowing Library and Archives Canada to reproduce, publish, archive, preserve, conserve, communicate to the public by telecommunication or on the Internet, loan, distribute and sell theses worldwide, for commercial or non-commercial purposes, in microform, paper, electronic and/or any other formats.

The author retains copyright ownership and moral rights in this thesis. Neither the thesis nor substantial extracts from it may be printed or otherwise reproduced without the author's permission.

AVIS:
L'auteur a accordé une licence non exclusive permettant à la Bibliothèque et Archives Canada de reproduire, publier, archiver, sauvegarder, conserver, transmettre au public par télécommunication ou par l'Internet, prêter, distribuer et vendre des thèses partout dans le monde, à des fins commerciales ou autres, sur support microforme, papier, électronique et/ou autres formats.

L'auteur conserve la propriété du droit d'auteur et des droits moraux qui protège cette thèse. Ni la thèse ni des extraits substantiels de celle-ci ne doivent être imprimés ou autrement reproduits sans son autorisation.

In compliance with the Canadian Privacy Act some supporting forms may have been removed from this thesis.

While these forms may be included in the document page count, their removal does not represent any loss of content from the thesis.

Conformément à la loi canadienne sur la protection de la vie privée, quelques formulaires secondaires ont été enlevés de cette thèse.

Bien que ces formulaires aient inclus dans la pagination, il n'y aura aucun contenu manquant.

Canada

ABSTRACT

This thesis explores methods to improve the stability of adsorbed ion-exchange sites on silica monoliths for ion chromatography. Recently, researchers have used reversed-phase columns coated with surfactants as ion-exchangers. Surfactant coatings can be removed and reapplied under different conditions to refine the column's capacity. However, the stability of surfactant coatings is unclear. Some researchers report stable coatings, while others observe a gradual decrease in analyte retention. Chapter 2 investigates a permanent coating of latex on a silica monolith. The latex-coated column was more stable and efficient than a surfactant-coated column. However, the capacity of the latex-coated column could not be optimized. Chapter 3 investigates improvements in surfactant coating stability. The decrease in retention observed by many researchers in the past was found to follow an exponential decay trend. This indicated that surfactant coatings are stable after a break-in period and explains contradictions about the stability of surfactant coatings.

ACKNOWLEDGEMENTS

I would first like to express my gratitude to my supervisor, Dr. Charles Lucy, for his guidance, patience and expertise over the past two years. His passion and enthusiasm for chemistry have been an important factor in the completion of this project. I am also thankful to the whole Lucy lab group for their advice, thoughtful discussions and most importantly for their friendship. Most notably Donna, Amy, Ting and Stu, whose humour and support have made my experience in graduate school an enjoyable one.

I'd also like to acknowledge the Natural Sciences and Engineering Research Council of Canada (NSERC) and Alberta Ingenuity for funding, and the Department of Chemistry at University of Alberta.

I am also appreciative of the faculty at St. Francis Xavier University, particularly Dr. Rom Palepu, for realizing my potential and setting me in the direction of graduate studies. It was him who ignited my interest in chemistry and research in the first place.

I would also like to thank my family and friends, especially Dave, for being a continuous source of support. I am forever grateful to my parents, Myles and Margie, for their endless support and encouragement for whichever path I choose to take.

Table of Contents

CHAPTER ONE: Introduction

1.1 Motivation and Thesis Overview.....1

1.2 Introduction to Ion Chromatography.....3

1.3 Chromatographic terms.....4

1.4 Instrumentation.....14

1.5 Detection.....16

1.6 Suppression.....17

1.7 Selectivity in ion chromatography.....23

1.7.1 Effect of analyte and eluent ions on selectivity.....23

1.7.2 Effect of stationary phase on selectivity.....26

1.8 Eluents.....27

1.9 Stationary Phases.....28

1.9.1 Monoliths vs. particle-packed columns.....28

1.9.2 Polymer-based stationary phases for IC.....32

1.9.3 Silica-based stationary phases for IC.....35

1.10 Modification of silica monoliths for use in ion chromatography.....38

1.10.1 Surfactant coatings.....38

1.10.2 Covalent modification of silica monoliths.....44

1.10.3 Latex coatings on silica monoliths.....45

1.11 Summary and Thesis Overview.....47

1.12 References.....48

CHAPTER TWO: Latex-coated silica monoliths for ion chromatography

2.1 Introduction....54

2.2 Experimental....58

2.2.1 Apparatus....58

2.2.2 Reagents and solution preparation....60

2.2.3 Coating and removing DDAB from the column....61

2.2.4 Latex coating....63

2.2.5 Determination of ion-exchange capacity....63

2.2.6 Stability tests....66

2.2.7 Calculations....66

2.3 Results and Discussion....66

2.3.1 Selectivity and optimization....67

2.3.2 Efficiency....75

2.3.3 Stability....77

2.4 Conclusions....79

2.5 References....80

CHAPTER THREE: Stability of Surfactant Coatings for Ion Chromatography

3.1.1 Introduction....82

3.1.2 Experimental....86

3.2.1 Apparatus....86

3.2.2 Reagents and solution preparation....87

3.2.3 Coating and removing CTAB from the column....88

3.2.4 Stability tests on 100 x 4.6 mm column..... 89

3.2.5 Determination of ion-exchange capacity on 5 x 4.6 mm column.....89

3.2.6 Calculation of efficiency.....90

3.2.7 Determination of critical micelle concentration (CMC).....90

3.3 Results and Discussion..... 91

3.3.1 The effect of coating conditions on the rate of surfactant leaching...91

3.3.2 Long-term stability of surfactant coatings.....97

3.3.3 Attempts to avoid the drastic initial decrease in retention.....107

3.3.4 Controlling the final ion-exchange capacity.....108

3.3.5 Possible causes for the exponential decay trend.....119

3.3.6 Clarifying contradictions about the stability of surfactant coatings..... 123

3.4 Conclusions..... 124

3.5 References..... 125

CHAPTER FOUR: Summary and Future Work..... 128

List of Tables

Table 1.1 Various surfactants used as ion-exchange coatings on reversed-phase silica..... 43

Table 2.1 Capacity of DDAB-coated column as a function of ACN content in the coating solution..... 68

Table 2.2 Comparison of k of 8 anions on latex and DDAB-coated monoliths..... 71

Table 3.1 Surfactant coatings in the literature..... 84

Table 3.2 Effect of coating conditions on ion-exchange capacity and stability.....94

Table 3.3 Long-term stability of surfactant coatings: exponential decay fits.....103

List of Figures

Figure 1.1 Chromatographic parameters for calculating peak efficiency.....7

Figure 1.2 Schematic representation of eddy diffusion.....10

Figure 1.3 Typical van Deemter plot 13

Figure 1.4 Schematic diagram of a typical IC system.....15

Figure 1.5 Schematic of a chemically regenerated membrane suppressor.....19

Figure 1.6 Schematic of an electrolytically regenerated membrane suppressor.....20

Figure 1.7 Schematic of Dionex Atlas Electrolytic Suppressor.....22

Figure 1.8 Flow through (A) particle-packed column, (B) monolithic column.....30

Figure 1.9 van Deemter plot comparing particulate and monolithic columns.....31

Figure 1.10 Schematic representation of (A) agglomerated particle, (B) particle with chemically grafted functionalities.....33

Figure 1.11 (A) Macropores and (B) mesopores of silica monolith.....37

Figure 1.12 Coating and uncoating process for DDAB.....42

Figure 1.13 Latex adhering to a bare silica surface.....46

Figure 2.1 Schematic of a DDAB surfactant coating on reversed-phase silica and a latex coating on bare silica.....57

Figure 2.2 Schematic of instrument set-up.....59

Figure 2.3 Surfactant breakthrough curve.....62

Figure 2.4 Calibration curve for bromide adsorption/desorption method.....65

Figure 2.5 Optimized anion separation on DDAB and latex-coated monoliths..... 70

Figure 2.6 Separation of 7 anions on DDAB and latex-coated monolithic columns..... 74

Figure 2.7 van Deemter plots for DDAB and latex-coated monolithic columns..... 76

Figure 2.8 Retention factor as a function of time: stability of latex and DDAB coatings..... 78

Figure 3.1 Linear fits for sulfate retention loss..... 93

Figure 3.2 Series of separations on CTAB-coated column..... 98

Figure 3.3 Efficiency of sulfate peak as a function of flush volume..... 99

Figure 3.4 Exponential decay fits for sulfate retention loss..... 102

Figure 3.5A Plateau retention factor for sulfate ion (A_∞) vs. $k_i(SO_4^{2-})$..... 105

Figure 3.5B Initial decay rate vs. initial retention factor for sulfate, $k_i(SO_4^{2-})$..... 106

Figure 3.6 Initial capacity according to surfactant breakthrough time (Q) vs. initial retention factor for sulfate ($k_i(SO_4^{2-})$)..... 111

Figure 3.7 Schematic of possible interactions between surfactant and C_{18} surface..... 115

Figure 3.8 Initial and final ion-exchange capacity as a function of %ACN in the coating solution..... 118

Figure 3.9 Retention factor on 100 x 4.6 mm column vs. flush volume..... 121

List of Symbols and Abbreviations

Symbol	Parameter
4-hba	4-hydroxybenzoic acid
α	selectivity
λ	packing factor
ψ	obstruction factor
A^-	monovalent analyte ion
A_1	fit parameter for single-exponential decay
A_∞	asymptotic value of single-exponential decay
A	van Deemter term for eddy diffusion
AAES	Anion Atlas Electrolytic Suppressor
ACN	acetonitrile
AES	Atlas Electrolytic Suppressor
AFM	atomic force microscopy
A_s	asymmetry factor
A^{x-}	analyte ion
B	van Deemter term for longitudinal molecular diffusion
$(B/A)_{0.1}$	ratio of distances to and from t_r at 10% height
C	van Deemter term for mass transfer in the stationary phase
C	surfactant concentration in coating solution
C_{18}	alkane with 18 carbon units
CE	capillary electrophoresis
CEC	capillary electrochromatography

CPC	cetylpyridinium chloride
CTAB	cetyltrimethylammonium bromide
CTAC	cetyltrimethylammonium bromide
CMC	critical micelle concentration
DDAB	didodecyldimethylammonium bromide
DDA^+	didodecyldimethylammonium ion
DDA-AA	(dodecyldimethylamino) acetic acid
DDMAU	N-dodecyl-N,N-(dimethylammonio)-undecanoate
d_f	average film thickness of liquid stationary phase
D_M	diffusion coefficient for solute in the mobile phase
DNA	deoxyribonucleic acid
DOSS	sodium dioctylsulfosuccinate
d_p	particle diameter
D_S	diffusion coefficient of solute in stationary phase
E^-	monovalent eluent ion
EMG	Exponentially Modified Gaussian
E^{y-}	eluent ion
F	flow rate
H	height equivalent to a theoretical plate
HPLC	high performance liquid chromatography
IC	ion chromatography
I.D.	inner diameter
IDA	iminodiacetic acid

k	retention factor
$k_i(SO_4^{2-})$	initial retention factor of sulfate
$K_{A,E}$	selectivity coefficient or equilibrium constant
K_c	distribution constant
k_{obs}	observed decay rate constant
L	column length
LC	liquid chromatography
Li-DS	lithium dodecylsulfate
LSER	linear solvation energy relationship
MW	molecular weight
N	plate number
ODS	octadecylsilyl
PEEK	polyether ether ketone
POE	polyoxyethylene
Q	initial ion-exchange capacity determined by surfactant
	breakthrough time
RP	reversed-phase
RP-18e	reversed-phase column with octadecylsilyl bonded
	phase and endcapped
R_s	resolution
RSD	relative standard deviation
SDS	sodium dodecylsulfate
t_0	hold-up or dead time

t_r	retention time
TTACl	tetradecyltrimethylammonium chloride
u	linear velocity
UV	ultra-violet
V	volume
V_M	volume of mobile phase
$w_{0.5}$	peak width at half height
w	mass of stationary phase
w_b	peak width at baseline
x	charge of analyte ion
y	charge of eluent ion

CHAPTER ONE: Introduction*

1.1 Motivation and Thesis Overview

The use of chromatography is widespread in industrial laboratories to separate a sample into its individual components, so that these components can then be identified, isolated or purified. The analysis of anions in water (in industrial, environmental, or drinking water samples) is one of the most common analyses performed by testing laboratories. In liquid chromatography, samples are transported by a liquid mobile phase (eluent) through a column packed with solid stationary phase, usually consisting of 5-15 μm silica or polymer particles. To analyze ionic species, such as a water sample containing trace ions, ion chromatography (IC) can be used to separate ions based on an ion-exchange mechanism. In IC, the traditional stationary phase consists of polymer particles with fixed ion-exchange sites. These packed columns, commercially available from Dionex Corporation, Metrohm and Alltech, can separate the common anions in water in about 10 minutes.[1]

Recently, monolithic columns, which consist of one continuous porous rod, have been used in many forms of liquid chromatography to obtain faster separations. The porous construction of monolithic columns allows for higher flow rates with lower backpressure than particulate columns, with little detriment to efficiency.[2-4] With the commercialization of silica monolithic columns in 2000, it seemed obvious to chromatographers to explore the possibility of silica monoliths for ion analysis.

---

* A version of Sec 1.9 was published in S.D. Chambers, K.M. Glenn and C.A. Lucy, "Developments in ion chromatography using monolithic columns", Journal of Separation Science, 2007, **30**, 1628-1645.

Indeed, many research groups have used silica monoliths for ion analysis in recent years. Hatsis and Lucy used an ion-interaction reagent to perform 30 s anion separations on a short (5 cm) C_{18} silica monolith.[5] More recent research has involved semi-permanently modifying the hydrophobic surface of C_{18} silica monoliths with ionic surfactants (Section 1.10.1). These coatings are termed "semi-permanent" because the coating can be easily removed by flushing the column with acetonitrile. However, there are contradictions within the literature about the stability of surfactant coatings. Some researchers report a stable coating, while others observe a decrease in retention time of the analytes due to the surfactant leaching from the column.

To circumvent the problems associated with surfactant coatings altogether, Chapter 2 explores the use of a silica-based monolith containing permanent ion-exchange sites. Permanent ion-exchange sites are anchored to the stationary phase through either covalent bonds or electrostatic forces, and cannot be removed from the column after coating. The column studied in Chapter 2 was prepared by flushing a suspension of positively-charged latex particles through a bare silica monolith, which has a negatively-charged surface. The performance of this column was then compared to a semi-permanent surfactant-modified column in terms of selectivity, efficiency and stability.

Ideally, a chromatographer should be able to purchase a commercially available monolithic column and apply a coating which does not leach from the column but can also be easily removed to allow the same column to be used with other coatings. This could be accomplished if the process of surfactant leaching is slowed or prevented altogether. Chapter 3 involves research to better understand

surfactant coatings on C_{18} silica columns. By altering coating conditions, such as surfactant concentration, temperature, ionic strength and organic modifiers, the possibility of a stable surfactant coating is explored. At the same time, an explanation is offered for the contradictions about the stability of surfactant coatings.

1.2 Introduction to Ion Chromatography

Chromatography is concerned with the separation of the components of a mixture. In liquid chromatography, samples are transported by a liquid mobile phase (eluent) through a column packed with solid stationary phase. Separation occurs if each of the sample components interact to differing extents with the stationary phase. The technique of chromatography was first introduced by Russian botanist Tswett in 1903, who used the method to isolate plant pigments.[6,7] Later, Van Deemter and Giddings established rate and efficiency theories of liquid chromatography and predicted that smaller particles of stationary phase would provide more efficient separations.[8,9] To accommodate the high pressures needed to flush liquid through these tightly packed small particles, new pumping systems were developed in the 1960's by Horvath and co-workers.[10,11] Since then, "High Performance Liquid Chromatography" (HPLC) has become the premier technique for analytical separations.

Ion chromatography (IC) refers to the determination of trace ions on low capacity high efficiency columns possessing fixed ion-exchange sites. These columns are commonly combined with suppressed conductivity detection to yield parts-per-billion detection of the seven common anions (F^-, Cl^-, NO_2^-, Br^-, NO_3^-,

HPO_4^{2-} and SO_4^{2-}), common cations (Li^+, Na^+, NH_4^+, K^+, Mg^{2+} and Ca^{2+}), carboxylic acids and small amines.[12] Modern ion chromatography evolved from the work of Hamish Small and co-workers in 1975.[13] Since then, there have been many new developments in instrumentation and stationary phases for ion chromatography.

Ion chromatography retains ions and ionizable compounds through an ion-exchange mechanism. For cation-exchange, the stationary phase contains negatively-charged sites. The analyses in this thesis involve anion-exchange, in which the stationary phase carries a fixed positive charge. In anion-exchange, eluent anions, E^{y-}, are displaced from the stationary phase (subscript *s*) by analyte ions, A^{x-}, initially in the mobile phase (subscript *m*). The equilibrium for anion-exchange can be expressed as:

$$xE_s^{y-} + yA_m^{x-} \leftrightarrow yA_s^{x-} + xE_m^{y-} \qquad (1.1)$$

The equilibrium constant ($K_{A,E}$) determines the relative retention of each analyte ion. Analytes that have a larger $K_{A,E}$ spend more time in the stationary phase and thus, have a longer retention time.

1.3 Chromatographic terms [14]

The time needed for an analyte to elute from a chromatographic system is known as its retention time (t_r). The analyte spends a portion of its retention time in the mobile phase, where it travels along the column toward the detector. The remainder of the time is spent in the stationary phase, where the analyte is not moving

downstream. The rate of migration of an analyte is governed by its distribution constant, K_c:

$$K_c = [A]_s / [A]_m \tag{1.2}$$

where $[A]_s$ and $[A]_m$ are the equilibrium concentrations of analyte in the stationary and mobile phases, respectively. The time taken for an unretained compound to elute from the column is known as the hold-up time or dead time, t_0. Most chromatographers use the retention factor, k, to express the extent of retention of an analyte:

$$k = \frac{t_r - t_0}{t_0} \tag{1.3}$$

Plate number, N, is a common term used to express the efficiency of a chromatographic system. N is a measure of the broadening of a peak, as it takes into account the dispersion that a peak undergoes as it travels through the system. Larger plate numbers indicate a more efficient chromatographic system, i.e., sharper peaks. For symmetrical (Gaussian) peaks, N can be calculated by the tangent method. In this method, tangent lines are drawn at the inflection points of the peaks and their intersection with the baseline determines the peak width (w_b) (Figure 1.1). For symmetrical peaks, N can be calculated as:

$$N = 16\left[\frac{t_r}{w_b}\right]^2 \tag{1.4a}$$

Alternately, the width at half-height ($w_{0.5}$) can be used to calculate efficiency (Figure 1.1):

$$N = 5.54\left[\frac{t_r}{w_{0.5}}\right]^2 \tag{1.4b}$$

However, equations 1.4a and 1.4b tend to overestimate the efficiency of non-Gaussian (asymmetrical) peaks.[15] To calculate the efficiency of asymmetric peaks, the exponentially modified Gaussian (EMG) model developed by Foley and Dorsey [16] should be employed:

$$N = \frac{41.7(t_r / w_{0.1})^2}{(B/A)_{0.1} + 1.25} \tag{1.5}$$

The term $w_{0.1}$ is the peak width at 10% height and $(B/A)_{0.1}$ is the asymmetry factor which is the ratio of the distances to and from t_r at 10% height (Figure 1.1). For asymmetry factors (A_s=B/A) higher than 1, peaks are said to be "tailed", and for A_s < 1, peaks are said to be "fronted."

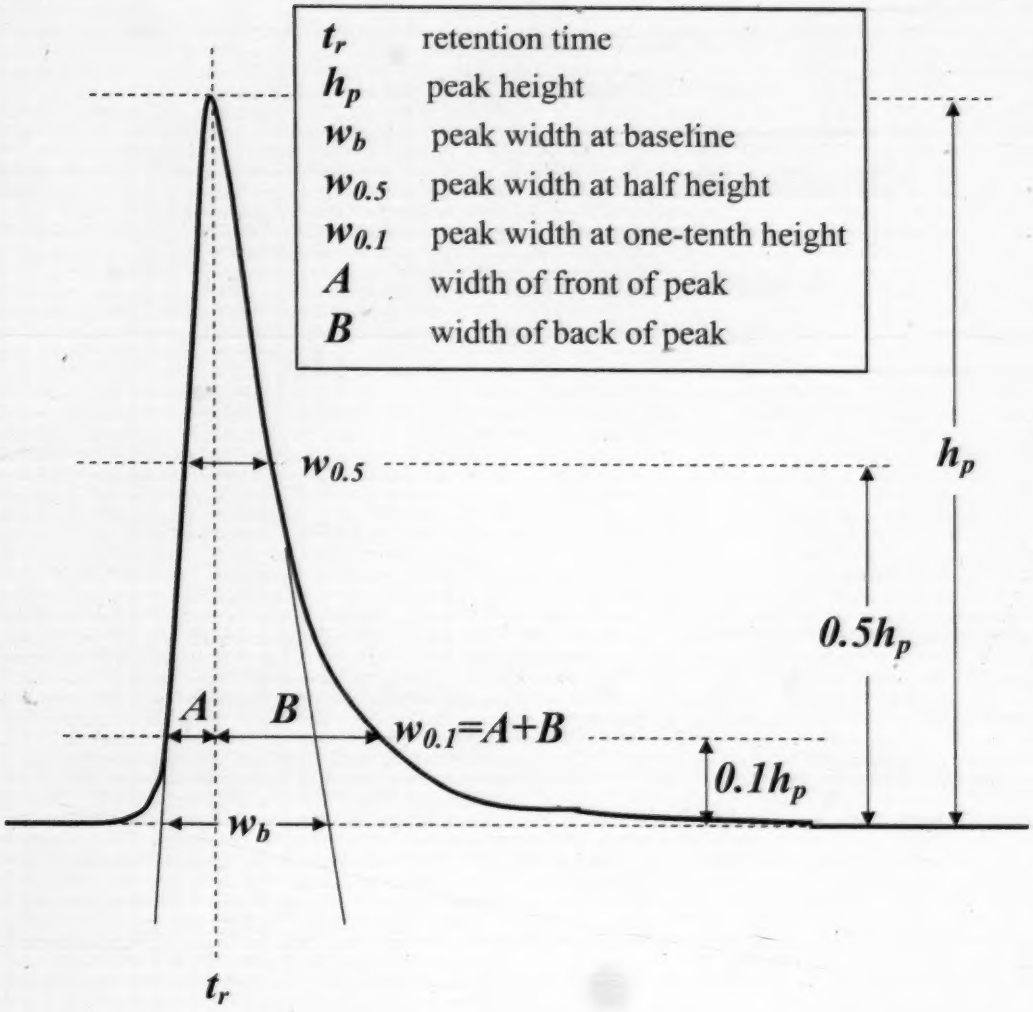

Figure 1.1. Chromatographic peak parameters for calculating peak efficiency (equations 1.4-1.6). Adapted from reference [17].

Plate number, however, depends on the length of the column, making it difficult to compare columns of varying length. The height equivalent to a theoretical plate, *H,* is a measure of efficiency that is independent of the length of the column (*L*):

$$H = L / N \tag{1.6}$$

The plate height is inversely proportional to *N*; thus, a smaller value for *H* indicates a more efficient chromatographic system.

Resolution, R_s, characterizes the separation between two peaks, relative to their peak widths at baseline:

$$R_s = \frac{t_{r2} - t_{r1}}{0.5(w_{b1} + w_{b2})} \tag{1.7}$$

where t_{r1} and t_{r2} are the retention times (min) of the first and second peaks, respectively, and w_{b1} and w_{b2} are their peak widths at the base (min). Peak width at the baseline can be measured by the tangent method, as described above. A resolution of 1.0 (about 90-94% resolution between two peaks) is considered adequate for separation. Baseline resolution is achieved when $R_s \geq 1.5$.

Selectivity, α, is a term used to describe the relative retention of two components. It is defined as the ratio of the adjusted retention times, or retention factors, of two different analytes:

$$\alpha = \frac{t_{r2} - t_0}{t_{r1} - t_0} = \frac{k_2}{k_1} \tag{1.8}$$

Ideally, when an analyte elutes from a column, it is detected as a sharp peak. However, there are several factors that contribute to the overall width of the peak by causing the analyte molecules to disperse as they travel along the column. van Deemter's rate theory[18] identifies three effects that contribute to band broadening: eddy diffusion (*A*); longitudinal molecular diffusion (*B*); and mass transfer in the stationary phase (*C*). These three parameters are related to the plate height, *H*, and to the linear velocity of the mobile phase, *u*, through the expression:

$$H = A + B/u + Cu \tag{1.9}$$

Thus, in order to minimize *H* and maximize the column efficiency, the terms *A, B* and *C* must be minimized.

Eddy diffusion, *A*, also known as the multiple-path term, arises due to the different flow paths that analytes can take in a packed column. Ideally, analyte molecules injected at the same time should also elute at the same time. But molecules that travel shorter paths through the particle-packed column will elute sooner than molecules that travel longer, more twisted paths around the particles (Figure 1.2). Eddy diffusion is related to the particle diameter (d_p) and the packing factor (λ):

$$A = 2\lambda d_p \tag{1.10}$$

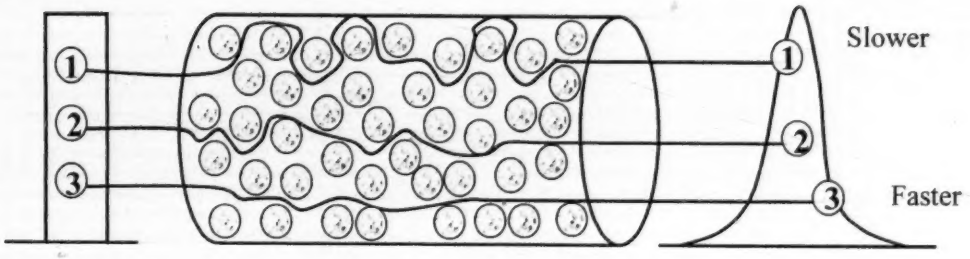

Figure 1.2. Schematic representation of Eddy diffusion. Adapted from reference [14]

Thus, to minimize A, small, tightly-packed particles should be used. However, particle size is limited by the operating pressure of the HPLC system.

Longitudinal molecular diffusion, B, is related to the diffusion coefficient for the solute in the mobile phase (D_M) and the obstruction factor (ψ), a term that allows for the nature of the packed beds:

$$B = 2\psi D_M \tag{1.11}$$

Molecules diffuse from a region of high concentration to that of lower concentration over time, causing the sample plug to become more diffuse with time. The van Deemter equation predicts that higher flow rates (or linear velocities, u) will minimize the B/u term. At higher flow rate, the analytes spend less time in the mobile phase and will have less time for molecular diffusion.

The C term of the van Deemter equation concerns the transfer of analyte molecules into and out of the stationary phase (sorption and desorption). Faster kinetics reduces the contribution of C to overall band broadening. For a liquid-liquid partitioning C is given by

$$C = \frac{8}{\pi^2} \frac{k}{(1+k)^2} \frac{d_f^{\,2}}{D_s} \tag{1.12}$$

where k is the retention factor, d_f is the average film thickness of the liquid stationary phase and D_s is the diffusion coefficient of the solute (analyte) in the stationary phase.

Thus, thin films and high diffusion coefficients minimize the C term. The ratio $k/(1+k)^2$ is minimized at large values of k, but there is little advantage to extending k beyond a value of 20 due to long analysis times.

A van Deemter plot refers to a plot of plate height, H, as a function of flow rate or more correctly the linear velocity. A typical van Deemter plot is shown in Figure 1.3 along with the individual contributions of the A, B and C terms. The minimum in the plot indicates the flow rate at which the lowest plate height (or maximum efficiency) is achieved. In the interest of speeding up analyses times, chromatographers often use linear velocities much higher than the optimal linear velocity, at the cost of reducing the efficiency of the separation. If the slope on the right-hand side of the van Deemter plot (i.e. the C-term) is not too steep, then the increase in plate height with higher flow rate will be negligible.

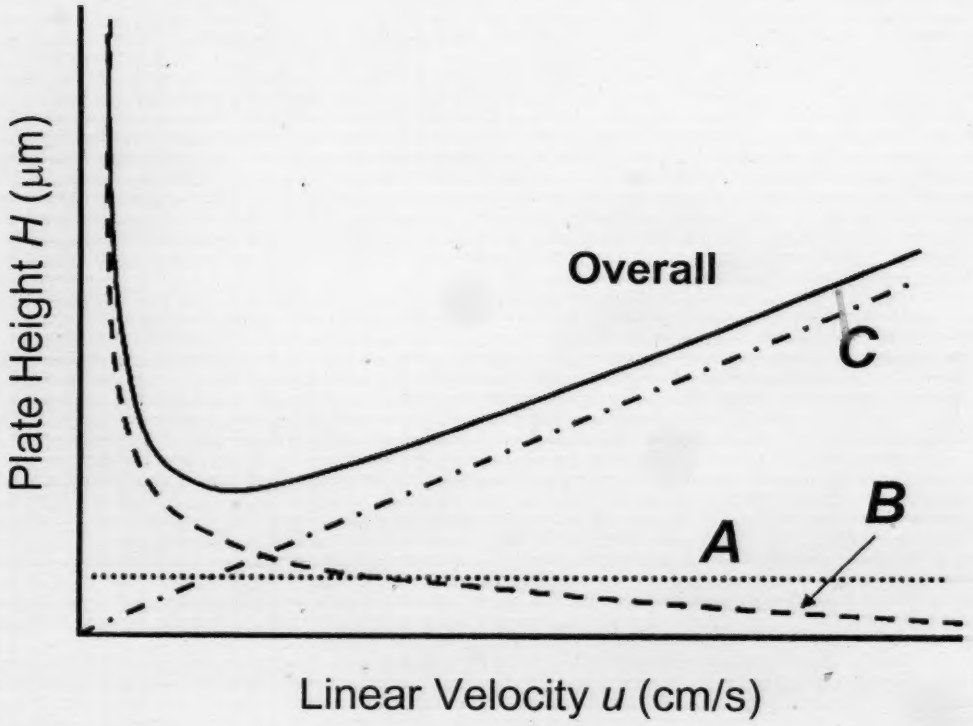

Figure 1.3. Typical van Deemter plot (solid line), with individual contributions from the A, B and C-terms shown in dashed lines. Adapted from reference [14]

1.4 Instrumentation

Modern HPLC instrumentation consists of high-pressure eluent pumps, an injector, separation column, detector, and computer for data collection and analysis, as well as connecting tubing and fittings to link the components together. Instrumentation for ion chromatography appears much like HPLC systems, except that the entire flow-path must be metal-free (Figure 1.4). The highly alkaline eluents commonly used in IC can cause stainless steel to release significant amounts of metal contaminants, which can alter retention characteristics, damage suppressors, and interfere with detection. Therefore, IC systems are made of polyether ether ketone (PEEK), a chemically inert polymer material capable of withstanding high pressures.

Pumps for IC are typically isocratic, although higher end IC systems can perform gradient elution. The flow range of IC pumps mirrors that of modern microbore (2 mm i.d.) or conventional (4.6 mm i.d.) column systems, but no capillary IC systems are commercially available, although this is an area of active research.[19] Eluents may either be prepared manually or generated on-line through electrodialysis. Manually prepared eluents were used throughout this thesis. Therefore eluent generation will not be discussed. For further information about eluent generation reference[20] is recommended. The typical injection volume is 20 μL, with 1 mL injections or preconcentrator columns used for trace (sub ppb) determinations.[1]

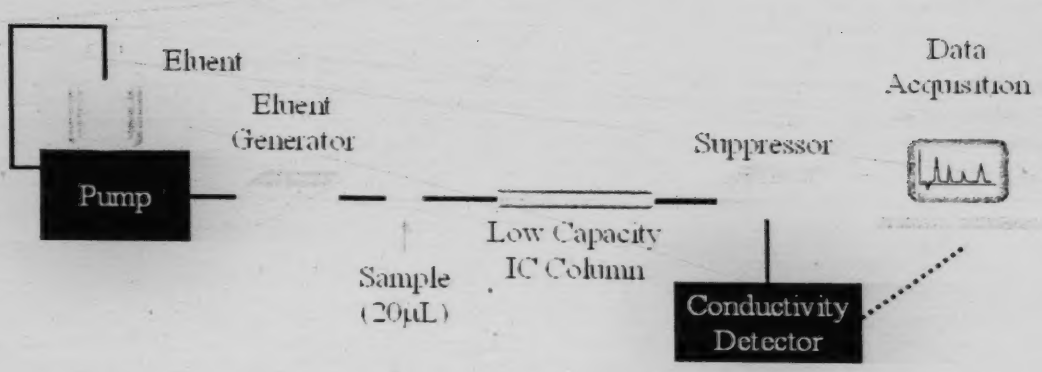

Figure 1.4. Schematic diagram of a typical IC system.

1.5 Detection

Most commonly, conductivity detection is used in IC because it is a universal detection mode for ionic species. Conductivity detection is achieved by passing the effluent through a detector cell containing two electrodes to which an electric potential is applied.[21] The ions move in response to the applied field, generating a current that can be measured. The current generated depends on the ionic conductance and the charge and concentration of the ions passing through the cell. When analyte ions are eluted from the column, there is a change in signal proportional to the difference in ionic conductance between the eluent and analyte ions. However, since the eluent is conductive itself, it causes a large conductivity background, worsening the limits of detection. To reduce this background, either low concentrations of weakly conductive eluent are used with low capacity columns (non-suppressed IC) or an eluent suppressor is added to the system between the column and the detector (suppressed IC). Suppressors are discussed in Section 1.6.

Direct UV absorbance can also be used for detection, which eliminates the need for a suppressor. However, only UV-absorbing anions (e.g., IO_3^-, NO_2^-, NO_3^-, Br^-, I^-, SCN^-) can be detected in this manner. More universal absorbance detection is achieved with indirect detection, where the displacement of a UV-absorbing eluent anion such as phenylphosphonic acid by the analyte ions is monitored by a UV detector.[22] Detection limits for indirect UV detection are typically medium to high ppb [1] which is significantly poorer than can be achieved by suppressed conductivity detection. Also, the presence of system peaks makes indirect UV detection challenging.

1.6 Suppression

Suppression is a post-column reaction designed to improve the sensitivity of conductivity detection. Suppressors are placed after the column and before the detector. Eluent suppression in anion exchange chromatography improves the detection limits of anions from the parts-per-million (ppm, μg/mL) to the parts-per-billion (ppb, ng/mL) level through two processes. First, the background conductivity is reduced by converting the eluent ion into its weak acid form (e.g., E^- in equation 1.1 is converted to HE). The background conductivity will then depend on the strength of the acid HE. It is for this reason that eluents with $pK_a>7$ are preferred, since their acidic form is only partially dissociated. For example, hydroxide eluents ($pK_w=14$) are converted to H_2O, which is essentially non-conductive (0.06 μS/cm background conductivity). Suppression also enhances the conductivity of the analyte anions by exchanging its associated counter-cation for H^+, which has a high ionic conductivity relative to all other cations (e.g, K^+Cl^- is converted to H^+Cl^-).[12]

There are a number of concerns to keep in mind when using suppressors. Namely, suppressors have a limited capacity and must be periodically regenerated or replaced. The capacity and pressure limits of suppressors also restrict the flow rate that can be used. Additionally, the extra volume added to the system by the suppressor contributes to band broadening.[23]

Commercially available suppressors have either a packed-bed or membrane construction, and can be regenerated by either chemical or electrolytic means. A packed-bed suppressor consists of a column packed with an ion-exchange resin, which requires frequent off-line regeneration and has a large dead-volume.

Membrane suppressors are most commonly used today and provide continuous regeneration and low dead-volumes.[24] Membrane suppressors contain a cation-exchange membrane, with effluent flowing on one side, and regenerant flowing on the other side in the opposite direction (Figure 1.5). Cations can move freely through the membrane, thus, H^+ transfers from the regenerant to the effluent to form H^+A^- and H_2O. The analyte counter-ion, Na^+, passes through the membrane into the regenerant flow. Two cation-exchange membranes are used to sandwich the effluent flow, to increase suppression capacity. Membrane suppressors that use an acid regenerant are termed "chemically suppressed."

The main shortcoming of chemical suppression is that the regenerant flow rate must be ten times the eluent flow to ensure complete suppression. As a result, a large supply of acid regenerant is needed, which usually must be prepared manually. As an alternative, a second mode of regeneration was developed, which relies on the electrolysis of water to generate a supply of H^+. Such suppressors are known as "electrolytic" or "self-regenerating" suppressors. Electrodes are situated within the suppressor to produce H^+ in situ (Figure 1.6), eliminating the need for large volumes of regenerant and a separate pumping system to deliver the regenerant. The suppressed eluent can be recycled through the outer chamber of the suppressor so that an external water supply is not needed. However, for determinations requiring greater sensitivity, fresh water can be delivered from an external source.

The thin membranes used in suppressors are quite delicate and care must be taken to avoid damage. Flow rates and backpressure must be limited. A new type of suppressor construction combines the ruggedness of packed-bed suppressors with

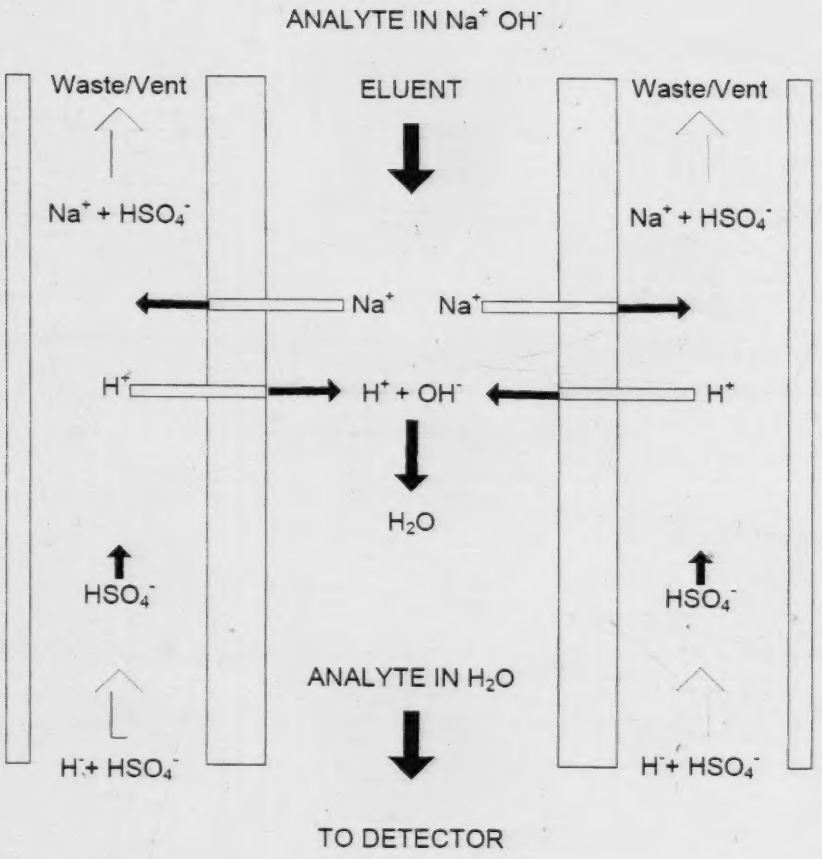

Figure 1.5. Schematic of a chemically regenerated membrane suppressor. Image courtesy of Dionex Corporation.

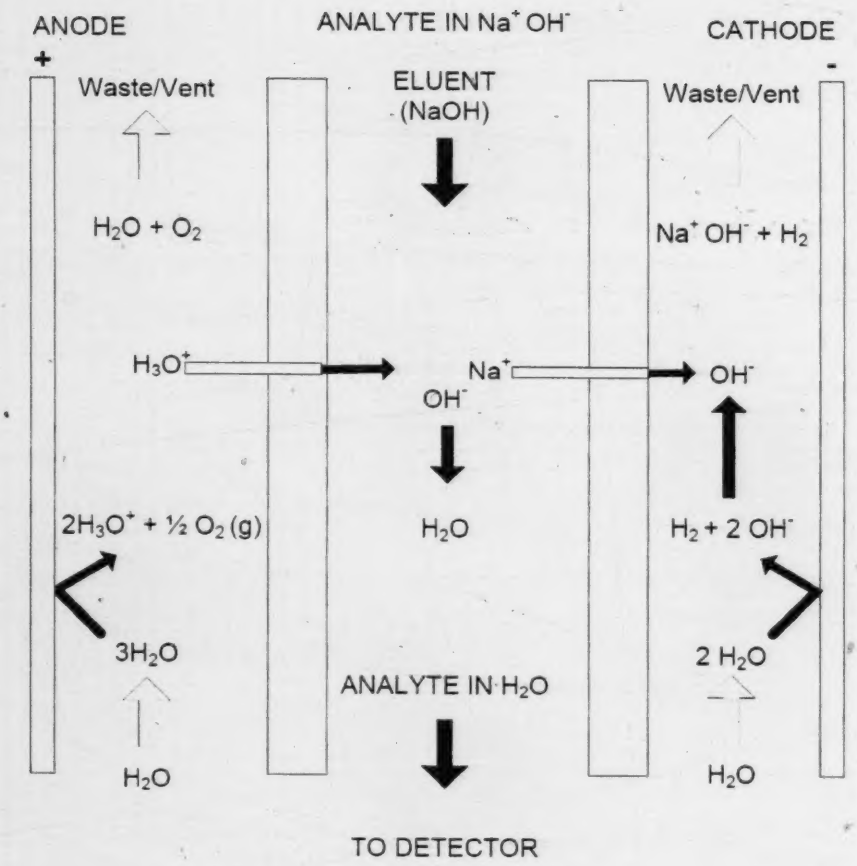

Figure 1.6. Schematic of an electrolytically regenerated membrane suppressor. Image courtesy of Dionex Corporation.

electrolytic regeneration. These suppressors are commercially available as the Atlas electrolytic suppressor (AES) by Dionex.[25] Instead of a packed-bed construction, the suppressor consists of six polyethylene cationic exchange monoliths which are functionalized with sulfonate groups.[20] (see Section 1.9.1 for more information on monoliths). The six monoliths are separated from each other by flow distribution discs to ensure that eluent flows through each monolith segment (Figure 1.7). Electrodes are placed at both sides of the monolithic bed for the electrolysis of water. This set-up requires less time for start-up, a faster equilibration time, and lower background noise than membrane suppressors in the chemical suppression mode. In this thesis, a Dionex Atlas electrolytic suppressor was used with an external water source.

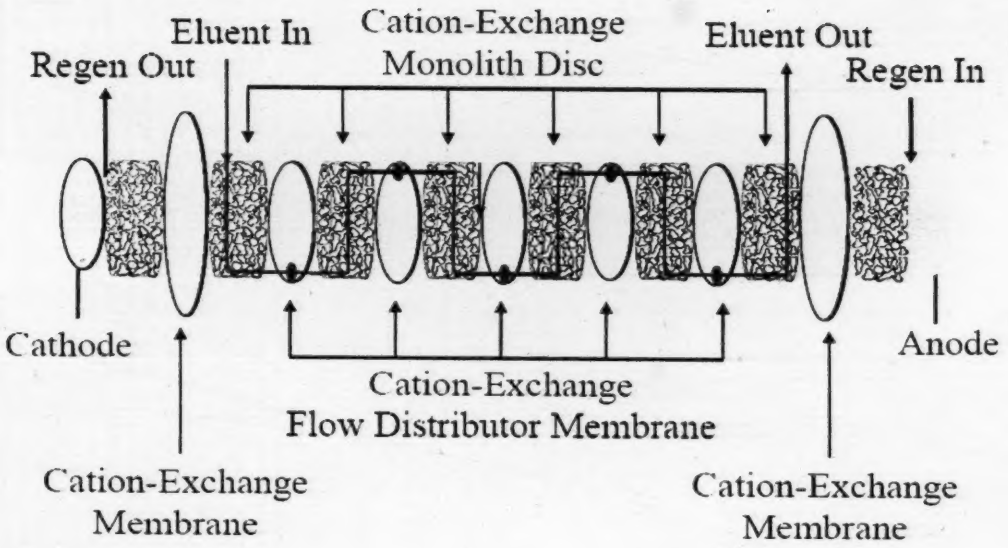

Figure 1.7. Schematic of Dionex Atlas Electrolytic Suppressor. Image courtesy of Dionex Corporation.

1.7 Selectivity in ion chromatography [12]

Selectivity, α, is a term used to describe the relative retention of two components (equation 1.8). There are several ways to alter selectivity in ion chromatography, through the nature of the mobile phase (e.g., eluent type, eluent strength, pH, additives) and the nature of the stationary phase (e.g. support and ion-exchange site). However, usually major changes in selectivity in IC are accomplished by changing the stationary phase, since the mobile phase is restricted to eluents that can be suppressed. As mentioned earlier, in anion-exchange, eluent anions E^{y-} are displaced from the stationary phase (subscript s) by analyte ions, A^{x-}, initially in the mobile phase (subscript m) (equation 1.1). Assuming that activity coefficients are approximately equal to one, the equilibrium constant, or selectivity coefficient $K_{A,E}$, is given by:

$$K_{A,E} = \frac{[A_s^{x-}]^y [E_m^{y-}]^x}{[A_m^{x-}]^y [E_s^{y-}]^x} \qquad (1.13)$$

The selectivity coefficient is a function of the analyte ion, the eluent ion, and the stationary phase, and thus, it can be altered in many ways.

1.7.1 Effect of analyte and eluent ions on selectivity

The charge on the analyte ion is the most apparent factor affecting its selectivity – polyvalent ions are more strongly retained than monovalent ions. As a result, there is often a gap in the chromatogram between ions of differing charge.

Increasing the eluent strength can alleviate this problem. Alternatively, if an analyte ion is the conjugate base of a weak acid, then altering the pH of the eluent can change its degree of ionization, and therefore, its retention. However, suppression requires that the eluent be basic for anion separations, and acidic for cation separations.

In addition to the charge on the ion, its hydration sphere also plays a role in selectivity. Highly hydrophilic ions have large hydration spheres that must be shed in order for the ion to interact with the ion-exchange site. The smaller the hydration sphere on the ion, the closer it can get to the ion-exchange site, and the more strongly it will be retained.

Polarizable ions, such as I^-, SCN^-, and ClO_4^-, are strongly retained on anion-exchange columns. These ions are rather large and poorly hydrated, and as such they do not form a proper hydration sphere in solution. They disturb the structure of water in the mobile phase and therefore enter into the stationary phase, where the structure of water is less ordered.[26] According to Diamond, polarizable ions may participate in water-structure enforced ion pairing with the anion-exchange site, thus increasing their retention.[27]

Ion retention can be predicted using the linear solvent strength model: [12]

$$\log k_A = \frac{1}{y}\log K_{A,E} + \frac{x}{y}\log\left[\frac{Q}{y}\right] + \log\left[\frac{w}{V_M}\right] - \frac{x}{y}\log[E_m^{\,y-}] \qquad (1.14)$$

where k_A is the retention factor of the analyte, $K_{A,E}$ is the selectivity coefficient for the analyte ion and competing eluent ion (E^{y-}), Q is the effective ion-exchange capacity of the column, w is the mass of the stationary phase, and V_M is the volume of mobile

phase. The values x and y are the charges of the analyte and the eluent, respectively. This model is quite accurate for separations using just one competing ion, but is not successful for mobile phases containing multiple ions (such as carbonate/bicarbonate or phthalate). Plots of $log\ k_A$ vs. $log(Q/y)$ or $log\ kA$ vs. $log\ [E_m^{y-}]$ have slopes of x/y and $-x/y$, respectively. In both plots, the slope for a doubly-charged analyte is twice that of a singly-charged analyte when eluted with the same eluent. Thus, the retention of polyvalent ions is more affected by changes in column capacity and eluent concentration than are monovalent analytes. Equation 1.14 can be reduced for a given column and given eluent ion:

$$\log k_A = const - \frac{x}{y}\log[E_m^{y-}] \qquad (1.15)$$

Thus, increasing the eluent strength will decrease the retention of an analyte. Eluent concentration is a convenient means of changing the retention of ions, but it has little effect on the selectivity of ions of the same charge. However, eluent concentration can have a dramatic affect on the selectivity of ions differing in charge. At high enough concentrations of eluent on a high-capacity column, doubly-charged ions can elute before singly-charged ones.

Weak eluents (such as hydroxide or borate for anion analysis) are sufficient for separation of singly-charged analytes; however, stronger eluents are required for multiply charged species. The combination of carbonate/bicarbonate is often used for mixtures of monovalent and polyvalent ions, since the eluent strength and pH can be

tuned by changing the ratio of carbonate:bicarbonate. For other considerations concerning eluent choice, see Section 1.8 on eluents.

1.7.2 Effect of stationary phase on selectivity

The most dramatic means of altering selectivity in ion chromatography can be accomplished by changing the stationary phase. A wide selection of stationary phases for IC is commercially available, or can be prepared in the lab. The types of stationary phases are discussed in Section 1.9. In this section, a brief discussion on the selectivity of stationary phases is offered.

The selectivity of a column is affected by the materials used to construct the stationary phase, the degree of cross-linking of polymer-based stationary phases, the ion-exchange capacity of the column, and the functional group on the ion exchanger. The structure of the ion-exchange site has the most profound effect on the selectivity of the column. Polymer-based columns for anion-exchange chromatography commonly contain a quaternary ammonium functionality ($-NR_4^+$). The structure of the quaternary ammonium groups can be changed by varying the alkyl chains. Lengthening some or all of the alkyl chains can produce a more hydrophobic, bulkier site. As the size of the ion-exchange group increases, its charge density decreases, thereby decreasing the electrostatic attraction between the analyte and ion-exchange sites. This results in a decrease in retention of polyvalent ions, such as SO_4^{2-} and HPO_4^{2-}. More hydrophilic anions, such as Cl^-, show a small increase in retention as the size of the ion-exchange site increases.

1.8 Eluents

Eluent ions are required for the process of ion-exchange (equation 1.1), and their nature and concentration affect the retention of analyte ions. Preferred eluents for anion separations are salts of weak acids (pH > 7) such as (in order of increasing strength): hydroxide (^-OH), bicarbonate (HCO_3^-) and carbonate (CO_3^{2-}). Such eluents are easily suppressed (see Section 1.6) and have adequate buffering capacity to ensure reproducibility and robustness. The mixture of bicarbonate and carbonate ions is often used as a powerful eluent for the separation of both singly and doubly charged analytes in a single sample.

The highly-alkaline eluents used in IC require a pH-stable stationary phase, such as polymeric materials. Recently, however, there has been significant interest in using silica-based IC columns, due to the higher chromatographic efficiency of silica over polymers.[1] Highly-alkaline eluents are not compatible with silica stationary phases, since silica dissolution is a concern above pH 8. [28] To circumvent this problem, weak acid eluents can be used as an alternative to highly-alkaline eluents.[1,29] Cyanophenols and 4-hydroxybenzoic acid (4-hba) have been shown to be good alternatives for silica stationary phases.[23,30,31] Such eluents have a low equivalent conductance, thus, they can be used with suppressed or non-suppressed conductivity detection.

1.9 Stationary Phases

The column is the heart of the chromatographic system, as it is responsible for the actual separation of the components of a mixture. The stationary phase has the greatest effect on ion exchange selectivity (Section 1.7.2); thus, a wide range of IC columns are commercially available.[32] Traditional ion-exchange columns are composed of polymeric materials, which can withstand the high pH of hydroxide and carbonate/bicarbonate eluents. However, the studies in this thesis are concerned with silica as a stationary phase for IC. Silica has been the traditional stationary phase for reversed-phase and normal phase HPLC, due to its higher chromatographic efficiency and mechanical strength over polymer-based columns.[1] Stationary phases, whether silica or polymer based, can be of particle-packed or monolithic construction. Zirconia titania and graphitic carbon based stationary phases are also available, but will not be discussed here.

1.9.1 Monoliths vs. particle-packed columns

Chromatography columns are available with particulate or monolithic stationary phases. Particulate columns are packed with small spherical particles, most commonly composed of silica or polymer, ranging from 1.5-15 μm in diameter. Smaller particles allow for more efficient separations, but there exists a point at which the pressure drop across the column exceeds the operating conditions of the HPLC instrumentation. Fortunately, monolithic columns are available which are much more permeable than particulate columns and can perform as well as 3 μm particles in terms of efficiency.[33-35] Monolithic columns are a continuous rod of porous silica or

polymer encased in a PEEK column housing. The porous structure allows for higher flow rates with lower backpressure than particulate columns, enabling faster separations with a traditional HPLC pump.[4,36,37] For these reasons, new possibilities in many modes of liquid chromatography have emerged, including ion chromatography.[37] A review has recently been released on the current developments in ion chromatography and capillary electrochromatography on monolithic columns.[38] An extensive review by Chambers et al. also discusses the recent developments in IC using both polymer and silica-based monoliths.[39]

Figure 1.8 illustrates the differences between particulate and monolithic columns in terms of solvent flow. In particle-packed columns, the eluent molecules are forced to flow around the particles in winding paths (Figure 1.8A). This causes the separation to be heavily dependent on diffusive mass transfer of the analytes, which can be slow and extremely unfavourable for large molecules. In contrast, monolithic columns are permeable enough to allow flow directly through the solid, porous rod (Figure 1.8B). This allows the transport of the solute to the surface to be dominated by convection instead of diffusion.[40]

Figure 1.9 shows van Deemter plots for a silica monolith and conventional columns packed with 3.5 and 5 μm silica particles.[41] This figure shows that monolithic columns are as efficient as 3.5 μm particulate columns. but higher flow rates can be used with monoliths..

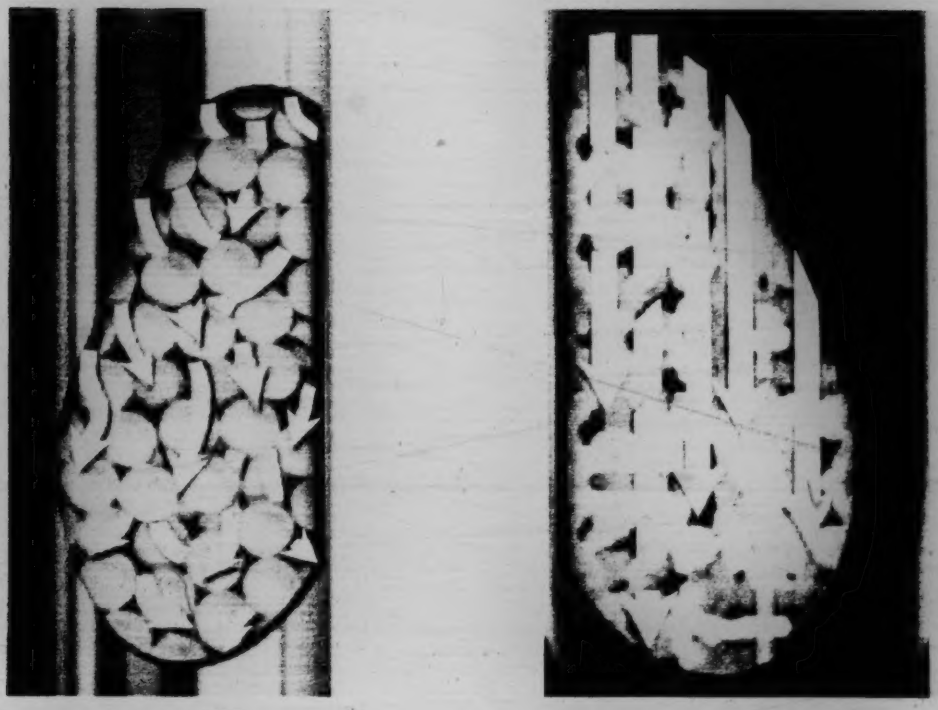

Figure 1.8. Flow through (A) particle-packed column, (B) monolithic column. Image courtesy of Phenomenex (www.phenomenex.com).

Figure 1.9 has been removed due to copyright restrictions. Figure 1.9 showed a comparison of van Deemter plots for silica monolithic column and conventional columns packed with silica particles of different diameters. The original source of Figure 1.9 can be found in Figure 6 of reference [41] (Cabrera, K., *J. Sep. Sci.* **2004**, *27*, 843-852).

1.9.2 Polymer-based stationary phases for IC

Due to the highly alkaline nature of IC eluents, stationary phases are traditionally made of pH-stable polymer materials. To circumvent the poor mass transfer within the pores of polymeric particles, agglomerated particles are most commonly used in IC. An agglomerated particle is composed of a solid inner core (essentially non-porous) on the surface of which is deposited a thin layer of stationary phase[1]), as is shown in Figure 1.10A. The inner core is commonly composed of a surface-sulfonated polystyrene/ divinyl-benzene substrate with particle diameters between 5-25 μm. Latex particles (~0.1 μm diameter), composed of fully aminated, high capacity polymers of polyvinylbenzyl chloride or polymethacrylate, are agglomerated to the surface of the internal polymer beads through electrostatic and van-der-Waals interactions.[1,42] The monolayer of charged latex particles determines the stationary phase functionality and selectivity. These stationary phases produce higher efficiencies than completely porous ion exchangers due to their faster kinetics and the high permeability of the pellicular layer. An example of this type of phase is the Dionex Ion Pac AS10 and the Ion Pac AS16 which have a capacity of 6.8 μeq/cm through attachment of 65/80 nm latex on 8.5/9 μm ethylvinylbenzene-divinylbenzene nonporous particles. A second format for polymeric particles, exemplified by the Dionex Ion Pac AS14A and Ion Pac CS12A, chemically grafts functionality directly onto the particles and is depicted in Figure 1.10B. The thin grafted film (1-5 nm) makes a high efficiency, high capacity stationary phase (4.8 and 112 μeq/cm for Ion Pac AS14A and CS12A, respectively).[42]

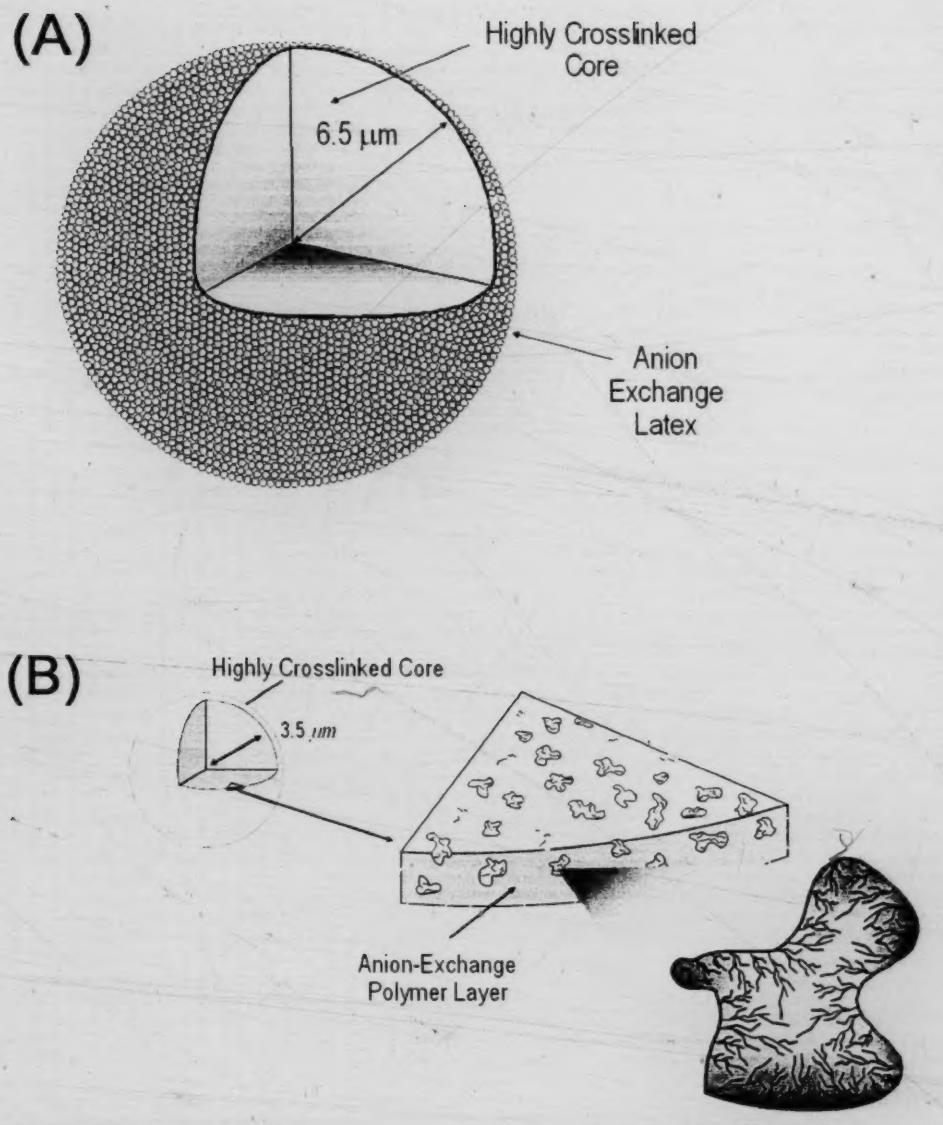

Figure 1.10. Schematic representation of (A) latex-agglomerated particle (Dionex IonPac AS9-SC packing particle) and (B) particle with chemically grafted functionalities (Dionex IonPac AS14 packing particle). Images courtesy of Dionex Corporation.

Polymer monolithic columns are not commercially available, except as monolithic discs,[43] but they can easily be synthesized in the laboratory.[44] To date, there have been only a few reports on the use of polymer monoliths for anion-exchange chromatography. Hilder *et al.* demonstrated the use of a polymer monolithic capillary coated with latex particles for use in micro ion chromatography.[45] Six of seven ionized sugars were resolved in under 6 minutes, with a modest efficiency of 2.6×10^4 plates/m. Less than a year later, Zakaria *et al.* also prepared a latex coated capillary polymer monolith for the separation of small inorganic anions.[46] Due to the polymer nature of the column, alkali metal hydroxide eluents could be used to provide a fast separation of seven inorganic ions in less than 2 minutes.

Polymer monoliths can also be synthesized in a disc format, and are commercially available from BIA separations in a length of 1 mm.[43] Although these IC discs provide fast separations of biomolecules, they do not provide efficient separations of small ions. For example, using a BIA monolith disc, the efficiency achieved for an oligomeric DNA sample was double that of citric and malic acids, which have 10–15 times lower MW.[47]

Polymer monoliths, because of their ease of preparation and pH stability, exhibit great potential to be a fast and efficient means of separating ions. Efforts to produce polymer monoliths with higher ion-exchange capacities have been described by Hutchinson et. al.[48] However, to date, the average efficiency of ion separations on polymer-based monoliths (10^4–10^5 plates/m) has not exceeded that of silica

monoliths, which can be in excess of 10^5 plates/m.[23] As a result, my research has been directed towards the use of silica monoliths for efficient IC separations.

1.9.3 Silica-based stationary phases for IC

Silica is the stationary phase of choice for traditional reversed phase and normal phase HPLC separations, due to its higher chromatographic efficiency over polymer-based columns.[1] Although silica has poor chemical stability at pH > 8, [1,28] it has a high mechanical strength (tolerates high pressures) and does not shrink or swell in the presence of organic solvents.[1] Silica also offers the advantage that it can be covalently modified by reacting chlorosilanes with the silanol groups on the silica surface.[14]

Silica can also be synthesized in a monolithic construction, and are commercially available from many suppliers, including Merck[49] and Phenomenex.[50] The use of silica monoliths in IC seems an attractive choice, given their high efficiencies for small molecules and their ability to operate at high flow rates for shorter separation times.[51] Additionally, the uniform mesoporous structure, with homogenously spaced and sized throughpores, provides a much larger surface area than their non-porous polymer counter parts. Commerically available silica monolith columns have macropores and mesopores of 2 μm and 13 nm (Figure 1.11), respectively, giving them a total porosity of greater than 80% and a surface area of about 300 m^2/g. Silica monolithic columns have been shown to be equivalent to 3 μm particulate columns in terms of efficiency and to 7-15 μm particles with respect to

permeability.[33-35] Recently, monolithic silica capillaries have been prepared to have even smaller sized domains (1.3 μm mesopores and silica skeletons of ~0.9 μm), with efficiencies comparable to 2-2.5 μm particle-packed columns and permeability of 5 μm columns.[52] However, all research in this thesis was conducted using commercial monoliths with 2 μm throughpores.

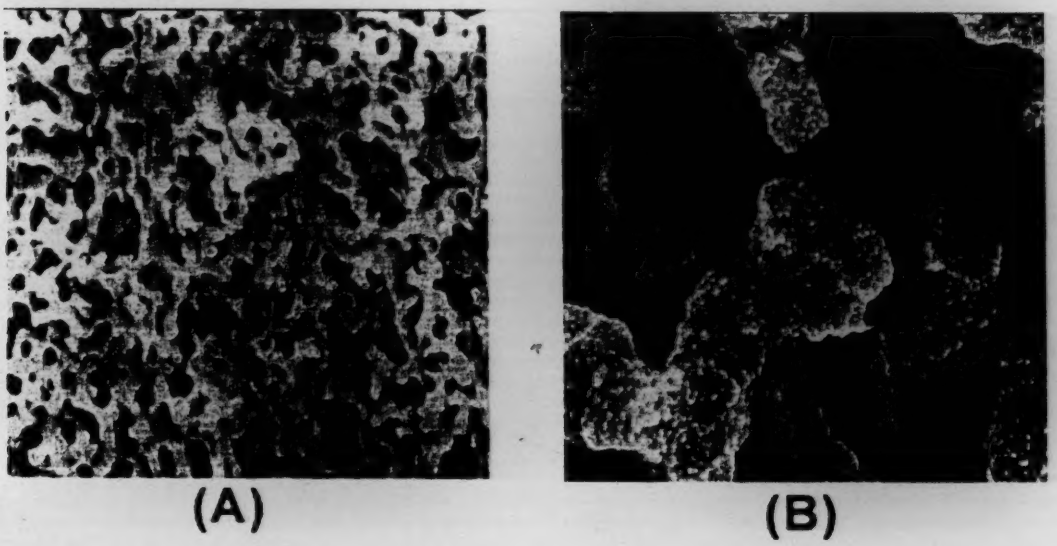

Figure 1.11. (A) Macropores and (B) mesopores of silica monolith. Reproduced with permission from Merck (www.merck.de).

1.10 Modification of silica monoliths for use in ion chromatography

The use of silica monoliths for applications in ion chromatography has received attention in recent years due to the high efficiency of these monoliths for small inorganic ions.[39] Recent applications of silica-based columns to IC involve semi-permanently coating a reversed-phase column with an ionic surfactant (Section 1.10.1), covalently attaching ion exchange sites to bare silica,[53-55] or coating bare silica with latex particles.[56]

1.10.1 Surfactant coatings

A reversed-phase column can be semi-permanently coated with an ionic surfactant to convert it into an ion-exchange phase. In this procedure, an aqueous solution of ionic surfactant, often containing an organic modifier such as acetonitrile (ACN), is flushed through the column until breakthrough of the surfactant is observed, as indicated by a sharp rise in conductivity. The ion-exchange capacity of the column can be calculated using equation 1.16: [30,57,58]

$$Q = CF(t_b - t_0) \qquad (1.16)$$

The term Q is the capacity (μeq/column), C is the surfactant concentration of the coating solution (μeq/mL), F is the flow rate (mL/min), t_b is the breakthrough time (min) indicated by a sharp rise in detector response and t_0 is the void volume of the column (min).

Early work with surfactant coatings employed particulate silica columns and included the surfactant in the eluent as an ion-interaction reagent.[59,60] Using tetrabutylammonium chloride as an ion interaction reagent on a 3 μm silica particulate column, Connolly and Paull[60,61] were able to separate five UV-absorbing anions in 45 seconds. Hatsis and Lucy[5] were able to further reduce analysis times by using very fast flow rates on a monolithic column. At the high flow rate of 16 mL/min, 8 inorganic ions were separated in just 15 seconds on a 5 cm silica monolithic column, using tetrabutylammonium phthalate as an ion-interaction reagent along with direct conductivity detection. The pressure drop across the monolithic column at 16 mL/min was 2500 psi, well within HPLC operating conditions.

Later work by Connolly and Paull[57] showed that these reversed-phase columns could be permanently coated with a double-chained cationic surfactant, didodecyldimethylammonium bromide (DDAB). The alkyl chains of the surfactant adhere to the C_{18} chains of the stationary phase through hydrophobic interactions, while the cationic head group acts as an anion exchange site. By applying DDAB coatings to a 50 x 4.6 mm silica monolithic column, Hatsis and Lucy[30] separated 7 anions in only 30 s using flow rates up to 10 mL/min. More recently, Pelletier and Lucy used more practical flow-rates to separate inorganic ions on short (0.5-1 cm) monolithic columns coated with DDAB.[23]

Surfactant coatings are semi-permanent, meaning they can be removed simply by flushing the column with acetonitrile. Upon recoating a column, a lower ion-exchange capacity can be obtained by increasing the amount of acetonitrile in the coating solution.[23,30] For this reason, surfactant coatings are an attractive choice since

the ion-exchange capacity can be adjusted to suit the separation. It also allows the user to try different surfactants and coating conditions on the same column in order to achieve the desired separation.

However, there have been contradictions in the literature regarding the stability of surfactant coatings. Some researchers found that surfactant coatings gradually leach from a column, resulting in decreasing retention of analytes over time.[23,30] while others report a stable coating.[57,62-65] Some studies have included a small amount of the surfactant in the eluent to maintain retention times.[66-70] Hatsis and Lucy observed a 10% decrease in the retention of sulfate after 12 hours of flow at 5 mL/min.[30] The surfactant coating can be removed and re-applied to restore original analyte retention, but this is a time consuming process and is not well suited to routine analyses. Efforts to slow the process of surfactant leaching have been made by Pelletier et al.[23], by placing a coated pre-column before the analytical column. As surfactant leaches from the analytical column, it is replaced by surfactant leaching from the coated pre-column. This method has been found to increase the stability of a surfactant coating by 15 fold, but by no means stopped the leaching completely.

There have also been reports of increased backpressure and reproducibility problems with multiple uncoating/recoating cycles of DDAB.[71] This may be due to the DDA^+ ($eluent^-$) ion pair precipitating on the column during the uncoating process, since DDAB is only partially soluble in pure acetonitrile (0.1 g/mL in 100% acetonitrile[23]). Pelletier and Lucy addressed this problem by introducing a new uncoating procedure in which the DDA^+($eluent^-$) is first converted back to DDA^+(Br^-), and then uncoated using a gradient from 0 to 50% acetonitrile[72] (Figure 1.12).

Although surfactant coatings do have their drawbacks, they are an attractive choice for chromatographers who wish to unite the high chromatographic efficiency of silica with ion chromatographic separations. Surfactant coatings also allow the chromatographer to tailor the ion-exchange capacity and selectivity of their column for their desired separation. Additionally, the coatings can be easily removed to allow the column to be used in its original reversed-phase form.

Experimenting with different surfactants allows the selectivity of the column to be varied. Table 1.1 displays the various surfactants that have been used as coatings for ion-exchange. O' Riordain et al.[73] recently reported interesting selectivity on particulate and monolithic columns coated with a carboxybetaine-type surfactant, (dodecyldimethyl-amino) acetic acid. This amphoteric surfactant contains a stong inner anion-exchange site and a terminal weak carboxylic acid group, and thus the degree of protonation (and therefore anion retention) could be varied with pH.

Coating a column with both an ionic and non-ionic surfactant has been shown to alter selectivity and improve analysis time, efficiency and coating stability.[74,75] The non-ionic surfactant is thought to make the stationary phase more hydrophilic and therefore more compatible with the aqueous mobile phase. Q. Xu et al. applied this dual-surfactant coating method to monolithic columns.[76] A reversed-phase silica monolith was first coated with a non-ionic surfactant (polyoxyethylene, or POE), then with the cationic surfactant cetyltrimethylammonium bromide (CTAB). This stationary phase, when used with a sodium sulfate eluent, was able to separate hydroxide from other ions in a mixture. By comparison to a column coated with

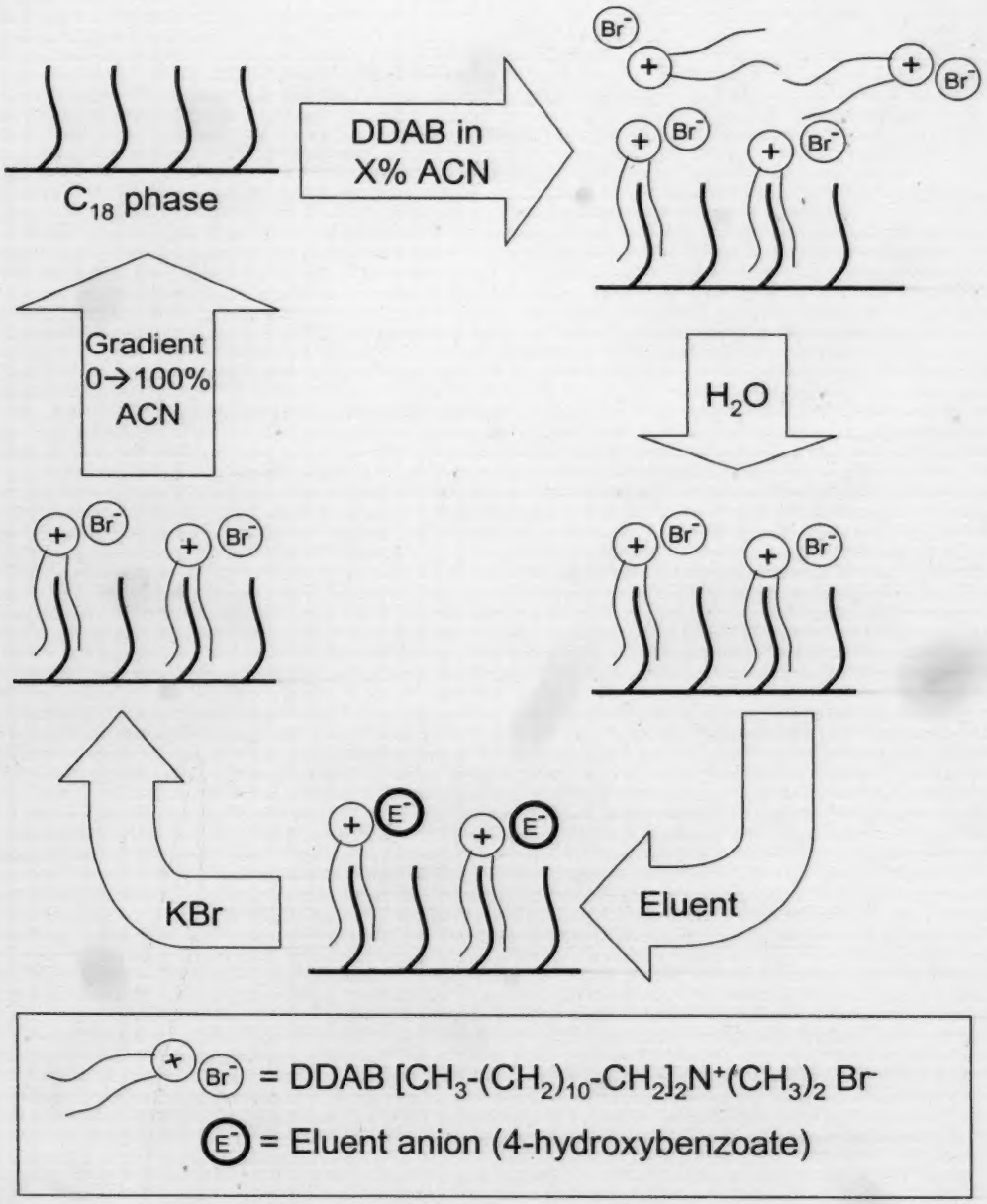

Figure 1.12. Coating and uncoating process for a DDAB-coated reversed phase column.

Table 1.1. Various surfactants used as ion-exchange coatings on reversed-phase silica.

Structure	Name	Abbreviation	Ref.
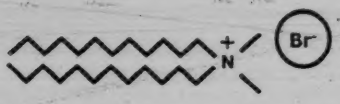	Didodecyldimethyl-ammonium Bromide	DDAB	23,30,31,56,57,77, 78
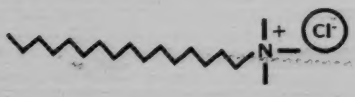	Cetyltrimetyl-ammonium Chloride	CTAC	66
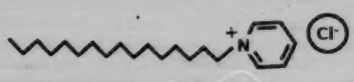	Cetylpyridinium Chloride	CPC	63,77-79
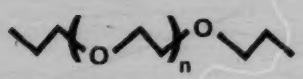	Polyoxyethylene	POE	65,77,78
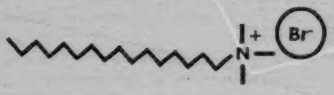	Cetyltrimethyl-ammonium Bromide	CTAB	65
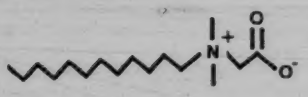	(Dodecyldimethyl-amino) acetic acid	-	68,80
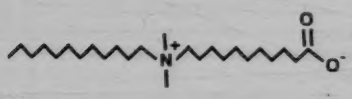	N-dodecyl-NN-(dimethylammonio) undecanoate	DDMAU	64
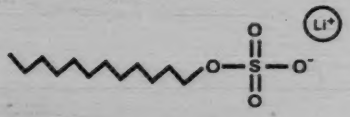	Lithium dodecylsulfate	Li-DS	67,81-83
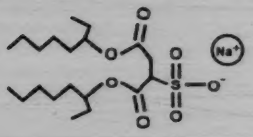	Sodium Dioctylsulpho-succinnate	Na-DOSS	62,84,85

CTAB only, improvements in efficiency (ΔN = 915 plates/column) and coating stability were confirmed.

Cations can also be analyzed by coating a reversed-phase column with an anionic surfactant. For example, lithium dodecylsulfate (Li-DS) and sodium dioctylsulfo-succinate (DOSS) have been used in cationic separations (Table 1.1). Paull's group recently used DOSS and DDAB-coated columns for simultaneous determination of anions and cations.[86]

1.10.2. Covalent modification of silica monoliths

Although surfactant coatings are reversible and easy to change or mainpulate, coating instability has led to a drive towards covalent (i.e., permanent) modification of monoliths. Chelating ion-exchange columns have been prepared by chemically bonding iminodiacetic acid (IDA) functionalized silane to a bare silica monolith.[53,54] The monolith was robust enough to determine trace levels (< 1 ppm) of magnesium and calcium in brine samples in under 40 s using 5 mL/min. Subsequent analysis of the monolithic column showed a non-uniform ion-exchange capacity along the length of the column, with the end of the column showing 30-40% less capacity.

Additionally, amino acids covalently bound to silica have been used for IC. Depending on the amino acid used and its pK_a, anionic, cationic or zwitterionic surfaces can result.[87-89] Elefterov et al.[90] showed retention of alkali and alkaline earth metals on a lysine-bonded silica particulate column when used at pH values of 2.5-2.9. A later study by Sugrue et al. explored the use of a bare silica monolith covalently bonded with lysine (2,6-diaminohexanoic acid) for use in both cation and

anion exchange chromatography.[91] Separation of 6 anions could be achieved in 100 s with efficiencies between $3x10^4$ to $4.8x10^4$ plates/m using a 50 mM phosphate buffer at pH 3.0. By changing the pH of the eluent, separations of cations were also performed.

1.10.3 Latex coatings on silica monoliths

Ideally, an ion-exchange phase should have its ion-exchange sites permanently adhered to the underlying surface, such as the Dionex agglomerated particles (Section 1.9.2). In these stationary phases, charged latex particles adhere to the negatively charged polymer surface underneath through strong electrostatic interactions. Bare silica monoliths have negatively charged silanol groups at their surface at pH > 2. Latex particles, functionalized with positively-charged quarternary ammonium groups, can be flushed through the column, adhering to the bare silica through electrostatic interactions (Figure 1.13). Breadmore et al. demonstrated this by coating an open-tubular silica capillary with quaternary ammonium functionalized latex particles for use in ion-exchange capillary electrochromatography, which requires applying a voltage across the capillary.[92] More recently, latex coatings have been applied to monoliths. Hutchinson et al. also separated ions in the ion-exchange capillary electrochromatography mode, using monolithic silica capillaries (50 and 75 μm i.d.) coated with latex particles.[93] Polymer capillary monoliths coated with latex have also been used to separate ions through the ion-exchange mode, as shown by Hilder et al.[45] and Zakaria et al.[46], Section 1.9.2.

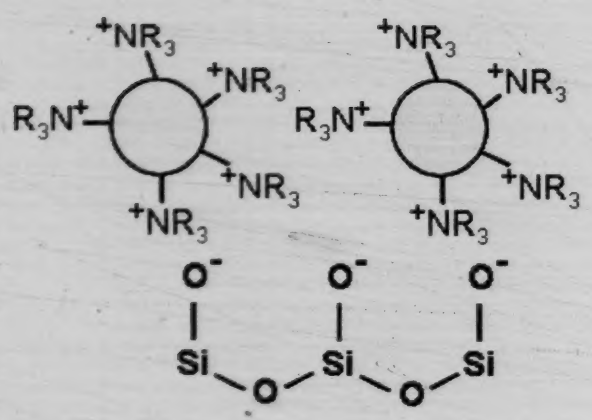

Figure 1.13. Latex adhering to a bare silica surface through electrostatic interactions.

1.11 Summary and Thesis Overview

This thesis focuses on methods of making ion chromatography on silica monoliths more stable. In Chapter 2 silica monoliths coated with the surfactant DDAB are compared with latex coated monoliths. The two approaches for introducing ion exchange sites are compared with respect to selectivity, stability and efficiency. Chapter 3 studies means of increasing the stability of surfactant coatings on reversed phase silica monoliths. Chapter 4 summarizes the thesis and briefly describes potential future studies.

1.12 References

(1) Weiss, J., *Handbook of Ion Chromatography*, 3rd edn., Wiley-VCH, Weinheim, 2004.

(2) Tanaka, N.; Kobayashi, H.; Nakanishi, K.; Minakuchi, H., Ishizuka, N., *Anal. Chem.* **2001**, *73*, 420A-429A.

(3) Paull, B.; Nesterenko, P. N., *TRAC Trends Anal. Chem.* **2005**, *24*, 295-303.

(4) Miyabe, K.; Guiochon, G., *J. Sep. Sci.* **2004**, *27*, 853-873.

(5) Hatsis, P.; Lucy, C. A., *Analyst* **2002**, *127*, 451-454.

(6) Ettre, L. S., *Evolution of Liquid Chromatography: A Historical Overview in HPLC Advances and Perspectives*, Academic Press, New York, 1980.

(7) Ettre, L. S., *LC GC North America* **2003**, *21*, 458-467.

(8) van Deemter, J. J.; Zuiderweg, F. J.; Klinkenberg, A., *Chem. Eng. Sci.* **1956**, *5*, 271-289.

(9) Giddings, J. C., *Anal. Chem.* **1963**, *35*, 2215-2216.

(10) Horvath, C.; Lipsky, S. R., *J. Chromatogr. Sci.* **1969**, *7*.

(11) Horvath, C.; Preiss, B. A.; Lipsky, S. R., *Anal. Chem.* **1967**, *39*, 1422-1428.

(12) Lucy, C. A.; Hatsis, P., in *Chromatography - 6th Edition, Chapter 4*, ed. E. Heftmann, Elsevier, Amsterdam, Editon edn., 2004, vol. 69A.

(13) Small, H.; Stevens, T. S.; Bauman, W. C., *Anal. Chem.* **1975**, *47*, 1801-1809.

(14) Miller, J. M., *Chromatography, Concepts and Contrasts*, 2 edn., Wiley Interscience, Hoboken, 2005.

(15) Bidlingmeyer, B. A.; Warren, F. V., *Anal. Chem.* **1984**, *56*, 1583A-1596A.

(16) Foley, J. P.; Dorsey, J. G., *Anal. Chem.* **1983**, *55*, 730-737.

(17) Sadek, P. C., *Troubleshooting HPLC Systems: A Bench Manual*, John Wiley & Sons, Inc., New York, 2000.

(18) van Deemter, J. J.; Zuiderweg, F. J.; Klinkenberg, A., *Chem. Eng. Sci.* **1956**, 13-25.

(19) Kuban, P.; Dasgupta, P. K., *J. Sep. Sci.* **2004**, *27*, 1441-1457.

(20) Liu, Y.; Srinivasan, K.; Pohl, C.; Avdalovic, N., *J. Biochem. Biophys. Methods* **2004**, *60*, 205-232.

(21) Buchberger, W. W., *J. Chromatogr. A* **2000**, *884*.

(22) Melanson, J. E.; Wong, B. L. Y.; Boulet, C. A.; Lucy, C. A., *J. Chromatogr. A* **2001**, *920*, 359-365.

(23) Pelletier, S.; Lucy, C. A., *J. Chromatogr. A* **2006**, *1118*, 12-18.

(24) Stevens, T. S.; Davis, J. C.; Small, H., *Anal. Chem.* **1981**, *53*.

(25) www.dionex.com, *ATLAS Supressor Manual* **2004**.

(26) Chu, B.; Whitney, D. C.; Diamond, R. M., *J. Inorg. Nucl. Chem.* **1962**, *24*, 1405.

(27) Diamond, R. M., *J. Phys. Chem.* **1963**, *67*, 2513.

(28) Pool, C. F., *The Essence of Chromatography*, Elsevier Science B.V., Amsterdam, 2003.

(29) Haddad, P. R.; Jackson, P. E., *Ion Chromatography: Principles and Applications*, Elsevier, New York, 1990.

(30) Hatsis, P.; Lucy, C. A., *Anal. Chem.* **2003**, *75*, 995-1001.

(31) Victory, D.; Nesterenko, P.; Paull, B., *Analyst* **2004**, *129*, 700-701.

(32) Pohl, C. A.; Stillian, J. R.; Jackson, P. E., *J. Chromatogr. A* **1997**, *789*, 29.

(33) Leinweber, F. C.; Lubda, D.; Cabrera, K.; Tallarek, U., *Anal. Chem.* **2002**, *74*, 2470-2477.

(34) Leinweber, F. C.; Tallarek, U., *J. Chromatogr. A* **2003**, *1006*, 207-228.

(35) Kobayashi, H.; Ikegami, T.; Kimura, H.; Hara, T.; Tokuda, D.; Tanaka, N., *Anal. Sci.* **2006**, *22*, 491-501.

(36) Tanaka, N.; Kobayashi, H.; Nakanishi, K.; Minakuchi, H.; Ishizuka, N., *Anal. Chem.* **2001**, *73*, 420A-429A.

(37) Paull, B.; Nesterenko, P. N., *TRAC* **2005**, *24*, 295-303.

(38) Schaller, D.; Hilder, E. F.; P.R.Haddad, *J. Sep. Sci.* **2006**, *29*, 1705-1719.

(39) Chambers, S. D.; Glenn, K. M.; Lucy, C. A., *J. Sep. Sci.* **2007**, *30*, 1628-1645.

(40) Svec, F.; Tennikova, T.; Deyl, Z. E., *Monolithic Materials: Preparation, Properties and Application*, Elsevier, Amsterdam, 2003.

(41) Cabrera, K., *J. Sep. Sci.* **2004**, *27*, 843-852.

(42) www.dionex.com.

(43) www.biaseparations.com.

(44) Svec, F.; Frechet, J. M. J., *Anal. Chem.* **1992**, *64*, 820-822.

(45) Hilder, E. F.; Svec, F.; Frechet, J. M. J., *J. Chromatogr. A* **2004**, *1053*, 101-106.

(46) Zakaria, P.; Hutchinson, J. P.; Avdalovic, N.; Liu, Y.; Haddad, P. R., *Anal. Chem.* **2005**, *77*, 417-423.

(47) Podgornik, A.; Barut, M.; Jaksa, S.; Jancar, J.; Strancar, A., *J. Liq. Chromatogr. Related Technol.* **2002**, *25*, 3099-3116.

(48) Hutchinson, J. P.; Hilder, E. F.; Shellie, R. A.; Smith, J. A.; Haddad, P. R., *Analyst* **2006**, *131*, 215-221.

(49) www.merck.de.

(50) www.phenomenex.com.

(51) Cabrera, K.; Lubda, D.; Eggenweiler, H. M.; Minakuchi, H.; Nakanishi, K., *J. High. Resolut. Chromatogr.* **2000**, *23*, 93-99.

(52) Hara, T.; Kobayashi, H.; Ikegami, T.; Nakanishi, K.; Tanaka, N., *Anal. Chem.* **2006**, *78*, 7632-7642.

(53) Sugrue, E.; Nesterenko, P.; Paull, B., *Analyst* **2003**, *128*, 417-420.

(54) Sugrue, E.; Nesterenko, P.; Paull, B., *J. Sep. Sci.* **2004**, *27*, 921-930.

(55) Sugrue, E.; Nesterenko, P. N.; Paull, B., *J. Chromatogr. A* **2005**, *1075*, 167-175.

(56) Glenn, K. M.; Lucy, C. A.; Haddad, P. R., *J. Chromatogr. A* **2007**, *1155*, 8-14.

(57) Connolly, D.; Paull, B., *J. Chromatogr. A* **2002**, *953*, 299-303.

(58) Conder, J. R.; Young, C. L., *Physicochemical Measurement by Gas Chromatography*, John Wiley & Sons, Toronto, 1979.

(59) Connolly, D.; Paull, B., *Anal. Chim. Acta* **2001**, *441*, 53-62.

(60) Connolly, D.; Paull, B., *J. Chromatogr. A* **2001**, *917*, 353-359.

(61) Connolly, D.; Paull, B., *Anal. Chim. Acta.* **2001**, *441*, 53-62.

(62) Connolly, D.; Victory, D.; Paull, B., *J. Sep. Sci.* **2004**, *27*, 912-920.

(63) Li, J.; Zhu, Y.; Guo, Y. Y., *J. Chromatogr. A* **2006**, *1118*, 46-50.

(64) Riordain, C. O.; Barron, L.; Nesterenko, E.; Nesterenko, P. N.; Paull, B., *J. Chromatogr. A* **2006**, *1109*, 111-119.

(65) Xu, Q.; Mori, M.; Tanaka, K.; Ikedo, M.; Hu, W. Z.; Haddad, P. R., *J. Chromatogr. A* **2004**, *1041*, 95-99.

(66) Ito, K.; Takayama, Y.; Makabe, N.; Mitsui, R.; Hirokawa, T., *J. Chromatogr. A* **2005**, *1083*, 63-67.

(67) Xu, Q.; Tanaka, K.; Mori, M.; Helaleh, M. I. H.; Hu, W. Z.; Hasebe, K.; Toada, H., *J. Chromatogr. A* **2003**, *997*, 183-190.

(68) Riordain, C. O.; Nesterenko, P.; Paull, B., *J. Chromatogr. A* **2005**, *1070*, 71-78.

(69) Hu, W.; Haddad, P. R.; Cook, H.; Yamamoto, H.; Hasebe, K.; Tanaka, K.; Fritz, J. S., *J. Chromatogr. A* **2001**, *920*, 95-100.

(70) Hu, W. Z.; Yang, P. J.; Hasebe, K.; Haddad, P. R.; Tanaka, K., *J. Chromatogr. A* **2002**, *956*, 103-107.

(71) Paull, B.; Victory, D., *International Ion Chromatography Symposium, Trier, Germany* **2004**.

(72) Pelletier, S., Ph.D., Ph.D. Thesis, Department of Chemistry, University of Alberta, 2006.

(73) Riordain, C. O.; Nesterenko, P.; Paull, B., *Journal of Chromatography A* **2005**, *1070*, 71-78.

(74) Fritz, J. S.; Yan, Z.; Haddad, P. R., *Journal of Chromatography A* **2003**, *997*, 21-31.

(75) Yan, Z.; Haddad, P. R.; Fritz, J. S., *Journal of Chromatography A* **2003**, *985*, 359-365.

(76) Xu, Q.; Mori, M.; Tanaka, K.; Ikedo, M.; Hu, W. Z.; Haddad, P. R., *Journal of Chromatography A* **2004**, *1041*, 95-99.

(77) Fritz, J. S.; Yan, Z.; Haddad, P. R., *J. Chromatogr. A* **2003**, *997*, 21-31.

(78) Yan, Z.; Haddad, P. R.; Fritz, J. S., *J. Chromatogr. A* **2003**, *985*, 359-365.

(79) Li, J.; Wu, G. F.; Zhu, Y., *J. Chromatogr. A* **2006**, *1118*, 151-154.

(80) Paull, B.; Riordain, C. O.; Nesterenko, P. N., *Chem. Commun.* **2005**, 215-217.

(81) Hu, W. Z.; Hasebe, K.; Tanaka, K.; Inoue, S.; Nagai, M., *Analyst* **2000**, *125*, 2160-2162.

(82) Hu, W. Z.; Hasebe, K.; Iles, A.; Tanaka, K., *Analyst* **2001**, *126*, 821-824.

(83) Xu, Q.; Mori, M.; Tanaka, K.; Ikedo, M.; Hu, W. Z., *J. Chromatogr. A* **2004**, *1026*, 191-194.

(84) Gillespie, E.; Macka, M.; Connolly, D.; Paull, B., *Analyst* **2006**, *131*, 886-888.

(85) Barron, L.; Nesterenko, P. N.; Diamond, D.; O'Toole, M.; Lau, K. T.; Paull, B., *Anal. Chim. Acta* **2006**, *577*, 32-37.

(86) Connolly, D.; Victory, D.; Paull, B., *Journal of Separation Science* **2004**, *27*, 912-920.

(87) Nesterenko, P. N., *HRC J. High Resolut. Chromatogr.* **1991**, *14*, 767-768.

(88) Nesterenko, P. N., *J. Chromatogr.* **1992**, *605*, 199-204.

(89) Nesterenko, P. N.; Haddad, P. R., *Anal. Sci.* **2000**, *16*, 565-574.

(90) Elefterov, A. I.; Nesterenko, P. N.; Shpigun, O. A., *J. Anal. Chem.* **1996**, *51*, 972-975.

(91) Sugrue, W.; Nesterenko, P. N.; Paull, B., *J. Chromatogr. A* **2005**, *1075*, 167-175.

(92) Breadmore, M. C.; Macka, M.; Avdalovic, N.; Haddad, P. R., *Analyst* **2000**, *125*, 1235-1241.

(93) Hutchinson, J. P.; Hilder, E. F.; Macka, M.; Avdalovic, N.; Haddad, P. R., *J. Chromatogr. A* **2006**, *1109*, 10-18.

CHAPTER TWO: Latex-coated silica monoliths for ion chromatography *

2.1 Introduction

Monolithic stationary phases have experienced a significant growth in research interest since the introduction of the first commercially available monolithic column in 2000.[1-3] The advantages of monolithic columns over particulate columns have been discussed in detail in Section 1.9.1. The bimodal porous structure of monolithic columns, consisting of small pores within an interconnected skeleton surrounded by larger through-pores, allows for higher solvent flow with lower back-pressure than traditional particulate columns.[4-6] Silica monolithic columns have been shown to be equivalent to 3 μm particulate columns in terms of efficiency and to 7-15 μm particles with respect to permeability.[7-9] For these reasons, new possibilities in many modes of liquid chromatography have emerged, including ion chromatography.[5] A review has recently been released on the current developments in ion chromatography and capillary electrochromatography on monolithic columns.[10] Chambers et al. have also written an extensive review on the use of monoliths in ion chromatography.[11]

Reversed-phase silica columns, whether particulate or monolithic, can be converted into ion-exchange materials through the use of surfactant coatings, as described in Section 1.10.1. Connolly and Paull[12] showed that a particulate silica reversed-phase column could be permanently coated with a double-chained cationic surfactant, didodecyldimethylammonium bromide (DDAB, Table 1.1). Hatsis and

---

* A version of this chapter has been published. K.M. Glenn, C.A. Lucy and P.R. Haddad, *Journal of Chromatography A* 1155 (2007) 8-14.

Lucy later showed that monolithic columns permanently coated with DDAB could separate seven inorganic ions in just 30 s using flow-rates up to 10 mL/min.[13] More recently, Pelletier and Lucy used lower flow-rates to separate inorganic ions on short (0.5-1 cm) monolithic columns coated with DDAB.[14] In fact, the back-pressure in this method was so low that the system could be pumped with a glass syringe. Paull and co-workers also investigated the use of short (1.0 x 0.4 cm) DDAB-coated silica monolith columns for ion chromatography, employing low-pressure micro-scale peristaltic pumps.[15]

However, the DDAB coatings have been found to leach gradually from the column, necessitating a periodic recoating of the column to avoid drift in retention times. The repeated removal and application of DDAB coatings leads to pressure build-up and reproducibility problems, possibly due to precipitation of DDAB in the column.[16] A stable ion-exchange stationary phase can be produced by coating a cationic latex onto a solid support. The agglomerated ion exchange columns of Dionex Corporation are an example of columns produced in this manner (see Section 1.9.2).[17] Recently, polymeric monolithic ion exchange phases have been reported based on the adsorption of latexes onto a polystyrene-divinyl benzene monolith.[18] Latex-coated monolithic polymeric stationary phases have been used for anion-exchange capillary electrochromatography and on-line sample preconcentration in capillary electrophoresis.[19-21] Also, Zakaria et al.[22] have reported capillary ion chromatography on latex-coated polymeric monoliths using hydroxide eluents. These polymer monolithic phases were prepared *in situ* within fused-silica capillaries, and ion-exchange sites were introduced by coating with cationic latex particles. Polymeric

monoliths are pH stable and are therefore compatible with strong eluents such as hydroxide or carbonate/ bicarbonate. However, to date, these latex-coated polymer monoliths have exhibited limited ion-exchange capacity and only modest separation efficiencies.[18] The low ion-exchange capacity is due to the limited amount of functional monomer that can be incorporated into the polymerization mixture. This leads to limited anionic charge on the monolith surface, which restricts the amount of cationic latex that can adhere to the surface.[18]

As an alternative, silica monoliths can be modified with latex coatings, with the cationic latex nanoparticles adhering electrostatically to the negatively charged silanol groups at the surface. Open-tubular fused silica capillaries have been coated with quaternary ammonium functionalized latex for use in capillary electrochromatography (CEC) and preconcentration techniques.[23-25] Monolithic silica capillaries have also been coated with latex for use in CEC,[26] with the advantage of higher ion-exchange capacities than the open-tubular columns. Silica monoliths are well suited for the separation of small molecules, due to their high surface area (~ 300 m^2/g) and mesoporous structure.[27] This study explores the use of latex-coated silica monolith columns for ion chromatography. Silica monoliths are coated with either functionalized latex nanoparticles or with DDAB to convert the columns into anion-exchangers (Figure 2.1), with direct comparisons then being made between the two coatings in terms of selectivity, efficiency and stability.

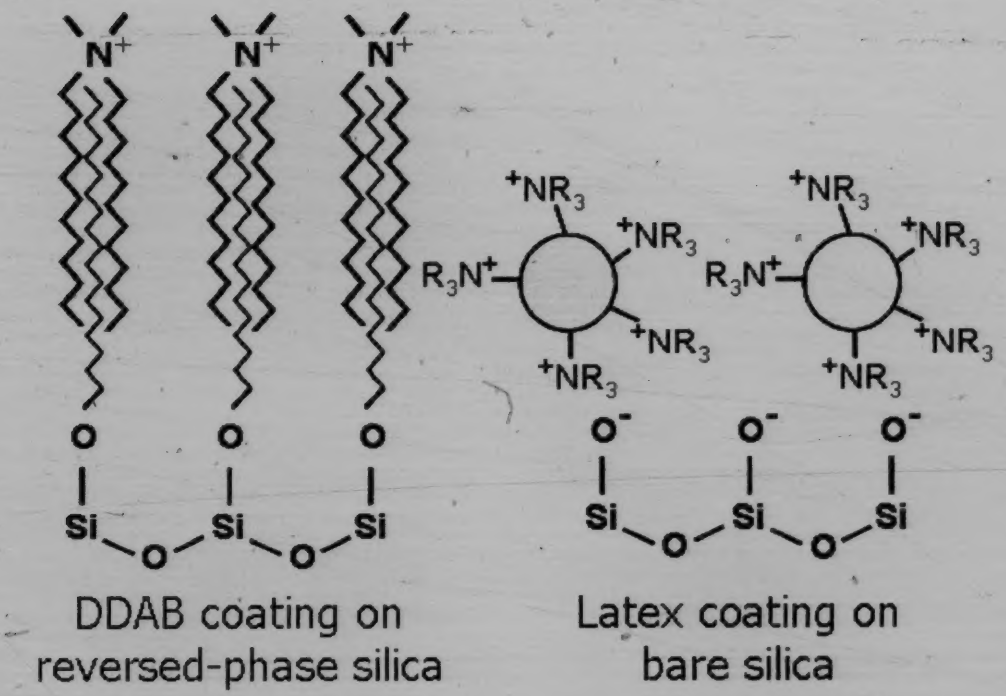

Figure 2.1. Schematic diagram of a DDAB surfactant coating on reversed-phase silica and a latex coating on bare silica.

2.2 Experimental

2.2.1 Apparatus

A model 625 LC Waters (Milford, MA, USA) HPLC pump was used in this study. A 0.5 μm stainless steel frit (Upchurch, Oak Harbor, WA, USA) or a Chromolith (Merck KGaA, Darmstadt, Germany) guard cartridge (5.0 x 4.6 mm ID) with cartridge holder was positioned before a Rheodyne (Berkeley, CA, USA) injection valve (model 9125) fitted with a 20 μL loop. Chromolith Performance monolithic silica 100 mm x 4.6 mm I.D. columns (Merck) were used. Chromolith columns are composed of high-purity silica and have macropores of 2 μm and mesopores of 13 nm. A RP-18e silica monolithic column was coated with didodecyldimethylammonium bromide (DDAB), and a bare silica monolithic column was coated with Dionex AS9-SC latex. For comparison purposes, an IonPac AS9-SC column (250 mm x 4.0 mm I.D., 13.0 μm polymer particles) from Dionex Corporation (Sunnyvale, CA, USA) was also used. Analyte ions were detected using suppressed conductivity detection using a Dionex Anion Atlas Electrolytic Suppressor (AAES) in the external water mode using a regenerant flow rate of ~2 mL/min. The suppressor was removed when coating and uncoating the columns with DDAB. For detection, a Dionex ED-50A electrochemical detector and a DS3 Detection Stabilizer (Dionex, model DS3-1) were used. A 10 cm length of 0.005" I.D. PEEK tubing (Upchurch) connected the column or suppressor directly to the cell, which was within the DS3 stabilizer. The volume of the conductivity cell was 1 μL,

the rise time was 0.05 s and data was collected with Dionex PeakNet 5.2 software at 20 Hz. See Figure 2.2 for a schematic of the instrument set-up.

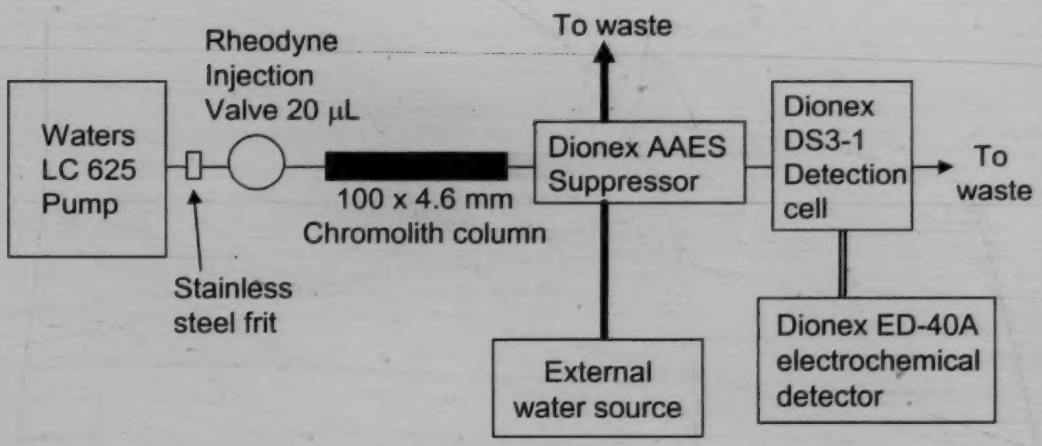

Figure 2.2. Schematic of instrument set-up.

For determination of the ion-exchange capacity of the columns, a Waters model 501 HPLC pump was used, along with a Rheodyne injection valve (model 7125) fitted with a 500 μL injection loop. UV absorbance detection was employed (Waters Lambda-Max Model 481 LC Spectrophotometer). Data were collected using StampPlot Pro V3 Release 2 (Selmaware Solutions) at 20 Hz.

All pH measurements were made with a Corning 445 pH-meter (Corning, New York, NY, USA) with a Corning electrode (3 in 1 combo P/N 476436).

2.2.2 Reagents and Solution Preparation

All solutions were prepared in deionised 18 MΩ water (Nanopure Water System, Barnstead, Chicago, IL, USA) that had been filtered through 0.22 μm Magna nylon membrane filters (GE Osmonic, Trevose, PA, USA). Chemicals were reagent grade or better. The sodium salts of chloride (EMD Chemicals, Gibbstown, NJ, USA), nitrite (BDH, Toronto, Canada), nitrate (ACP Chemicals, Montreal, Canada), sulfate (BDH) and phosphate ($NaH_2PO_4 \cdot H_2O$, EMD) were used. Potassium salts of bromide (Fisher, Fair Lawn, NJ, USA), iodate (ACP Chemicals), iodide (BDH) and perchlorate (Fisher) were used.

The eluents were prepared by dissolving the appropriate amount of 4-hydroxybenzoic acid (99%, Aldrich, St. Louis, MI, USA) in water, adjusting the pH with a 2.5 M solution of sodium hydroxide (Fisher) and diluting to volume with water.

The DDAB coating solutions used were 1 mM DDAB in 30.0% to 35.0% v/v acetonitrile (ACN, HPLC grade, Fisher). To prepare the solutions, the appropriate

amount of DDAB was added to a plastic volumetric flask and dissolved in water by sonicating for 30 minutes with a Bransonic 220 sonicator (Sigma). Acetonitrile was added via pipette, and the solution was diluted to volume with water.

2.2.3 Coating and removing DDAB from the column

The Chromolith RP-18e columns were coated using the procedure of Hatsis and Lucy.[13] Briefly, the column was equilibrated with X% ACN / (100-X)% water (see Table 2.1 for the %ACN used) and then flushed with 1 mM DDAB in X% ACN / (100-X)% water at 2 mL/min until DDAB breakthrough was observed (indicated by a rapid increase in conductivity, Figure 2.3). The column was flushed with water for at least 20 min at 1 mL/min to remove any unbound DDAB. The suppressor was reattached and then the coated column was equilibrated with the eluent at 1 mL/min until the conductivity stabilized (about 20 min). The ion-exchange capacity of the coated columns was estimated from the DDAB breakthrough time using equation 1.16. As shown in Table 2.1 the ion-exchange capacity of the column can be varied by adjusting the ACN content in the coating solution.[13]

Although DDAB coatings were stable up to 3 weeks,[14] our columns were typically uncoated and recoated after 3-5 days of use to maintain reproducibility. To remove the DDAB coating, the column was first flushed with 1 mM KBr to return the DDA^+ to its bromide form to prevent precipitation of $DDA^+(eluent^-)$ on the column [28]. The column was then flushed with water at 1 mL/min to remove unretained bromide, before changing the mobile phase to aqueous ACN. The % ACN in the mobile phase was gradually increased to 50% over a period of 1 min and held at 50% for 7 minutes

to remove the DDAB. The % ACN was then gradually reduced to the % ACN to be used for the next coating. The coating and uncoating process is outlined in Figure 1.12.

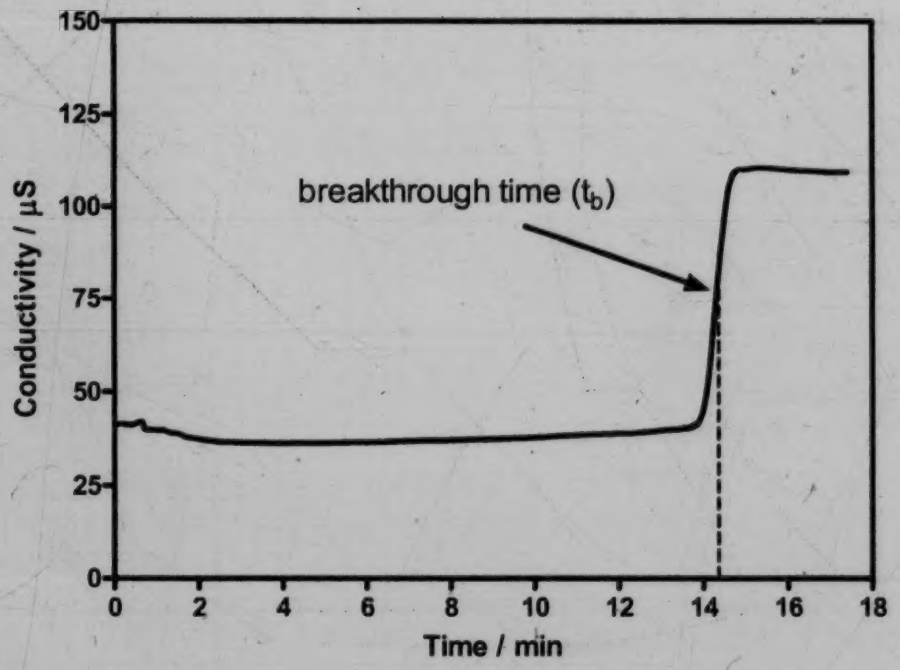

Figure 2.3. Surfactant breakthrough curve. Conditions: 100 x 4.6 mm RP-18e silica monolith, 1 mM DDAB in 35% ACN, 2 mL/min, non-suppressed conductivity detection.

2.2.4 Latex coating

Dionex AS9-SC latex particles are 110 nm in diameter and are composed of a polyacrylate backbone (20% cross-linked) and functionalized with alkyl quaternary ammonium groups. The latex coating was applied based on the procedure described by Hutchinson et al.[26] A Chromolith Performance monolithic silica 100 mm x 4.6 mm I.D. column was pre-rinsed with 0.01 M HCl (filtered through 0.45 μm nylon) for 20 min at 2 mL/min. A coating solution was prepared by dialyzing a suspension of Dionex AS9-SC latex using 30 cm of cellulose membrane dialysis tubing (Sigma D-9652) which had been soaked in deionized water prior to use. Dialysis removes fine particulates in the suspension which could clog the column or other system components during coating. The dialyzed latex suspension was diluted ten-fold in 0.01 M HCl. The resulting solution was rinsed through the column at 2 mL/min until breakthrough was observed (5 min), then flushed for an additional 5 min at 0.5 mL/min. The column was then rinsed with deionized water (2 mL/min for 15 min) to remove any interstitial latex.

2.2.5 Determination of ion-exchange capacity

The ion-exchange capacities (in μeq/column) of both the DDAB-coated and latex-coated monolithic columns were determined using a bromide adsorption/desorption method.[18,21] The term μeq is a measure of the amount of charge adsorbed onto the column (i.e., the concentration of surfactant adsorbed to the column, multiplied by the charge of the surfactant). The columns were flushed at 2

mL/min with a 20 mM KBr solution until all ion-exchange sites were saturated with bromide. Interstitial bromide was then removed by flushing the column with water. The bound bromide was eluted with 100 mM $KClO_4$ at 1 mL/min and monitored using direct UV absorbance detection at 230 nm. Detection by UV absorbance was used as opposed to conductivity detection because both Br^- and ClO_4^- are conductive, whereas only Br^- will absorb in the UV region. The bromide peak area was compared to a calibration curve (Figure 2.4) constructed by replacing the column with a union and injecting varying concentrations of KBr into the system. Peak areas were calculated using Microsoft Excel 97 software (Microsoft Corporation, Seattle, WA). The data were fit with a second-order polynomial using GraphPad Prism 4.00 (GraphPad Software Inc., San Diego, CA).

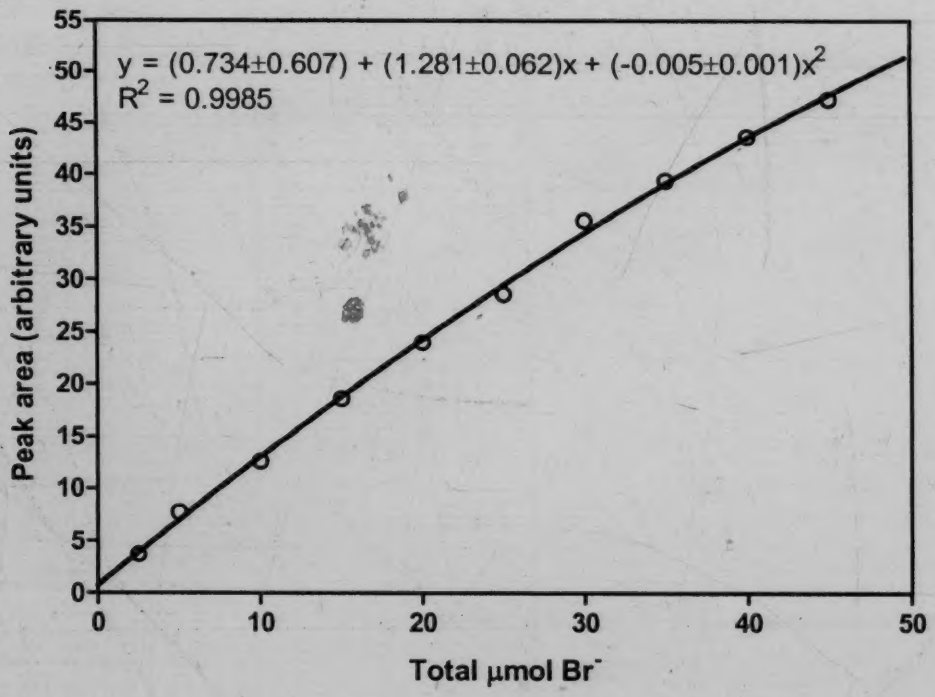

Figure 2.4. Calibration curve for bromide adsorption/desorption method. Conditions: 500 µL of KBr solutions (varying in concentration) were injected into the detector (column was replaced by a union). UV detection at 230 nm.

2.2.6 Stability Tests

To determine coating stability, the columns were continuously flushed at 1 mL/min with 5.0 mM 4-hydroxybenzoic acid (4-hba) pH 7.0 and a solution containing 0.050 mM of seven common anions was injected every hour. Retention times and retention factors of the ions were monitored.

2.2.7 Calculations

Since our peaks were slightly tailed (giving a peak asymmetry [A_S = B/A, see below] value of ~ 1.1), the exponentially modified Gaussian (EMG) peak model (equation 1.5)[29] was used to calculate efficiency (N). This method does not overestimate the plate count for tailed peaks like some of the more common methods (tangent or half peak height).[30]

2.3 Results and Discussion

Silica monolith stationary phases were chosen for this study due to their higher chromatographic efficiency in comparison to polymeric phases (Section 1.9.3).[17] Weak acid eluents must be used with silica-based columns to prevent the dissolution of silica at high pH values (Section 1.8). Cyanophenols and 4-hydroxybenzoic acid (4-hba) have been shown to be good alternatives for silica stationary phases and suppressed conductivity detection.[13-15] In this study, 4-hydroxybenzoic acid eluent was chosen, since it has previously been found to be a more effective eluent than cyanophenols in terms of resolution and separation time.[14]

The eluent 4-hba can be used with suppressed or non-suppressed conductivity; however, a reduction in background conductivity from 350 to 122 μS was observed upon suppressing 5.0 mM 4-hba (pH 7.0). All eluents used in this study were kept at pH 7.0 to prevent the degradation of silica.

It is important to note, in the case of the latex-coated monolith, that the ion-exchange sites are located only in the larger macropores (or transport pores, 2 μm diameter) of the monolithic structure. The latex particles (110 nm in diameter) cannot fit into the small mesopores, which are only 13 nm in diameter. Thus, a large portion of the surface area of the monolith is unusable for anion-exchange.

2.3.1 Selectivity and Optimization

Before efficiency and selectivity could be compared, the retention properties of the two columns had to be matched by adjusting the eluent concentration and column capacity. From the bromide adsorption/desorption method, the capacity of the latex column was 41 ± 4 μeq/column. As will be discussed in Section 2.3.3, the latex coating was found to be irreversible. Thus, it was not possible to alter the capacity of the latex-coated column after the column has been coated. Therefore, the capacity of the DDAB-coated column was altered by adjusting the % ACN in the coating solution, in order to ensure that the latex-coated and DDAB-coated columns were of similar capacity. Table 2.1 gives the column capacities as a function of acetonitrile content in the coating solution. To closely match the latex-coated column capacity, a DDAB coating solution containing 33% ACN was chosen, yielding a capacity of 44 μeq/column (according to the DDAB breakthrough time). When this same DDAB

coating was assessed using the bromide adsorption/desorption method, a capacity of 48 μeq/column was obtained. Previously, Hatsis and Lucy coated an analogous 5 cm silica monolith with DDAB and reported the column capacity as a function of % ACN in the coating solution [13]. Extrapolating their data to 33% ACN gives an approximate value of 24 μeq/column (or ~48 μeq/column for a 10 cm column). This value is comparable to the 46 ± 2 μeq found on our 10 cm column.

Table 2.1. Capacity of DDAB-coated column as a function of ACN content in the coating solution.

%ACN	Capacity (μeq/column)
33.0	44
35.0	36
36.0	32

Conditions: 1 mM DDAB (%ACN varied) at 2 mL/min until breakthrough occurred. Ion-exchange capacity calculated using equation 1.16. Standard error of capacity measurements by surfactant breakthrough method is about 2-3%.

As for eluent concentration, 5.0 mM 4-hba was chosen for the DDAB-coated column, as it was the highest concentration that did not cause ions in the test mixture to be co-eluted. This concentration of 4-hba has previously been used in our group to obtain efficient separations on DDAB-coated columns.[28] To closely match the retention observed on the DDAB column with this eluent, a concentration of 7.5 mM 4-hba was chosen for the latex-coated column. All eluents were adjusted to pH 7.0.

Separations of 8 common anions using these eluents are shown in Figure 2.5 and the k values for each column are listed in Table 2.2. The fluoride peak is lost in the water dip on the latex-coated column, which is a common problem with this highly hydrated ion. A sample containing iodate was injected onto the latex-coated column as well, but this ion also could not be distinguished from the water dip. Fluoride and iodate did, in fact, elute from the column (with retention times of 1.73 and 1.70 min, respectively), as determined by injecting a sample of each ion made up in the eluent to eliminate the water dip (which spanned from 1.68 to 1.83 min). In contrast, separations using 4-hba eluent on a polymer-based anion-exchange material, composed of polystyrene/divinylbenzene particles surface-aminated with trimethyl amine, showed a fluoride peak well resolved from the water dip.[31] It is unknown why the fluoride peak could not be resolved from the water dip on our latex-coated column, especially since resolution was achieved on the DDAB-coated column. More confusingly, AS9-SC latex provides resolution of F^- from the water dip with Dionex columns (IonPac AS9-SC column) when a carbonate/ bicarbonate eluent is used[17] and when 4-hba eluent is used, as shown in our own experiments (Table 2.2).

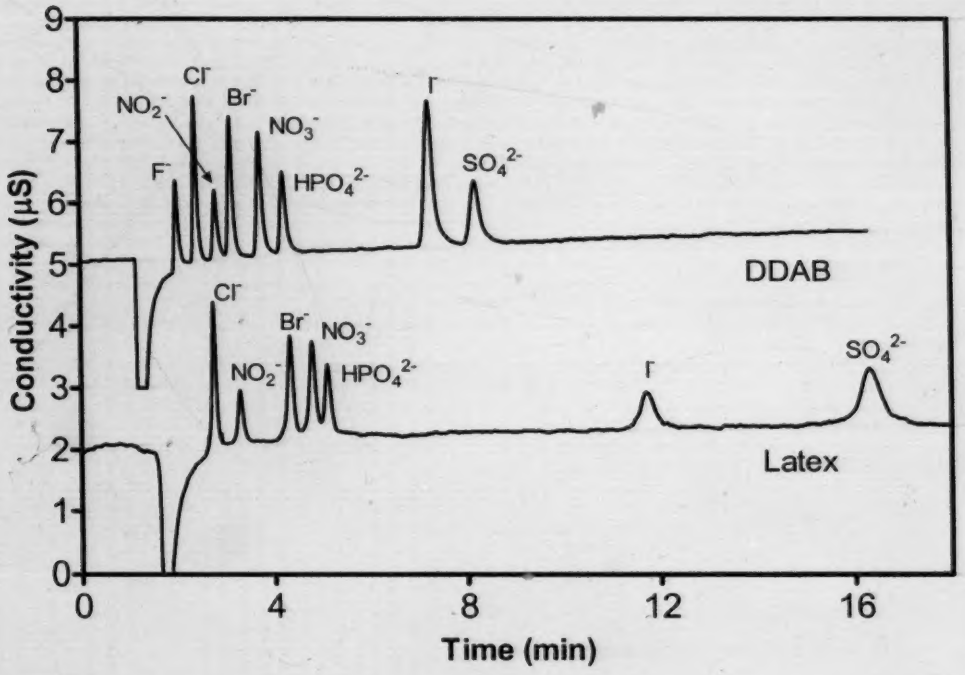

Figure 2.5. Anion separation on 100 x 4.6 mm monolithic columns. Conditions: 0.050 mM analyte ions, 20 µL injection volume, 1.00 mL/min flow rate, 5.0 mM (DDAB column) and 7.5 mM (Latex column) 4-hydroxybenzoic acid pH 7.0, suppressed conductivity detection at 17 mA (DDAB column) and 26 mA (Latex column).

Table 2.2. Comparison of k of 8 anions on latex and DDAB-coated silica monoliths.

Peak	Retention factor, k (DDAB-coated column, 5.0 mM 4-hba)	Retention factor, k (Latex-coated column, 7.5 mM 4-hba)	Retention factor, k (IonPac AS9-SC column, 2.0 mM 4-hba)
F^-	0.49	<0.01	0.21
Cl^-	0.79	0.51	0.68
NO_2^-	1.11	0.80	0.90
Br^-	1.35	1.37	1.34
NO_3^-	1.80	1.62	1.52
HPO_4^{2-}	2.16*	1.80*	2.99*
I^-	4.44	5.43	4.37
SO_4^{2-}	5.17*	7.95*	11.13*

*Direct comparison between divalent anions is not possible due to the differing ionic strength of the eluents used.

Conditions: 0.050 mM all 8 ions, 20 µL injection volume, 1.00 mL/min flow rate, 2.0-7.5 mM 4-hydroxybenzoic acid pH 7.0, suppressed conductivity detection at 10-26 mA.

Additional experiments with an IonPac AS9-SC column and a 4-hba eluent were carried out to compare its selectivity to the latex-coated monolith. Due to the lower capacity of the IonPac column (30-35 μeq/column) in comparison to the latex-coated monolith (45 μeq/column), a lower concentration of 2.0 mM 4-hba (pH 7.0) separated the mixture of 8 anions (k values are listed along with the DDAB and latex-coated columns in Table 2.2). The same order of elution is shown for monovalent anions for the latex-coated monolith and the IonPac column, but because divalent anions are more affected by changes in eluent concentration (see Section 1.7.1), a direct comparison between sulfate and phosphate ions is not possible. The more hydrophilic singly-charged ions (F^-, Cl^-, NO_2^-) show less retention on the latex-coated silica than on the IonPac, while the more hydrophobic ions (NO_3^-, I^-) show more retention. This results in the peaks of the singly-charged ions being more resolved on the latex-coated silica column than on the IonPac. The reason behind such a change in selectivity is unknown, but the differing underlying matrices (silica monolith vs. polymeric particles) must be a factor.

It is interesting to note that the latex-coated column had a greater void volume than the DDAB-coated column, as indicated by the positions of the water dips in Figure 2.5. Void volumes were found to be 1.27 mL and 1.76 mL for the DDAB-coated and latex-coated columns, respectively. Both columns have the same physical dimensions (100 x 4.6 mm), but with different chemistries. The latex was coated onto a bare silica monolith, while the DDAB was coated onto a C_{18} reversed-phase silica monolith. The extra space occupied by the C_{18} chains could account for the smaller void volume of the DDAB-coated column. Gritti and Guiochon[32]

investigated void volume as a function of the amount of bonded C_{18} on silica stationary phases. Their results show that the void volume gradually decreases with increasing amount of carbon bonded onto the silica particles. The magnitude by which the void volumes changed between 0% carbon content (i.e. bare silica) and 18% carbon content on a 150 x 4.6 mm silica column in Gritti and Guiochon's study agree well with the difference in magnitude found here. They found a void volume of ~1.95 mL and ~1.50 mL for 0% and 18% carbon content, respectively (interpolated from Figure 1a of reference[32]). The Chromolith RP-18e column used in our study has a carbon content of 18% and a void volume of 1.27 mL, while the bare silica column has a void volume of 1.76 mL. The void volume values found here differ from Gritti and Guiochon's findings due to the shorter length of column and the differences in stationary phase geometry (i.e., monolithic vs. particulate columns).

For comparison of selectivity, the same eluent used on the DDAB-coated column (5.0 mM 4-hba, pH 7.0) was used on the latex-coated column. The resulting separation is shown in Figure 2.6 along with the optimized separation on the DDAB-coated column. On the latex-coated column, the highly-retained sulfate ion takes almost 30 min to be eluted, but the iodate peak is still overwhelmed by the water dip.

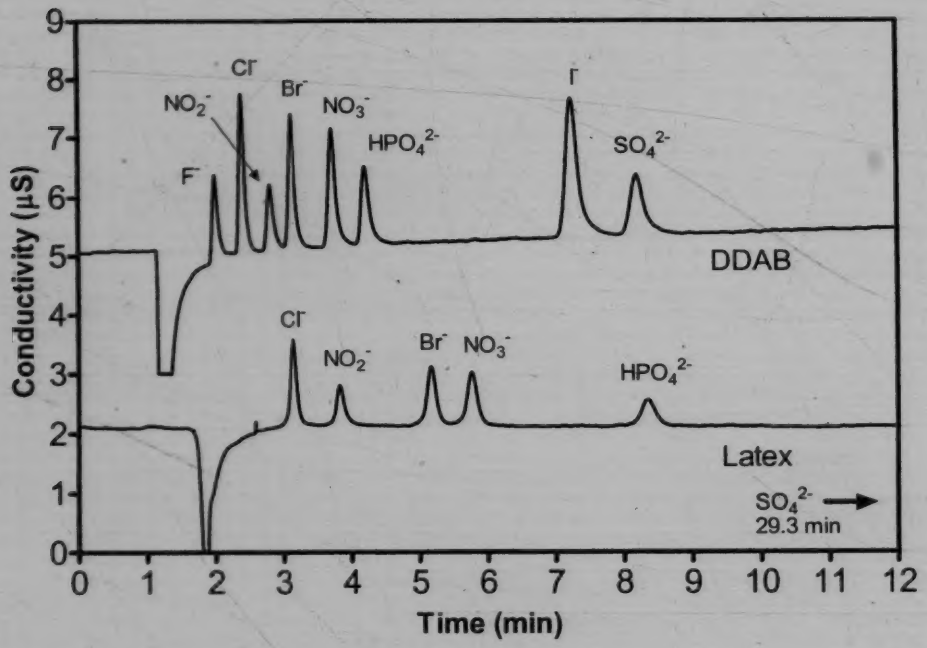

Figure 2.6. Separation of 7 anions on DDAB-coated and latex-coated 100 x 4.6 mm monolithic columns. Conditions: 5.0 mM 4-hydroxybenzoic acid pH 7.0 at 1.00 mL/min, 0.050 mM analyte ions, 20 µL injection volume, suppressed conductivity at 17 mA. Fluoride peak is in the water dip on latex-coated column's chromatogram.

2.3.2 Efficiency

Figure 2.7 shows the van Deemter plots obtained for the DDAB-coated and latex-coated columns, with 5.0 mM and 7.5 mM 4-hba as the eluent, respectively. Under these conditions bromide exhibited similar retention on both columns. Peak efficiencies were calculated using equation 2.2 since the bromide peaks were slightly tailed (A_S~1.1 on latex column and A_S~1.7 on DDAB column). Although the monolithic construction of the stationary phase allows for the use of high flow-rates, flow-rates more than 2 mL/min could not be utilized due to the limitations of the suppressor.

The plate height values obtained in this study were nearly double that of the previous work of Hatsis and Lucy on a 50 x 4.6 mm DDAB-coated silica monolithic column.[13] The different values could be due to the different suppressors used in the studies. Extra dead-volume in the suppressor, detector cell, connecting tubing, injector, etc. can contribute to the overall variance of the peak.[33] However, the suppressors used in both studies have about the same void volume (~35 μL). The suppressor used in this study was a membrane suppressor whereas Hatsis et al. used a packed-bed suppressor, but it is unclear if the difference in the type of suppressor would contribute to band broadening. Nonetheless, data was collected under the same conditions for the two columns used in this particular study, so any differences in efficiencies between the two columns could therefore be attributed to the columns themselves. Figure 2.7 clearly shows that the latex-coated column was more efficient over the range of flow-rates studied. The IonPac column showed poorer efficiency than both the DDAB and latex-coated monoliths (81 μm plate height for

Br^- at 1 mL/min), which is not surprising because of its large polymeric particles (13 μm).

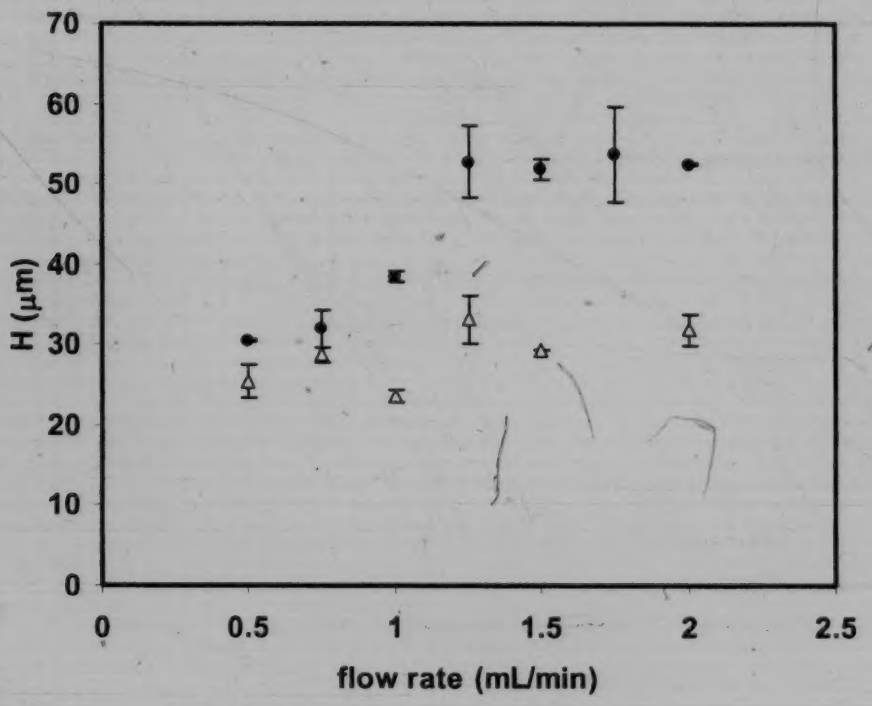

Figure 2.7. van Deemter plots for DDAB-coated (•) and latex-coated (Δ) monolithic columns. Efficiencies of bromide peaks calculated using the Foley-Dorsey equation (equation 1.5). conditions: 0.050 mM all 8 ions, 20 μL injection volume, 1.00 mL/min flow rate, 5.0 mM (DDAB column) and 7.5 mM (latex column) 4-hydroxybenzoic acid pH 7.0, suppressed conductivity detection at 17 mA (DDAB column) and 26 mA (latex column).

2.3.3 Stability

As mentioned earlier, one drawback of DDAB-coated columns was that the surfactant gradually leached from the column, causing a drift in retention times of the analytes as the ion-exchange capacity of the column was diminished progressively. Previously, a 7% decrease in retention times was observed after pumping 2900 column volumes (~8 h at 1 mL/min) of 8 mM 4-cyanophenol pH 7.3 through a 1 cm DDAB-coated silica monolith.[14] The most significant change in retention times was seen with the later eluted ions. For this reason, the retention time of sulfate was monitored as a function of time on the DDAB-coated column used in this study. To enable direct comparison, the same concentration of eluent (5.0 mM 4-hba) was used also on the latex column, but the retention of nitrate was monitored on this column as it showed similar retention to sulfate on the DDAB-coated column. The retention data for nitrate on the DDAB-coated column was also included for comparison. Figure 2.8 shows the k values of sulfate and nitrate on the DDAB-coated and latex-coated columns, respectively, as 5.0 mM 4-hba was flushed continuously through the column.

As expected, Figure 2.8 indicates that the electrostatically bound latex coating was more stable than the DDAB coating, which adheres to the stationary phase simply through hydrophobic interactions with the C_{18} chains on the silica monolith. The DDAB-coated column showed a 10% decrease in k for sulfate and nitrate after just 11 h of continuous use at 1 mL/min, which is in excellent agreement with previous findings in our group.[14] In contrast, retention changed by < 1% over 12.5 h of flushing on the latex-coated column. Even after 2.5 months of periodic use, the

retention of nitrate had not changed by more than 1%. The stability of the DDAB-coating could be improved by placing a DDAB-coated pre-column prior to the injector, as surfactant leaching from this column replaces any lost from the analytical column. Previous work[14] showed nearly a 15-fold improvement in the stability of the coating when a pre-column was used.

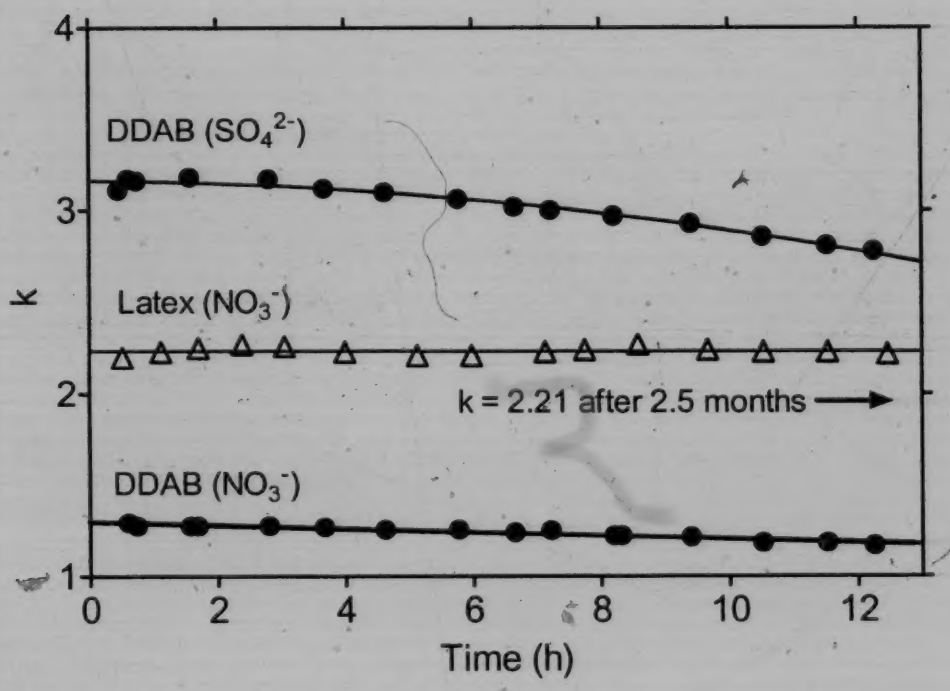

Figure 2.8. Retention factor as a function of time: stability of latex coating and DDAB coating. Conditions: 5.0 mM 4-hydroxybenzoic acid, pH 7.0, at 1.00 mL/min. Suppressed conductivity detection at 17 mA, 0.050 mM analyte ions, 20 μL injection volume. Parentheses indicate the analyte ions monitored.

2.4 Conclusions

Comparisons in selectivity, efficiency and stability were made between a monolithic silica RP-18e column coated with DDAB and a monolithic silica column coated with functionalized latex nanoparticles. Both columns, because they are silica based, lack pH stability. The DDAB coating exhibited the favourable qualities that it was dynamic and its ion-exchange capacity could be modified to suit the separation, while the latex coating was permanent and its ion-exchange capacity could not be adjusted once the coating had been applied. On the other hand, latex did not leach from the column and cause drift in retention times, in contrast to the DDAB-coating which must be periodically removed and reapplied (a time consuming task and one poorly suited to routine analysis). The results presented in this paper show that the latex-coated column demonstrated superior efficiency and stability to the DDAB column. However, the latex-coated column could not resolve fluoride or iodate from the water dip, even when eluent concentration was lowered to the point where sulfate took over 30 min to be eluted. Nonetheless, latex-coated silica shows considerable potential as a new anion-exchange material for ion chromatography.

2.5 References

(1) Cabrera, K.; Lubda, D.; Eggenweiler, H. M.; Minakuchi, H.; Nakanishi, K., *J. High. Resolut. Chromatogr.* **2000**, *23*, 93-99.

(2) Rabel, F.; Cabrera, K.; Lubda, D., *Am. Lab.* **2000**, *32*, 20.

(3) Cabrera, K., *J. Sep. Sci.* **2004**, *27*, 843.

(4) Tanaka, N.; Kobayashi, H.; Nakanishi, K.; Minakuchi, H.; Ishizuka, N., *Anal. Chem.* **2001**, *73*, 420A-429A.

(5) Paull, B.; Nesterenko, P. N., *TRAC* **2005**, *24*, 295-303.

(6) Miyabe, K.; Guiochon, G., *J. Sep. Sci.* **2004**, *27*, 853-873.

(7) Leinweber, F. C.; Lubda, D.; Cabrera, K.; Tallarek, U., *Anal. Chem.* **2002**, *74*, 2470-2477.

(8) Leinweber, F. C.; Tallarek, U., *J. Chromatogr. A* **2003**, *1006*, 207-228.

(9) Kobayashi, H.; Ikegami, T.; Kimura, H.; Hara, T.; Tokuda, D.; Tanaka, N., *Anal. Sci.* **2006**, *22*, 491-501.

(10) Schaller, D.; Hilder, E. F.; P.R.Haddad, *J. Sep. Sci.* **2006**, *29*, 1705-1719.

(11) Chambers, S. D.; Glenn, K. M.; Lucy, C. A., *J. Sep. Sci.* **2007**, *30*, 1628-1645.

(12) Connolly, D.; Paull, B., *J. Chromatogr. A* **2002**, *953*, 299-303.

(13) Hatsis, P.; Lucy, C. A., *Anal. Chem.* **2003**, *75*, 995-1001.

(14) Pelletier, S.; Lucy, C. A., *J. Chromatogr. A* **2006**, *1118*, 12-18.

(15) Victory, D.; Nesterenko, P.; Paull, B., *Analyst* **2004**, *129*, 700-701.

(16) Paull, B.; Victory, D., *International Ion Chromatography Symposium, Trier, Germany* **2004**.

(17) Weiss, J., *Handbook of Ion Chromatography*, 3rd edn., Wiley-VCH, Weinheim, 2004.

(18) Hutchinson, J. P.; Hilder, E. F.; Shellie, R. A.; Smith, J. A.; Haddad, P. R., *Analyst* **2006**, *131*, 215-221.

(19) Hilder, E. F.; Svec, F.; Frechet, J. M. J., *J. Chromatogr. A* **2004**, *1053*, 101-106.

(20) Hutchinson, J. P.; Macka, M.; Avdalovic, N.; Haddad, P. R., *J. Chromatogr. A* **2006**, *1106*, 43-51.

(21) Hutchinson, J. P.; Zakaria, P.; Bowie, A. R.; Macka, M.; Avdalovic, N.; Haddad, P. R., *Anal. Chem.* **2005**, *77*, 407-416.

(22) Zakaria, P.; Hutchinson, J. P.; Avdalovic, N.; Liu, Y.; Haddad, P. R., *Anal. Chem.* **2005**, *77*, 417-423.

(23) Breadmore, M. C.; Macka, M.; Avdalovic, N.; Haddad, P. R., *Analyst* **2000**, *125*, 1235-1241.

(24) Boyce, M. C.; Breadmore, M.; Macka, M.; Doble, P.; Haddad, P. R., *Electrophoresis* **2000**, *21*, 3073-3080.

(25) Breadmore, M. C.; Palmer, A. S.; Curran, M.; Macka, M.; Avdalovic, N.; Haddad, P. R., *Anal. Chem.* **2002**, *74*, 2112-2118.

(26) Hutchinson, J. P.; Hilder, E. F.; Macka, M.; Avdalovic, N.; Haddad, P. R., *J. Chromatogr. A* **2006**, *1109*, 10-18.

(27) Svec, F.; Geiser, L., *LCGC* **2006**, *24*, 22-27.

(28) Pelletier, S., Ph.D., Ph.D. Thesis, Department of Chemistry, University of Alberta, 2006.

(29) Foley, J. P.; Dorsey, J. G., *Anal. Chem.* **1983**, *55*, 730-737.

(30) Bidlingmeyer, B. A.; Warren, F. V., *Anal. Chem.* **1984**, *56*, 1583A-1596A.

(31) Samanidou, V. F.; Zacharis, C. K.; Papadoyannis, I. N., *J. Liq. Chromatogr. Relat. Technol.* **2002**, *25*, 803-818.

(32) Gritti, F.; Guiochon, G., *J. Chromatogr. A* **2006**, *1115*, 142-163.

(33) Miller, J. M., *Chromatography, Concepts and Contrasts*, 2 edn., Wiley Interscience, Hoboken, 2005.

CHAPTER THREE: Stability of Surfactant Coatings for Ion Chromatography

3.1 Introduction

Surfactant coatings have gained popularity in recent years as a means of converting reversed-phase columns into ion-exchangers.[1-6] The attractiveness of surfactant coatings arises from their semi-permanent nature, allowing different ion-exchange capacities and selectivities to be achieved simply by altering the coating conditions. Hatsis and Lucy [2] showed that by simply changing the percentage of acetonitrile in the coating solution, the ion-exchange capacity of the column could be varied. Different selectivities for anion separations have been introduced by using amphoteric surfactants instead of cationic surfactants,[7-9] or by applying a non-ionic surfactant coating before coating with a cationic surfactant.[4,10,11]

As indicated in Table 3.1, many research groups have used surfactants to coat silica-based reversed-phase columns for the purpose of ion-exchange. An extensive review by Chambers et al. outlines the use of monolithic columns in ion chromatography, along with various surfactant coatings and other modification methods.[12] However, there are contradictions about the stability of surfactant coatings. Some studies report very stable coatings that did not exhibit any significant decrease in ion retention over time,[1,3,9,11,13] while others found that the coatings gradually leached from the column[2,14-16] or that a small amount of the surfactant had to be included in the eluent to stabilize retention times.[5-7,17-19] For example, Hatsis and Lucy[2] observed a 10% decrease in sulfate retention after 12 h of continuous operation at 5 mL/min when a coating solution of 1 mM DDAB in 5%

acetonitrile/water was used, while Connolly and Paull[1] reported a stable coating when 10 mM DDAB in water was used as the coating solution.

Does the content of organic modifier or the concentration of surfactant affect the coating stability? Are there other factors that may affect coating stability? Can the process of surfactant leaching be slowed or prevented? The following study addresses these questions by exploring the effect of different coating conditions on the stability of surfactant coatings used for ion exchange chromatography. The surfactant concentration, acetonitrile content, temperature, and ionic strength of the coating solution were varied to document the affect on stability. The double-chained surfactant didodecyldimethyl-ammonium bromide (DDAB, Table 1.1) has been widely used in this group and by other researchers. However, DDAB has been linked with backpressure and reproducibility problems.[14,20] Therefore in this study, the surfactant cetyltrimethylammonium bromide (CTAB, Table 1.1) was used because it has also been widely used to prepare surfactant-coated IC columns[11,17] and does not exhibit any deleterious properties such as increased backpressure or precipitation in eluent.

Table 3.1. Surfactant coatings in the literature.

Coating solution[a*]	Column dimensions (Capacity)	Flush volume	Stability	Ref.
10 mM DDAB	30 x 4.6 mm 3 µm particulate (40 µeq/cm)	Not specified	Reported to be stable.	1
1 mM DDAB (5% ACN)	50 x 4.6 mm monolith (20 µeq/cm)	150 mL water + 75 mL eluent (225 mL total)	10% decrease in retention after 3.60 L.	2
1 mM DDAB (5% ACN)	25 x 4.6 mm monolith (N/A)	150 mL water	Reported to be stable.	3
1 mM DOSS (5% ACN)	50 x 4.6 mm monolith (N/A)	150 mL water	Stable over 3 month period.	3
5 mM CTAC	50, 100 x 4.6 mm monoliths (27 µeq/cm)	water + eluent (vol. not specified)	0.2 mM CTAC in eluent to stabilize retention times.	17
1 mM DDAB (5% ACN)	5 x 4.6 mm 10 x 4.6 mm monolith (24 µeq/cm)	water + eluent (vol. not specified)	10% decrease in retention after 0.66 L (1 cm column). Increased stability 15-fold by using coated pre-column.	14
5 mM CPC	25 x 4.6 mm monolith (N/A)	Not specified	Stable up to 3 months of continuous use at 3 mL/min.	13
40 mM Li-DS	50 x 4.6 mm monolith (N/A)	Not specified	0.1 mM Li-DS in eluent to stabilize retention times.	18
1 mM DOSS	150 x 0.1 mm monolith (N/A)	60 µL water	Decrease in capacity after 240 µL. After another 980 µL, coating stabilized.	15
2 mM DDMAU	150 x 0.1 mm monolith (N/A)	90 µL water	Indications of column bleed over time.	16
20 mM DDA-AA	250 x 4.6 mm 5 µm particle, 100 x 4.6 mm monolith (N/A)	Not specified	0.2 mM surfactant in eluent to stabilize retention times.	7
20 mM DDMAU	100, 50, 25 x 4.6 mm monoliths (63 µeq/cm)	45 mL water, then eluent (vol. not specified)	Stable for >17,000 column volumes.	9
5 mM DDAB or CPC + 5 mM non-ionic surfactant	100 x 4.6 mm 150 x 3.9 mm particulate (N/A)	Equilibrated with eluent (vol. not specified)	Stable for at least 360 h of use.	4

5% w/w POE 25 mM CTAB	100 x 4.6 mm monolith (N/A)	Not specified.	Stable for at least 1 month	11
TTACl Zwittergent-3-14	250 x 4.6 mm 5 μm particle (N/A)	Not specified.	10% v/v surfactant in eluent to stabilize retention times.	5,19

a. Abbreviations: DDAB, didodecyldimethylammonium bromide; DOSS, sodium dioctylsulphosuccinate; CTAB/CTAC: cetyltrimethylammonium bromide/ chloride;DDA-AA, (dodecyldimethylamino) acetic acid; LiDS: lithium dodecylsulfate; DDMAU: N-dodecyl-N,N-(dimethylammonio)-undecanoate; CPC: cetylpyridinium chloride; POE: polyoxyethylene; TTACl: tetradecyltrimethyl-ammonium chloride; Zwittergent-3-14, 3(N,N-dimethyltetradecylammonio)propane sulfonate.

* All coating solutions are in 100% water unless otherwise stated.

Experimental

3.2.1 Apparatus

A model 625 LC Waters (Milford, MA, USA) HPLC pump was used. A 0.5 μm stainless steel frit (Upchurch, Oak Harbor, WA, USA) was positioned before a model 9125 Rheodyne (Berkeley, CA, USA) injection valve fitted with a 20 μL loop. Separations were carried out on a Chromolith Performance monolithic silica RP-18e 100 mm x 4.6 mm I.D. column (Merck KGaA, Darmstadt, Germany). A 5 mm x 4.6 mm I.D. Chromolith guard column housed within a guard cartridge (Merck) was used in the study of ion-exchange capacity. Both columns were coated with the cationic surfactants cetyltrimethylammonium bromide (CTAB) or cetyltrimethylammonium chloride (CTAC). A CH-30 column heater and TC-50 temperature controller (Eppendorf, Mississauga, Ontario, Canada) was used to maintain a constant temperature (30 or 40°C) throughout the coating and separation processes. Analyte ions were detected using non-suppressed conductivity detection with a Dionex ED-50A electrochemical detector and a DS3-1 Detection Stabilizer (Dionex, Sunnyvale, CA, USA). A 10 cm length of 0.005" I.D. PEEK tubing (Upchurch, Oak Harbor, WA, USA) connected the column directly to the cell, which was within the DS3-1 stabilizer. The volume of the conductivity cell was 1 μL, rise time was 0.05 s and data was collected with Dionex PeakNet 5.2 software at 20 Hz.

For determination of the ion-exchange capacity of the columns, UV absorbance detection at 210 nm was employed (Waters Lambda-Max Model 481 LC

Spectrophotometer). Data were collected using StampPlot Pro V3 Release 2 (Selmaware Solutions) at 20 Hz.

All pH measurements were made with a Corning 445 pH-meter (Corning, New York, NY, USA) with a Corning electrode (3 in 1 combo P/N 476436).

3.2.2 Reagents and Solution Preparation

Solutions were prepared in deionised 18 MΩ water (Nanopure Water System, Barnstead, Chicago, IL, USA) that had been filtered through 0.22 μm Magna nylon membrane filters (GE Osmonic, Trevose, PA, USA). Chemicals were reagent grade or better. The sodium salts of chloride (EMD Chemicals, Gibbstown, NJ, USA), nitrite (BDH, Toronto, Canada), nitrate (ACP Chemicals, Montreal, Canada), sulfate (BDH) and phosphate ($NaH_2PO_4.H_2O$, EMD) were used. Potassium salts of bromide (Fisher, Fair Lawn, NJ, USA), iodate (ACP Chemicals), iodide (BDH) and perchlorate (Fisher) were used. Phenol crystals (ACP chemicals), CTAB (95% purity, Aldrich, Oakville, Ontario, Canada) and CTAC (Aldrich, St. Louis, MI, USA) were used without further purification.

To prepare the 10.0 mM 4-hydroxybenzoic acid (4-hba) eluent, the appropriate amount of 4-hba (99%, Aldrich) was dissolved in water, the pH adjusted to 4.6 with a 2.5 M solution of sodium hydroxide (Fisher), and diluted to volume with water.

The CTAB coating solutions used were 1-20 mM CTAB in 0% to 35% v/v acetonitrile (ACN, HPLC grade, Fisher) in an aqueous component. The aqueous component consisted of either water or an aqueous solution of 10-20 mM 4-hba. To

prepare the solutions, the appropriate amount of CTAB was added to a plastic volumetric flask, acetonitrile was added, and the solution was diluted to volume with the aqueous component.

3.2.3 Coating and removing surfactant from the column

The Chromolith RP-18e columns were coated using the procedure of Hatsis and Lucy.[2] Briefly, the column was equilibrated with X% ACN / (100-X)% aqueous component and then flushed with 1-20 mM CTAB or CTAC in X% ACN / (100-X)% aqueous component at 0.5-2 mL/min until surfactant breakthrough was observed, as indicated by a rapid increase in conductivity (see Figure 2.3 for an example breakthrough curve). The column was flushed with water for 20 min at 1 mL/min to remove any unbound surfactant, and then equilibrated with the eluent at 2 mL/min until the conductivity stabilized (~10-20 min). The initial ion-exchange capacity of the coated columns was estimated from the surfactant breakthrough time using equation 1.16 [1,2,21].

To remove the surfactant coating, the column was first flushed with 1 mM KBr to return the CTA^+ to its bromide form. The column was then flushed with water at 1 mL/min to remove unretained bromide, before changing the mobile phase to aqueous ACN. The % ACN in the mobile phase was gradually increased to 50% over a period of 1 min and held at 50% for 7 minutes to remove the CTAB. The % ACN was then gradually reduced to the % ACN to be used for the next coating. Figure 1.12 shows an outline of this coating/uncoating method for the surfactant DDAB. To confirm that this procedure completely removed the surfactant coating,

0.05 mM of sulfate was injected into the uncoated column and eluted using 10.0 mM 4-hba, pH 4.6. The retention time for sulfate was statistically equivalent to the water dip, indicating that the column possesses no residual ion exchange character.

3.2.4 Stability tests on 100 x 4.6 mm column

Surfactant coating stability tests were carried out on the 100 x 4.6 mm column under various coating conditions. First, the column was coated with CTAB or CTAC and then continuously flushed with 10.0 mM 4-hba, pH 4.6 at 2-4 mL/min. A standard containing 0.050 mM of seven ions was injected at regular intervals and separated at 2 mL/min and the retention times were monitored. Between injections, the flow rate was increased to 4 mL/min to reduce the time of the experiment. A total volume of 1-4 L was flushed through the column.

3.2.5 Determination of ion-exchange capacity on 5 x 4.6 mm column

The 5 x 4.6 mm guard column was too short to give significant retention of the ions. Therefore the stability of the coating was monitored by measuring the initial and final ion-exchange capacity. The initial capacity was given by the breakthrough time of CTAB. The capacity was then re-determined using another breakthrough curve method, a variation of the bromide adsorption/desorption method used by Hutchinson et al.[22-24] First, a 20 mM KCl solution was flushed through the column for 2 mL/min until all ion-exchange sites were converted to the Cl^- form (about 5-10 min). Then a 0.5 mM solution of KBr was flushed at 1 mL/min and the breakthrough curve was monitored using UV detection at 210 nm. The ion-exchange capacity was

calculated from the breakthrough time using equation 1.16. Next, the column was flushed for 50 min at 4 mL/min with 10.0 mM 4-hba, pH 4.6. The capacity was then re-determined using the bromide breakthrough curve method.

3.2.6 Calculation of efficiency

The efficiency (N) of separation was monitored throughout the stability studies using the width-at-half-height method (equation 1.4b).

3.2.7 Determination of critical micelle concentration (CMC)

The critical micelle concentration, or CMC, of CTAB was determined through surface tension titrations. A Fisher Model 20 surface tensiometer with 13 mm diameter Pt-Ir ring was employed. A 50 mL aliquot of acetonitrile/water solution was dispensed into a glass beaker at room temperature. The apparent surface tension was measured by immersing the ring into the solution and measuring the force, in dynes/cm, needed to pull the ring from the surface. Then, solutions of increasing concentration of surfactant were measured. A plot of ln[surfactant] vs. apparent surface tension revealed a breakpoint, which indicated the CMC.

3.2 Results and Discussion

Silica based columns dissolve in alkaline eluents.[25] Therefore, in this study, a weak acid eluent was used instead of the more traditional highly-alkaline IC eluents such as hydroxide or carbonate/bicarbonate. In this case, 10 mM 4-hba was buffered at its pKa (4.6) to avoid changes in pH over the course of the experiments and to minimize silica dissolution.

3.3.1 The effect of coating conditions on the rate of surfactant leaching

The retention of sulfate on a 4.6 x 100 mm monolithic column coated under various conditions was monitored as a function of the volume of eluent flushed through the surfactant-coated column up to a total eluent volume of 1 L. The conditions varied include temperature, the presence of the organic modifier, the concentration of surfactant, and the ionic strength of the solvent. The results are shown in Figure 3.1A and 3.1B, along with a linear fit for each coating condition. The y-axis of this plot has been normalized to the initial retention factor (k) observed for a given coating. Table 3.2 documents the initial retention factor for sulfate, the column capacity, the slope of the line (indicating the rate of surfactant leaching), and the percent decrease in retention factor after 1 L of eluent has passed through the column (calculated from the linear fit).

Figure 3.1A shows the effect of the ionic strength of the coating solution. These studies used a coating solution containing 1 mM CTAB in 23% acetonitrile / 77% aqueous component. The aqueous component of the coating solution was composed of water, eluent (10.0 mM 4-hba), or 20.0 mM 4-hba. As shown in Table 3.2, the

initial capacity was greatly affected by the presence of the eluent (50, 86 and 106 μeq/column, respectively). Berthod et al.[26] also observed an increase in the amount of adsorbed CTAB onto C_{18} silica stationary phases with increasing ionic strength. This phenomenon has been studied in detail by Bartha et al.[27], who proposed that a "salting-out" effect lowers the electrostatic repulsions between the surfactant headgroups and enhances the hydrophobic interactions between the surfactant tail and the C_{18} phase. Thus, a higher ion-exchange capacity is observed upon increasing the ionic strength of the coating solution.

The change in ionic strength of the coating solution also had a slight effect on the rate of surfactant desorption from the column. By increasing the 4-hba concentration from 0 to 10 to 20 mM, a 9.0%, 6.2%, and 5.5% decrease in retention after 1 L of flushing was observed, respectively. However, this is not an overly significant improvement in surfactant coating stability.

Next, the effect of the surfactant concentration was investigated. Through comparison of 1 mM and 20 mM CTAB in 23% acetonitrile / 77% 10 mM 4-hba (Figure 3.1B), there seemed to be no significant improvement in coating stability. However, adjusting the concentration of surfactant provided an additional means by which to alter the capacity of the column (Table 3.2). By increasing the CTAB concentration from 1 to 20 mM, the ion-exchange capacity increased more than 5-fold. Adsorption isotherms for CTAB onto C-18 silica by Berthod et al.[28] show a significant increase in the amount of adsorbed CTAB with increasing CTAB solution concentration in the sub-micellar region, which plateaus after the CMC is reached. Measurements of the CMC (Section 3.2.7) were unable to determine the precise value

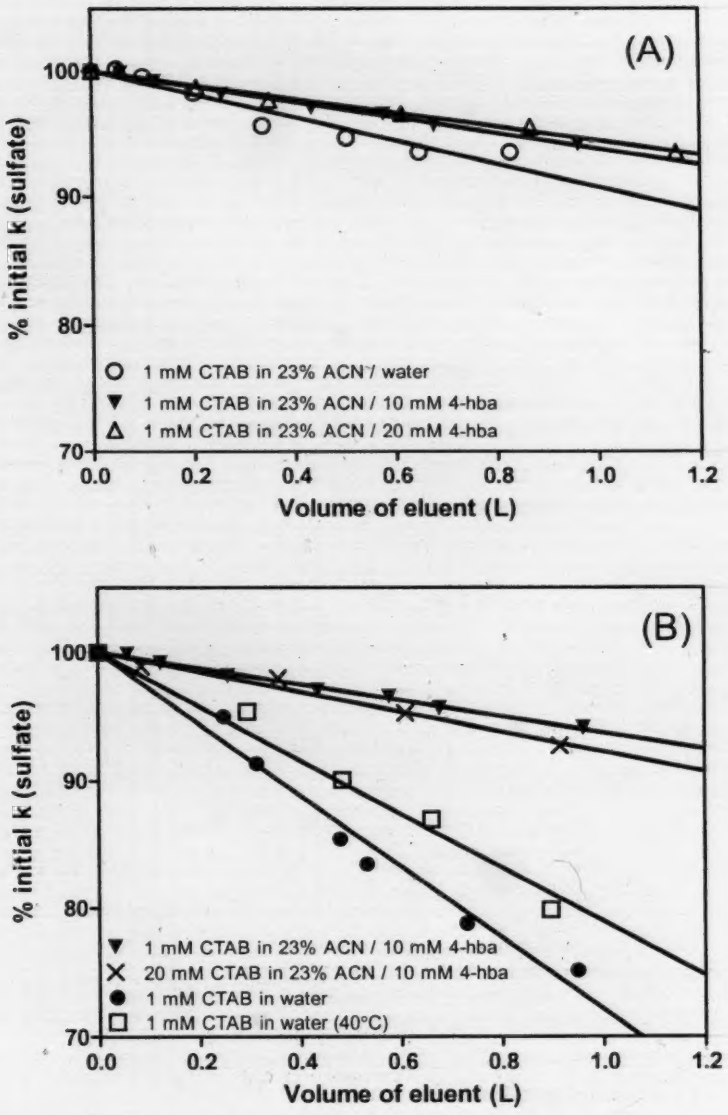

Figure 3.1 Linear fits for sulfate retention loss for: **A)** different ionic strengths of coating solutions; and **B)** various other coating conditions. Conditions: 100 x 4.6 mm RP-18e Chromolith column coated until breakthrough. Separations using 10.0 mM 4-hydroxybenzoic acid (pH 4.6) at 2 mL/min, 0.05 mM sulfate, 20 µL injection, non-suppressed conductivity detection. Temperature 30°C unless otherwise stated.

Table 3.2: Effect of coating conditions on ion-exchange capacity and stability[a]

Coating conditions	Initial Capacity[b] (μeq/col.)	Initial k (SO_4^{2-})[c]	Slope	R^2	% retention loss after 1 L of flushing[d]
1 mM CTAB in 23% ACN / water	51	9.25 ± 0.06	-9.28 ± 0.64	0.9257	9.3
1 mM CTAB in 23% ACN / 10 mM 4-hba	86	18.0 ± 0.0$_3$	-6.24 ± 0.13	0.9929	6.2
1 mM CTAB in 23% ACN / 20 mM 4-hba	106	21.9 ± 0.1	-5.57 ± 0.18	0.9864	5.6
20 mM CTAB in 23% ACN / 10 mM 4-hba	300	35.7 ± 0.2	-7.71 ± 0.37	0.9783	7.7
1 mM CTAB in water	310	49.9 ± 0.9	-27.9 ± 1.0	0.9759	28
1 mM CTAB in water (40°C)	270	44.7 ± 0.9	-21.0 ± 0.9	0.9790	21

a. Conditions: as in Figure 3.1.
b. According to surfactant breakthrough time (equation 1.16)
c. Initial k(SO_4^{2-}) calculated from linear regression of k(SO_4^{2-}) vs. eluent flush volume when x = 0.
d. Calculated from linear fit for sulfate ion.

of the CMC for CTAB in 23% acetonitrile but indicated that it was greater than 20 mM. Thus, for the conditions used in this study, the CTAB is in the sub-micellar region, and so the increased capacity observed in Table 3.2 is consistent with the results of Berthod et al.[28] Berthod et al.[28] and Geoffry et al.[29] explain that the amount of adsorbed surfactant remains constant after the CMC because the concentration of surfactant monomers remains constant after this point. Levchenko et al. observed similar behaviour for the adsorption of purified SDS on self-assembled monolayers of undecanethiol on gold.[30]

A more common way to change the ion-exchange capacity of a surfactant-coated column is to adjust the percent of organic modifier in the coating solution.[2,14,31,32] Hatsis and Lucy[2] observed an increase in ion-exchange capacity upon decreasing the percent acetonitrile in the coating solution. To see this effect most dramatically, the acetonitrile was excluded from the coating solution altogether in this study. Through comparison of 1 mM CTAB in 23% acetonitrile/water and in pure water, a drastic increase in the ion-exchange capacity is observed in pure water (50 vs. 310 μeq/column, Table 3.2). Unfortunately, the rate of capacity loss for CTAB in pure water was 3-fold that of CTAB in the ACN/water mixture. Further, the retention time for sulfate was over 25 min at such a high capacity. Both of these observations suggest that reducing the %ACN in the CTAB coating solution will not achieve useful and stable ion exchange columns.

In recent years temperature has been increasingly used as a variable in liquid chromatography to speed up analysis times, and to adjust retention and selectivity.[33] In general, increasing the column temperature results in a decrease in reversed phase

retention. An increase in column temperature of 4°C is about equivalent to a 1% increase in the methanol content of the mobile phase.[34] Therefore column temperature was investigated as an alternate means of adjusting the capacity of a surfactant-coated ion exchange column.

Table 3.2 shows that by increasing the temperature from 30 to 40°C, a 13% decrease in ion-exchange capacity (i.e., retention of the surfactant) is observed for coating solutions containing 1 mM CTAB in pure water. With regard to the coating stability, sulfate retention clearly decreases more rapidly on the column coated at 30 °C (•) than at 40 °C (□), Figure 3.1A. The slopes of the linear fits for 1 mM CTAB in water at different temperatures (Table 3.2) show a 25% improvement in the CTAB stability upon increasing the temperature. However, the capacity at 40°C is still too high to be useful for IC. Unfortunately higher temperatures could not be used because the Chromolith column is rated to just 45°C.[35] Further, operating the Chromolith column at 40 °C for ~45 hours resulted in an 89% decrease in efficiency. Due to this catastrophic loss of efficiency adjustment of the column temperature was not explored further.

To summarize, the initial ion-exchange capacity of the column could be altered in many ways: by changing the acetonitrile content, the ionic strength, the temperature, or the surfactant concentration. However the only significant decrease in the rate of capacity loss was achieved by increasing the column temperature during coating. Unfortunately this approach is limited due to the limited temperature stability of the Chromolith column.[35] Other attempts to increase the stability of the

coating, such as varying surfactant concentration or ionic strength, did not yield significant improvements.

3.3.2 Long-term stability of surfactant coatings

The main purpose for conducting the experiments in Sec. 3.3.1 was to slow the loss of ion exchange capacity due to surfactant leaching by optimizing the coating conditions. These experiments were unsuccessful. However, during the analysis of the stability of the various coatings, an interesting observation directed this work towards a different objective. Close inspection of the linear fits in Figures 3.1A and 3.1B reveals a slight positive deviation from linearity at higher volumes of eluent. This is most prominent in Figure 3.1B for the 1 mM CTAB in water (30°C, •). To determine if some leveling off of capacity loss was occurring, additional experiments were carried out over a longer range of eluent flush volumes (up to 4 L, which corresponds to ~ eight 8-hour workdays at 1 mL/min).

Figure 3.2 shows a series of separations on a column coated with 1 mM CTAB in 23% acetonitrile / 77% water. The most significant decrease in retention occurs before 1 L of eluent has passed through the column, after which the retention appears to stabilize. The efficiency of our column also remained constant throughout the entire experiment, as shown in Figure 3.3A (4.2% RSD for sulfate peak efficiency).

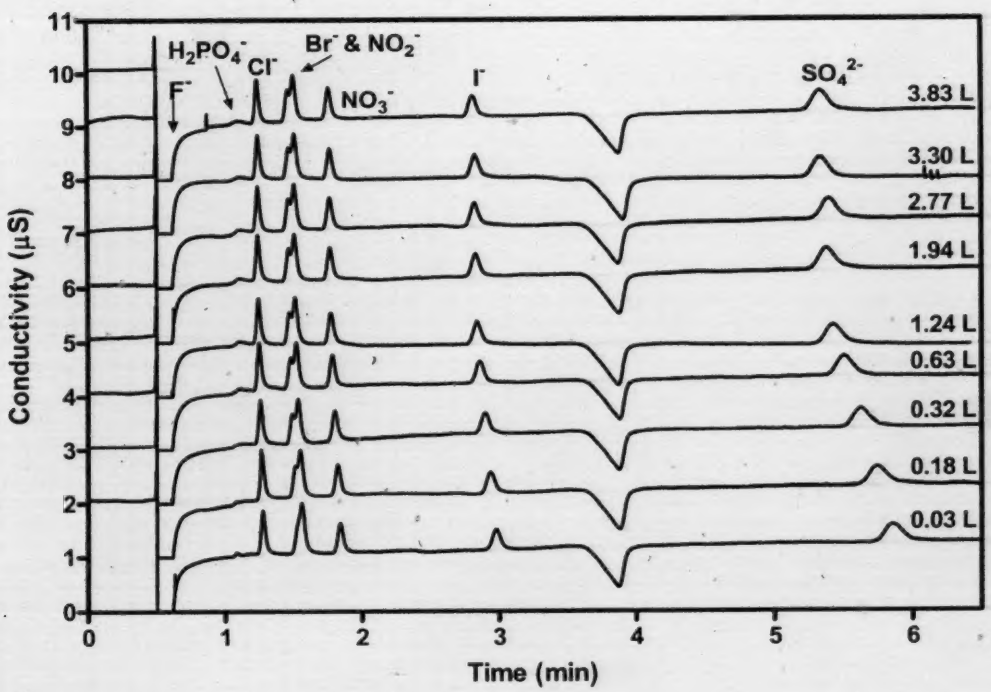

Figure 3.2 Series of separations of 8 anions on a 100 x 4.6 mm RP-18e Chromolith column coated with 1 mM CTAB in 23% ACN / water, 30°C. Conditions: 0.05 mM analyte ions, 20 µL injection, 10.0 mM 4-hydroxybenzoic acid eluent (pH 4.6), 2 mL/min, non-suppressed conductivity detection.

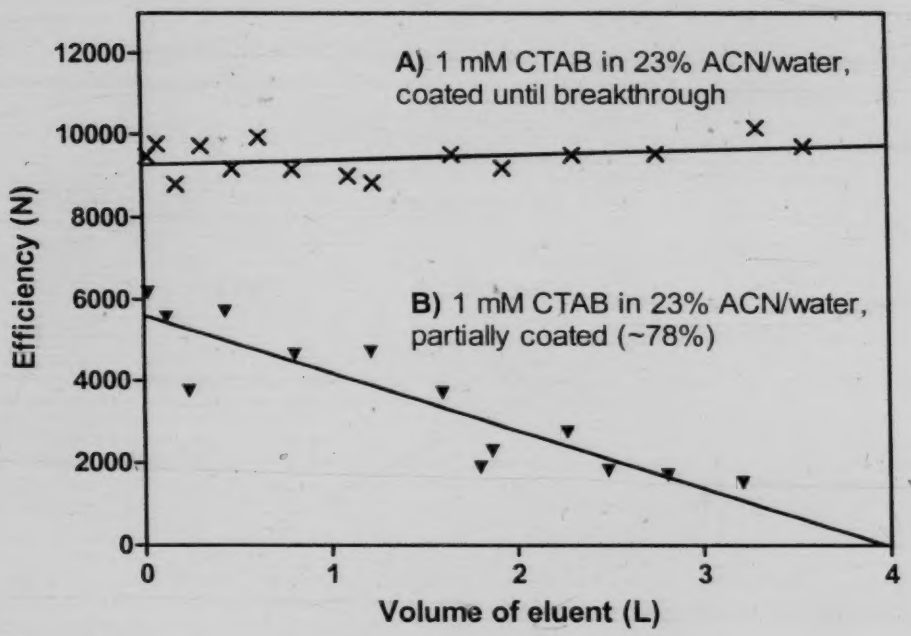

Figure 3.3 Efficiency of sulfate peak, calculated from width at half-height (equation 1.4b), as a function of flush volume, fitted with line of best fit. Conditions: 100 x 4.6 mm RP-18e Chromolith column coated with 1 mM CTAB in 23% ACN / water **A)** until breakthrough, **B)** for 18 min (~78% coated). Anion separations using 10.0 mM 4-hydroxybenzoic acid eluent (pH 4.6) at 2 mL/min, 0.05 mM sulfate, 20 μL injection, non-suppressed conductivity detection. Temperature 30°C.

Based on findings by Tiberg et al.,[36] the Lucy research group has used a single-exponential decay with a nonzero asymptotic value to describe the desorption of DDAB from and the adsorption of a phospholipid onto fused silica.[37,38] In this study, a similar equation has been fit to the sulfate retention data on a column modified with various CTAB coatings (Prism Version 4.00, GraphPad Software Inc., San Diego, CA):

$$k(SO_4^{2-}) = A_1 \exp(-k_{obs}V) + A_\infty \quad (3.1)$$

The term k_{obs} is the observed rate constant for the decay of the retention factor of sulfate ($k(SO_4^{2-})$), V is the volume of eluent flushed through the column, A_1 is a fit parameter, and A_∞ is the asymptotic value of the retention factor (plateau region). The half-life of the exponential decay in volume units is $0.69/k_{obs}$.

To determine if this exponential decay trend holds over a wide range of surfactant coating conditions, the same coating conditions as in Section 3.3.1 were used, but this time up to 4 L of eluent was flushed through the column after coating. The objective at this point is not to slow or prevent the loss of retention, but to arrive at the later stable retention behaviour as soon as possible. In addition to the coating conditions in Section 3.3.1, two new conditions were introduced – 1 mM CTAC in water, and a partial coating of 1 mM CTAB in 23% ACN/water. The reasons for introducing these new conditions will be explained later in the chapter.

Figure 3.4 shows the observed retention of sulfate vs. eluent flush volume under the various coating conditions. The curves in Figure 3.4 are the fit of the data to equation 3.1. The parameters of the exponential fits, including half-life and the retention factor for sulfate at the plateau (A_∞), are listed in Table 3.3. The initial

retention factor for sulfate, $k_i(SO_4^{2-})$, can be calculated by $A_1 + A_\infty$. It is reasonable to assume that the term $k_i(SO_4^{2-})$ should scale linearly with the initial capacity. I believe the term $k_i(SO_4^{2-})$ is actually a better reflection of the initial ion-exchange capacity of the column than the initial capacity determined by surfactant breakthrough (Q), because Q depends only on the amount of surfactant flushed through the column, and not how much of it actually adheres or acts as an ion-exchange site.

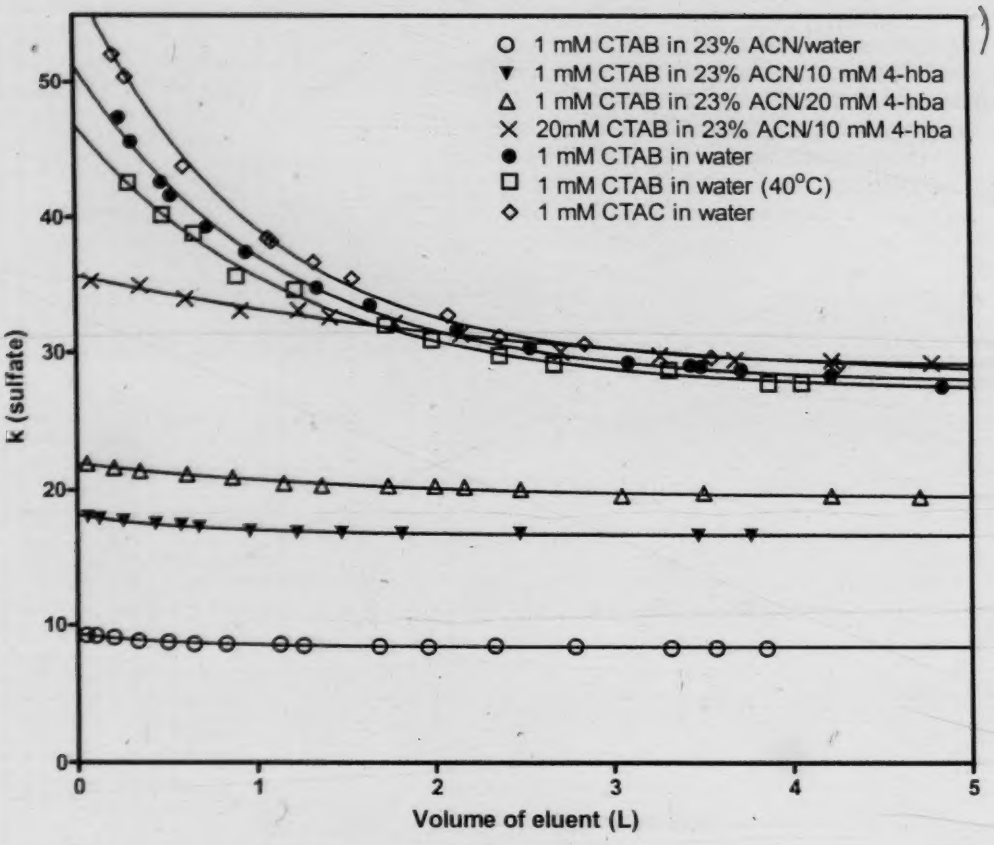

Figure 3.4 Exponential decay fits (equation 3.1) for sulfate retention loss under various coating conditions. Conditions: 100 x 4.6 mm RP-18e Chromolith column coated until breakthrough. Anion separations using 10.0 mM 4-hydroxybenzoic acid eluent (pH 4.6) at 2 mL/min, 0.05 mM sulfate, 20 µL injection, non-suppressed conductivity detection. Temperature 30°C unless otherwise stated.

Table 3.3. Long-term stability of surfactant coatings: exponential decay fits[a]

Coating conditions	$k_i(SO_4^{2-})$	A_1	A_∞	k_{obs} (L^{-1})	Half-life (L)	R^2
1 mM CTAB in 23% ACN / H_2O	9.34 ± 0.06	0.93 ± 0.05	8.41 ± 0.03	1.79 ± 0.24	0.39 ± 0.05	0.9656
1 mM CTAB in 23% ACN / 10 mM 4-hba	18.2 ± 0.1	1.44 ± 0.05	16.7 ± 0.0_3	1.45 ± 0.13	0.47 ± 0.04	0.9885
1 mM CTAB in 23% ACN / 20 mM 4-hba	21.9 ± 0.2	2.50 ± 0.11	19.5 ± 0.1	0.65 ± 0.08	1.07 ± 0.14	0.9797
20 mM CTAB in 23% ACN / 10 mM 4-hba	35.7 ± 1.1	8.16 ± 0.70	27.5 ± 0.81	0.36 ± 0.08	1.93 ± 0.40	0.9812
1 mM CTAB in H_2O	51.2 ± 0.5	23.4 ± 0.5	27.9 ± 0.3	0.91 ± 0.05	0.76 ± 0.04	0.9958
1 mM CTAB in H_2O (40°C)	46.8 ± 0.6	19.6 ± 0.4	27.3 ± 0.3	0.84 ± 0.06	0.82 ± 0.06	0.9960
1 mM CTAB in 23% ACN / H_2O (78% coated)	9.01 ± 0.16	0.77 ± 0.16	8.24 ± 0.03	5.03 ± 1.45	0.14 ± 0.04	0.8993
1 mM CTAC in H_2O	58.2 ± 0.5	29.1 ± 0.4	29.1 ± 0.3	1.04 ± 0.04	0.67 ± 0.03	0.9978

a. Conditions: as in Figure 3.4

There are a few interesting trends that result from the exponential decay data. Table 3.3 shows a clear relationship between the $k_i(SO_4^{2-})$ values and the plateau k values (A_∞), which are presented graphically in Figure 3.5A. In the initial portion of the graph ($k_i(SO_4^{2-}) < 30$), A_∞ scales linearly with $k_i(SO_4^{2-})$. Then, for $k_i(SO_4^{2-}) > 30$, which roughly corresponds to an ion-exchange capacity of 150 μeq on a 10 cm column, the A_∞ values level off, much like a Langmuir isotherm. This holds implications for chromatographers who wish to control the final capacity of their column by increasing the initial capacity through means such as changing the ACN content, surfactant concentration, ionic strength, etc. Section 3.3.4 discusses the control of the final ion-exchange capacity in more detail.

Table 3.3 also shows that each coating decays at different rates (k_{obs}), with the most drastic decay occurring in the initial ~500 mL of flushing volume (Figure 3.4). Figure 3.5B shows a plot of the initial decay rate vs. $k_i(SO_4^{2-})$. Here, the initial decay rate remains relatively constant and small until a $k_i(SO_4^{2-})$ value of about 30. After this point, the initial decay rate increases dramatically with increasing initial ion-exchange capacity. Geffroy et al.[29] also reported an increase in the desorption rate at higher surfactant surface concentrations on a hydrophobic polystyrene surface with adsorbed non-ionic alkyl ethylene oxide surfactants. The existence of the two regimes of stability in Figure 3.5B may explain the contradictory information in the literature regarding the stability of surfactant coatings, as discussed in Section 3.3.6.

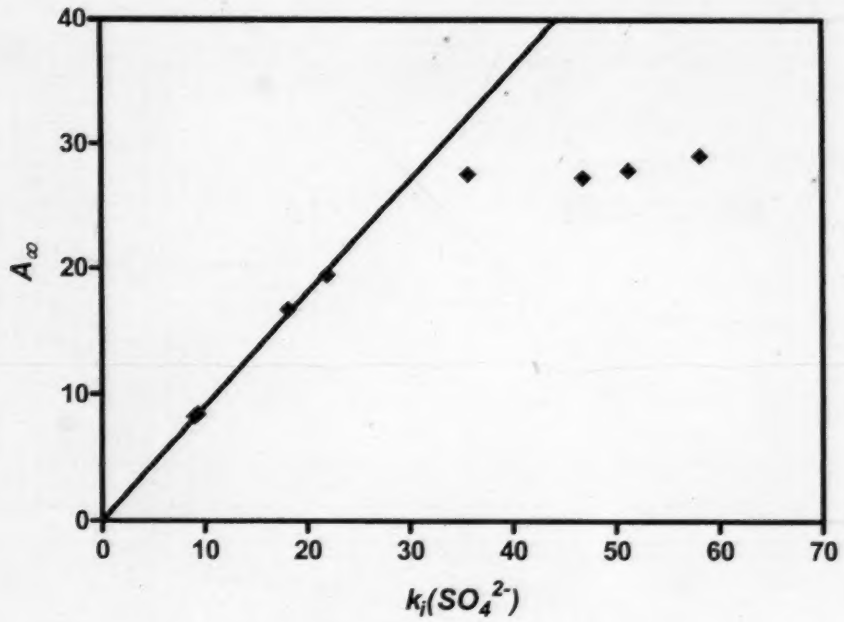

Figure 3.5A Plateau retention factor for sulfate ion (A_∞) vs. initial retention factor ($k_i(SO_4^{2-})$), as determined by exponential decay fits. Line of best fit through points $k_i(SO_4^{2-}) < 30$. Conditions: 100 x 4.6 mm RP-18e silica monolith, coated with CTAB or CTAC under the various coating conditions listed in Table 3.3.

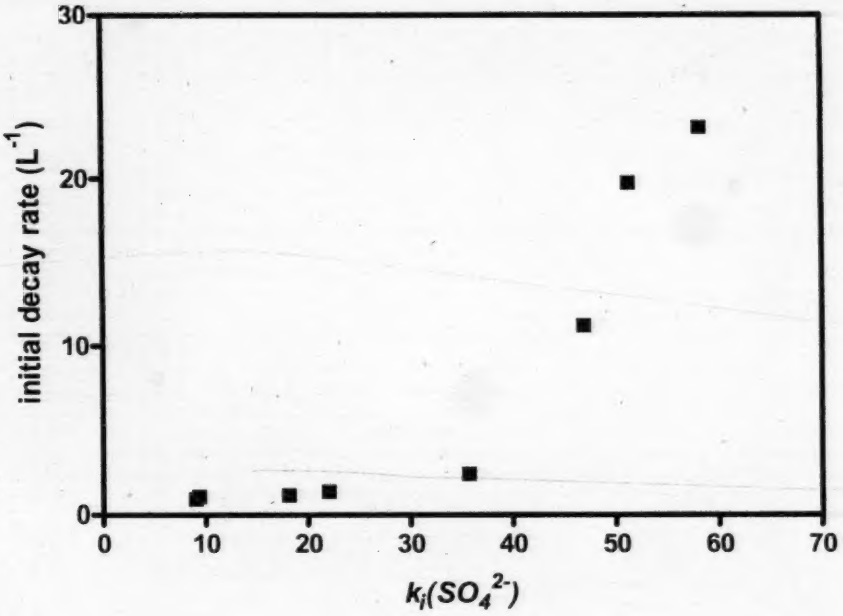

Figure 3.5B Initial decay rate vs. initial retention factor for sulfate, $k_i(SO_4^{2-})$. Initial decay rate is the slope of a linear fit of the initial ~500 mL of flushing. Conditions: 100 x 4.6 mm RP-18e silica monolith, coated with CTAB or CTAC under the various coating conditions listed in Table 3.3.

It is evident from Figure 3.4 that flushing a 100 x 4.6 mm column with a 1 L of eluent (~900 column volumes) ensures that a stable coating is reached under most coating conditions. This requires about 3.3 hours of continuous flow at 5 mL/min – a flow rate easily obtainable on monolithic columns. After this flushing period, both retention times and efficiency (Figure 3.3A) remain stable for ≥ 3000 column volumes. Thus, I propose a new strategy for preparing surfactant-coated ion exchange columns. Rather than coating a column and trying to use it immediately, I propose that a surfactant-coated column should be flushed for a period of time before being put to use. This is much less time-consuming than uncoating and recoating the column, which is what has been done in the past to maintain retention times.[2,14] If the user wishes, the column can easily be uncoated and used in its original reversed-phase format, or coated again under different conditions to optimize the ion-exchange capacity. Guidelines for controlling the final ion-exchange capacity are presented in Section 3.3.4.

3.3.3 Attempts to avoid the drastic initial decrease in retention

Preventing the initial decrease in analyte retention would result in much shorter start-up times for routine separations. Pelletier et al.[14] recently introduced an interesting method to maintain retention times on a surfactant-coated column. By placing a coated pre-column before the injector, the stability of the surfactant coating on the analytical column was increased 15-fold. The theory behind this approach was that any surfactant lost from the analytical column was replaced by surfactant leaching from the coated pre-column. Inspired by this method, in this study the

analytical column was only *partially* coated, allowing the front portion of the column to act as the coated pre-column, from which surfactant molecules would gradually leach off and be re-deposited further along the column. Additionally, Nagashima et al.[39] reported excellent stability on a graphitic carbon stationary phase coated with CTAB, which, upon comparison to studies done by Chambers et al.[40] had been unintentionally only partially coated.

In this study, the 100 x 4.6 mm monolith was once again re-coated with 1 mM CTAB in 23% ACN / 77% water, but the coating was terminated before complete breakthrough (the column was ~78% coated, according to previous breakthrough times for this particular coating solution). The hypothesis was that the initial decrease in surfactant leaching would be avoided and the retention would remain constant over the entire 4 L flush volume. However, in practice, this method showed no advantage over coating until complete breakthrough. The partial surfactant coating still showed a similar exponential decay trend (Table 3.3). Not only that, but the efficiency of the column decreased ~3-fold over the 4 L flush period (Figure 3.3B), with signs of double-peaking. Thus, my proposal that columns should be flushed to equilibrium before being put into use still stands.

3.3.4 Controlling the final ion-exchange capacity

As mentioned earlier, the most popular method to adjust the initial column capacity is to vary the percent acetonitrile in the coating solution.[2,14,31,32] However, I am proposing that a column be coated and then allowed to equilibrate to its plateau capacity before being put into use. Thus, it would be more useful to the

chromatographer to know what variables to control to achieve a specific final column capacity.

Figure 3.5A shows that the initial retention factor, $k_i(SO_4^{2-})$, and the final retention factor, A_∞, scale linearly for $k_i(SO_4^{2-}) < 30$, after which constant final retention factors are observed. This indicates that the final capacity of the column can be optimized by adjusting the initial capacity only within the linear portion of Figure 3.5A. Within the plateau region of Figure 3.5A, efforts to adjust the final capacity of the column are ineffective. That is, there is a limit to the highest ion-exchange capacity that can be achieved on a surfactant-coated column. According to Figure 3.5A, this maximum capacity is reached at $k_i(SO_4^{2-}) > 30$.

However, when chromatographers wish to adjust the capacity of a column, most commonly they do so by adjusting the percent acetonitrile in the coating solution and then calculate the initial capacity according to the surfactant breakthrough time (Q, equation 1.16). I proposed earlier that the $k_i(SO_4^{2-})$ is actually a better reflection of the initial capacity than Q because Q assumes that all surfactant molecules that are flushed through the column adsorb and act as ion-exchange sites. Figure 3.6 is a plot of Q vs. $k_i(SO_4^{2-})$. Points A-C were fitted with a linear regression, with the dotted lines indicating the 95% confidence interval. For $k_i(SO_4^{2-}) < 30$, Q scales linearly with $k_i(SO_4^{2-})$. For $k_i(SO_4^{2-}) > 30$, the Q values lie outside the 95% confidence interval and show little correlation with $k_i(SO_4^{2-})$.

Figures 3.5A, 3.5B and 3.6 all show a change in the behaviour of surfactant coatings at $k_i(SO_4^{2-}) = 30$. To gain a better understanding as to how to control the final capacity of the column, it may be useful to know if there is an underlying cause

which can explain or connect all of these trends. The table accompanying Figure 3.6 lists the CMC values for each condition from surface tension measurements and/or literature sources. Keep in mind that CMC values are not exact, but rather micelles begin to form over a range of concentrations. Points A-C which lie in the linear range of Figure 3.6 are below the CMC, while points D-F lie above the 95% confidence interval of the line and are above or very close to the CMC. The further the point D-F is above the CMC, the more it deviates from the line. Although Point "G" is below the CMC, it lies slightly below the 95% confidence interval of the line, likely because this point refers to CTAC and may not be directly comparable to the CTAB data. In short, Figure 3.6 shows that surfactant coating solutions above or very close to the CMC result in a Q value that overestimates the initial capacity of the column. This overestimation of initial capacity means that when micellar aggregates are present in the coating solution, either more surfactant is being flushed through the column than adsorbed onto it, and/or not all adsorbed surfactant molecules participate in ion-exchange.

These findings are consistent with Figures 3.5A and 3.5B, which also show a change in behaviour at $k_i(SO_4^{2-}) = 30$ that can be correlated with CMC values. In both figures, surfactant solutions are below the CMC for $k_i(SO_4^{2-}) < 30$ and above or around the CMC for $k_i(SO_4^{2-}) > 30$. Figure 3.5A shows that the final capacity stays relatively constant for surfactant coating solutions above the CMC. As mentioned

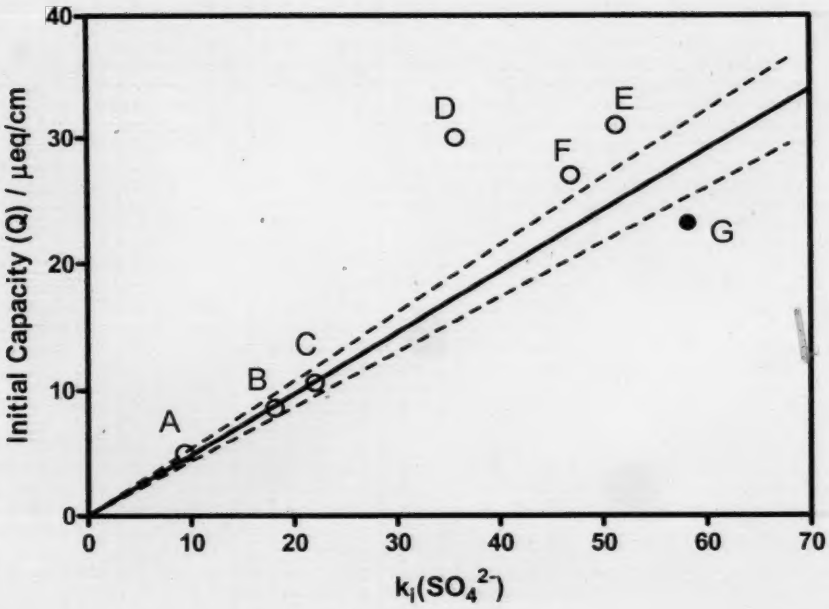

Point	Coating	CMC (mM)[a]
A	1 mM CTAB in 23% ACN / water	> 20
B	1 mM CTAB in 23% ACN / 10 mM 4-hba	3.0
C	1 mM CTAB in 23% ACN / 20 mM 4-hba	1.3
D	20 mM CTAB in 23% ACN / 10 mM 4-hba	3.0
E	1 mM CTAB in water (30°C)	0.9 – 1.0 [b]
F	1 mM CTAB in water (40°C)	~ 1.1 [c]
G	1 mM CTAC in water (30°C)	1.3 [d]

a. Determined by surface tension measurements (error ~ ±5%) unless otherwise indicated
b. CMC from reference [41] and surface tension measurements
c. CMC from reference [42]
d. CMC from reference [41]

Figure 3.6 Initial capacity according to surfactant breakthrough time (Q) vs. initial retention factor for sulfate ($k_i(SO_4^{2-})$). Coating conditions listed in accompanying table along with CMC values. Conditions: 100 x 4.6 mm RP-18e monolith, eluent: 10.0 mM 4-hba (pH 4.6) at 2 mL/min, 0.05 mM sulfate, 20 µL injection, non-suppressed conductivity detection.

earlier, Berthod et al.[28] and Geoffry et al.[29] explained that the amount of adsorbed surfactant remains constant after the CMC because the concentration of surfactant monomers remains constant after this point. In other words, micelles, which have their hydrophobic portion encased in a shell of charged groups, do not adhere to hydrophobic surfaces. This is consistent with the idea that when micelles are present, more surfactant is being flushed through the column than is actually adsorbing onto it; thus leading to an overestimation of the initial capacity if calculated using surfactant breakthrough times (equation 1.16).

Figure 3.5B suggests a much larger initial rate of surfactant desorption for coatings prepared from surfactant solutions containing micelles. A study of the adsorption of the anionic surfactant SDS on self-assembled monolayers of undecanethiol on gold by Levchenko et al. suggest that hemi-micelles form on hydrophobic surfaces.[30] At SDS concentrations well below the CMC, atomic force microscopy (AFM) images indicated the presence of surfactant aggregates with distorted structures, which were distributed evenly over the surface. At the CMC of SDS, the aggregates filled the surface, although their structure was not well-defined. At SDS concentrations well above the CMC, AFM images suggested that cylindrical hemi-micellar aggregates filled the surface in evenly-spaced parallel stripes. I propose that these different surfactant conformations may desorb from the surface at different rates, depending on how strong the interactions are between the surfactant structure and the underlying surface.

Based on Figures 3.5B and 3.5A, I propose that CTAB also exhibits these different surfactant conformations on C_{18} silica depending on whether the coating was

prepared with a solution below, at or above the CMC. Evidence of the formation of CTAB surface hemi-micelles was reported by Paruchuri et al. [43] in a study of the surface charge densities of CTAB adsorbed onto hydrophobic graphite surfaces. The authors reported that above the CMC of CTAB, the surface charge density does not change with concentration, suggesting the formation of surface hemi-micelles (this was confirmed through AFM images.

Based on the evidence presented in this section, a schematic representation of what could be happening at the column's C_{18} surface at surfactant concentrations above and below the CMC is shown in Figure 3.7. Above or at the CMC, surfactant monomers are in dynamic equilibrium with micelles in the solution and with hemi-micelles at the C_{18} surface (Figure 3.7A). Below the CMC, only surfactant monomers are present in the mobile phase and hemi-micelles do not form at the surface. Lack of evidence in the literature makes it difficult to deduce the conformation of surfactants at the C_{18} surface at concentrations below the CMC, but some possible representations are shown in Figure 3.7B. The surfactant monomers may adsorb to the surface with the hydrophobic tails extending into or laying on top of the bonded phase, or the surfactant molecules may form a bilayer with the underlying C_{18} chains (Figure 3.7B). The surfactant extending into the bonded phase maximizes hydrophobic interactions with the stationary phase, which may result in a more stable conformation which does not desorb from the surface very easily. Above the CMC, Paruchuri et al. [43] suggested that CTAB monomers initially adsorb to a graphite surface in a tail-to-tail and head-to-head fashion. The authors then explained that these adsorbed surfactants act as nucleation sites for the further adsorption of

surfactant, resulting in the formation of cylindrical hemi-micelles. It is possible that a similar phenomenon happens on the C_{18} surface at CTAB concentrations above the CMC, with the initially adsorbed surfactant monomers rearranging on the surface to form hemi-micelles (Figure 3.7A). It is likely that surfactant desorption occurs in a reverse manner, with the hemi-micelles changing to individually adsorbed surfactant monomers as surfactant is washed away from the surface. The hemi-micellar structures may be more easily washed away due to weaker interactions with the underlying bonded phase. This would explain the drastic initial decrease in retention observed for surfactant coatings prepared with solutions containing micelles as compared to those prepared with solutions below the CMC, as shown in Figure 3.5B. The small initial decrease in retention observed for coatings prepared with solutions below the CMC can be owed to differences in the way that individual surfactant monomers can adsorb to the surface, as depicted in Figure 3.7B. In addition, Figure 3.5A showed that the residual amount of adsorbed surfactant is constant for coating solutions above the CMC, suggesting that these coating solutions yield the maximum amount of stably adsorbed surfactant. Thus, by increasing the surfactant concentration in the coating solution further above the CMC, no gain in final ion-exchange capacity is achieved.

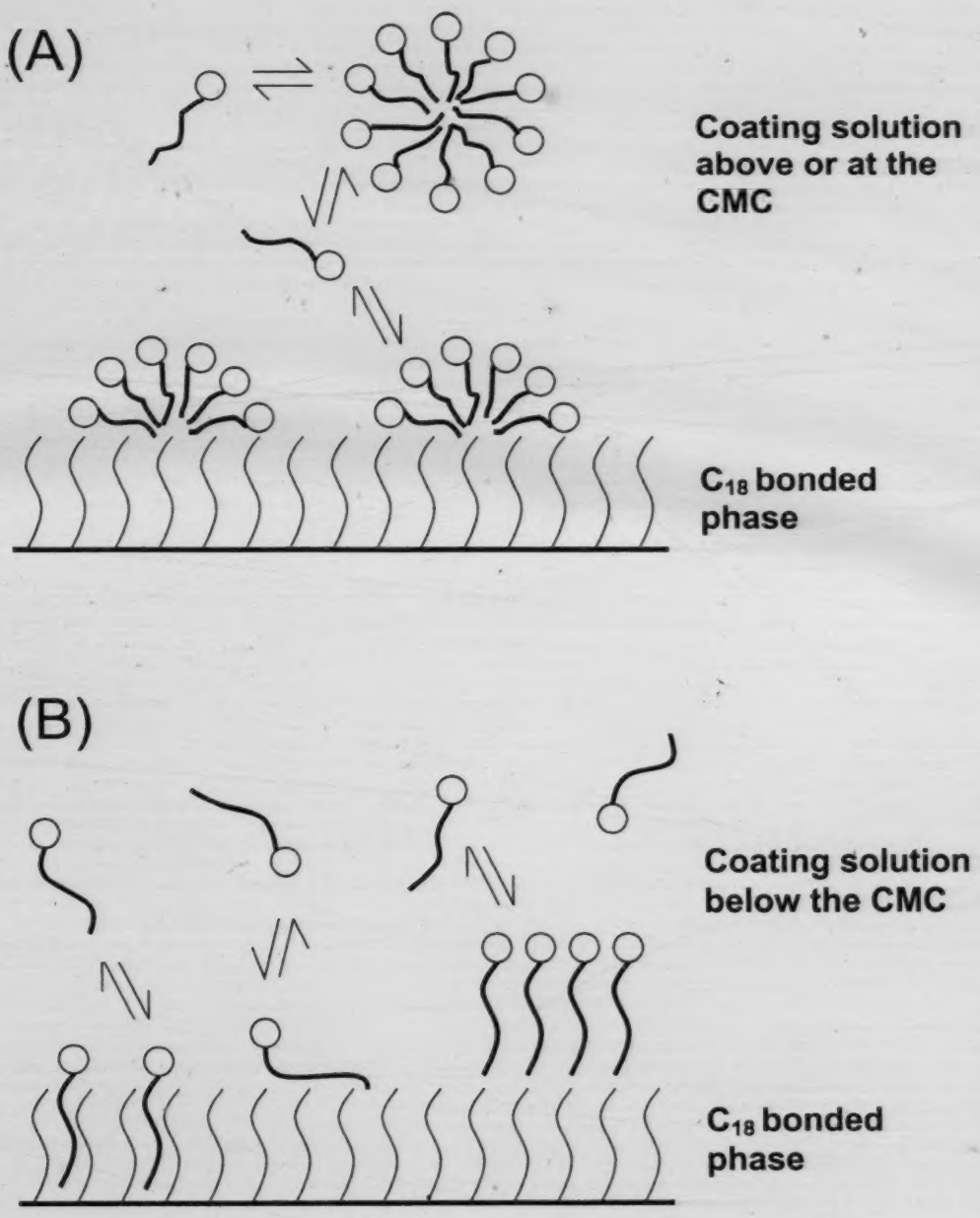

Figure 3.7. Schematic of possible processes occurring at the column's C_{18} surface during coating with a surfactant solution **(A)** above or at the CMC, and **(B)** below the CMC.

From the discussion in this section thus far, it can be concluded that the rate of desorption, the final capacity, and the accuracy of Q depend on whether the coating solution is above or below the CMC. However, the traditional method of adjusting initial capacity has been to adjust the ACN content (which, in effect, changes the CMC). Therefore, it would be more useful to the chromatographer if the relationship between Q and final capacity was presented in terms of the ACN content of the coating solution.

In this study, a short monolithic guard column (5 x 4.6 mm) was used. The initial and final capacities of the 5 x 4.6 mm CTAB-coated column were monitored as a function of ACN content. The initial ion-exchange capacities were determined from the surfactant breakthrough times, while the final capacities were determined using the bromide adsorption/desorption method (Section 3.2.5).

The studies on the 5 mm long columns can be directly correlated with the behaviour of 100 mm long analytical columns. Both a 5 x 4.6 mm and a 100 x 4.6 mm column were coated with 1 mM CTAB in 23% ACN/water. An initial capacity of 2.5 μeq was obtained on the 5 mm column, while the 100 mm column had an initial capacity of 51 μeq. This equals ~5 μeq/cm on both columns. Thus, the columns display the same coating behaviour. However, the 100 mm column required about 1000 mL to equilibrate to a stable coating (Section 3.3.2), while the 5 mm column required only about 50 mL. Thus, both the initial capacity and the required flush volume scale with column length. Further evidence of this phenomenon can also be seen in other studies in the Lucy research group. Hatsis and Lucy[2] observed a 10% decrease in retention after 3.60 L of eluent flushing on a 50 x 4.6 mm monolith,

while Pelletier and Lucy[14] found that a 10% decrease occurred after only 0.66 L of eluent flushing on a 10 x 4.6 mm monolith coated under identical conditions. By using the 5 mm column instead of the 100 mm column for the experiments in this section, the volume of eluent required and therefore the duration of the experiment was reduced.

The results obtained for initial and final capacities for coatings of 1 mM CTAB as a function of ACN content are displayed in Figure 3.8. At 0% and 5% ACN (i.e., to the left of the dotted line), the final capacity is far below the initial value. With %ACN greater than 10% the initial and final capacities match more closely.

Figure 3.5A and 3.6 together explain the trend seen in Figure 3.8. The points to the left of the dotted line in Figure 3.8 are above the CMC, while those points right of the line are below the CMC. All solutions used in Figure 3.8 have a concentration of 1.0 mM CTAB. For coating solutions above the CMC, Figure 3.6 indicates that Q overestimates the initial capacity, which explains why there is a larger discrepancy between initial and final capacities for low %ACN values in Figure 3.8. Figure 3.5A shows that the final capacity remains relatively constant for coating solutions above the CMC, which is also consistent with Figure 3.8, although there is some degree of scatter.

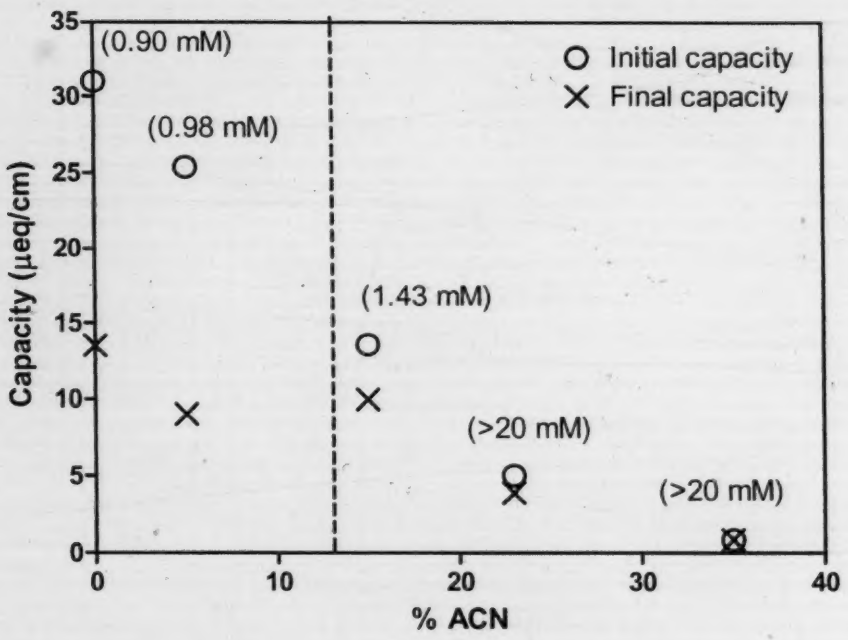

Figure 3.8 Initial (○) and final (×) ion-exchange capacity (μeq/cm) as a function of %ACN in the coating solution. Values in parentheses above data points indicate CMC determined from surface tension measurements. Initial capacity determined from surfactant breakthrough times, and final capacity (after flushing with ~4000 column volumes) determined from bromide adsorption/desorption method (Section 3.2.5). Conditions: 1 mM CTAB in X% ACN / water coated onto 5 x 4.6 mm Chromolith column.

The results in this section indicate that the final ion-exchange capacities can be optimized by adjusting *Q*, but only in the linear range of Figures 3.5A and 3.6 (i.e., when the coating solution is below the CMC). The *Q* value can be fine-tuned by any of the means described in Section 3.3.1; namely, varying the %ACN, surfactant concentration, ionic strength or temperature (or any combination of these). However, at higher initial capacities (i.e., when the coating solution is above or around the CMC), *Q* does not indicate the ion-exchange capacity of the column and any efforts to adjust *Q* result in no change in the final capacity. Thus, it is essential to know the CMC of the surfactant in the coating conditions in order to adjust the capacity or have an accurate measure of the capacity.

3.3.5 Possible causes for the exponential decay trend

It is desirable to understand the mechanism responsible for the exponential decay in the column capacity seen in Figure 3.4. It is possible that this decay behaviour is an intrinsic characteristic of surfactants. Tiberg et al.[36] and Geoffry et al.[29] observed similar desorption behaviour for nonionic surfactants, and Levchenko et al. observed similar desorption behaviour of anionic (SDS) surfactants from hydrophobic surfaces.[30] However, it is also possible that additional factors contribute to the exponential decay trends. Possible contributing factors are: 1) a change in the reversed-phase capacity of the column; and 2) the exchange of the surfactant counterion for the eluent ion. Two experiments were carried out to address these hypotheses.

The first experiment investigates the hypothesis that the exponential decay is due to a change in the reversed-phase capacity of the column. Octadecylsilyl ($C_{18}H_{37}$, ODS) bonded phases are very hydrophobic. Under typical reversed phase conditions (i.e., in the presence of acetonitrile) the bonded phase has a "brush structure."[44] However, under highly aqueous conditions this brush structure collapses into a folded, matted structure.[45,46] Such a collapse may cause adsorbed surfactant molecules to be "hidden" from the analytes, rendering them unusable for ion-exchange. To investigate whether a change in the ODS structure might be affecting retention, our RP-18e silica monolith was uncoated and used in the reversed-phase mode with water as the eluent. Phenol, a UV-absorbing molecule, was polar enough to be eluted with water, but sufficiently non-polar to exhibit retention on a reversed-phase column. First, the column was equilibrated with 23% ACN/water (this step is analogous to the surfactant coating step), and then the column was equilibrated with the eluent (water). The retention of phenol was monitored immediately upon switching to the water eluent and for a total flush volume of 4 L. The retention of phenol remained relatively constant for the entire experiment (0.5% RSD), as shown in Figure 3.9, suggesting that there has been no significant change in the structure of the ODS. Thus it is unlikely that underlying changes in the ODS are responsible for the exponential change in ion-exchange retention observed in Figure 3.5. Similarly, Chambers and Lucy[47] observed an exponential decay in ion retention on carbon-clad zirconia coated with cetylpyridinium chloride (CPC). Carbon is a hydrophobic surface whose structure does not change with organic modifier concentration. Thus,

changes in the ion retention in their work cannot be attributed to changes in the reversed phase media.

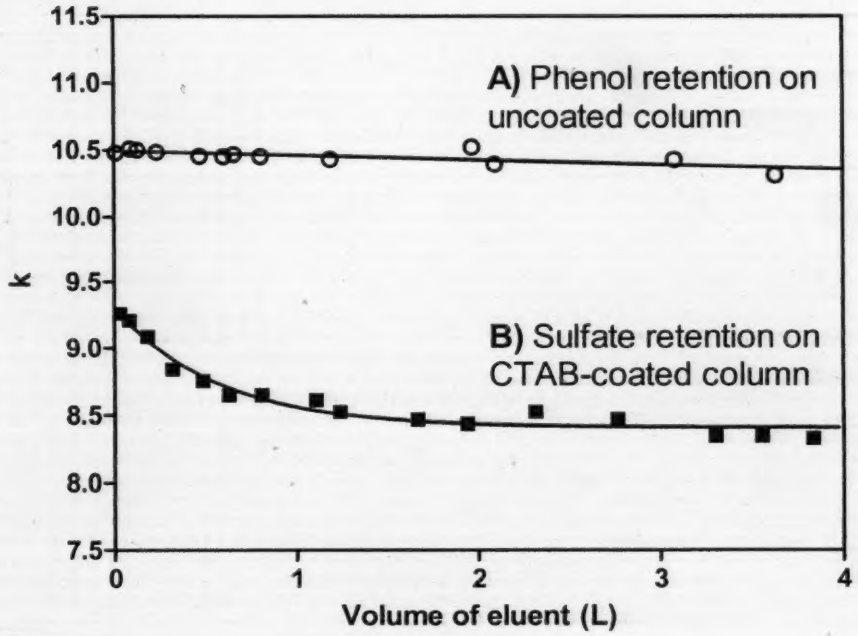

Figure 3.9 Retention factor on 100 x 4.6 mm Chromolith column as a function of flush volume, 30°C. **A)** Phenol on uncoated column, 0.00112 g/mL phenol + 0.05 mM NO_3^- (for dead-time marker), 20 µL injection, 2 mL/min water as eluent, 195 nm UV detection. **B)** sulfate on column coated with 1 mM CTAB in 23% ACN / water, 0.05 mM sulfate, 20 µL injection, 2 mL/min 10.0 mM 4-hydroxybenzoic acid (pH 4.6).

The second experiment deals with the exchange of the surfactant counterion for the eluent ion as a possible contributor to the exponential decay trend. To understand the role of the surfactant counterion, a coating was prepared using a solution of 1 mM CTAC in water. CTAC contains a chloride counterion instead of bromide. The chloride ion is more weakly retained on our column than the bromide ion. Thus, if the exponential decay trends were affected by the exchange of the surfactant counterion with the eluent ion, then a column coated with CTAC would come to the plateau region faster than a column coated with CTAB. Table 3.3 shows that the k_{obs} (based on normalized capacities) were 0.91 ± 0.05 for CTAB and 1.04 ± 0.04 for CTAC, which are statistically different at the 95% confidence interval. Thus, a minor change in the desorption rate is attributable to the counterion exchange.

Further evidence that the effect of counterion exchange comes from the studies of of coatings prepared from 1 mM CTAB in 20 mM 4-hba (Table 3.3). It is expected that the surfactant would be completely in the 4-hba form in the presence of 20 mM 4-hba. Nonetheless, Table 3.3 shows the exponential decay behaviour was still observed under these conditions. Thus, while the counterion exchange may contribute to the exponential decay rate, it is apparent that the exponential decay is an intrinsic characteristic of surfactant desorption.

3.3.6 Clarifying contradictions about the stability of surfactant coatings

Table 3.1 (Section 3.1) lists a number of studies using surfactant coatings to coat reversed-phase columns for ion-exchange. Along with the surfactant coating conditions used, Table 3.1 also indicates the initial ion-exchange capacity according to the surfactant breakthrough (Q), the column dimensions, the flush volume (i.e., the volume of water and/or eluent that was flushed through the column before separations were carried out) and the authors' statement about the stability of the surfactant coating.

Several observations throughout this chapter work together to explain the discrepancies in the stability of surfactant coatings reported in Table 3.1. First, Section 3.3.3 showed that surfactant desorption from the stationary phase as a function of flush volume follows an exponential decay trend. Different coating conditions result in different rates of decay, which affects the volume of eluent needed to reach a stable coating. We also found in Section 3.3.5 that shorter columns require less flush volume to reach a stable coating. Each of the studies listed in Table 3.1 employ different surfactant coating solutions, flush volumes, and column dimensions. Thus, some authors may have used short columns and/or large flush volumes for equilibration, thereby skipping over the initial rate of loss of surfactant, allowing the plateau region to be reached by the time the first injection was made. Other researchers may have used longer columns and/or smaller equilibration volumes, and so were under the impression that the surfactant coating was not stable. With the findings in this chapter, I maintain that surfactant coatings are indeed stable after an initial break-in period.

3.4 Conclusions

Many efforts have been made to permanently anchor ion-exchange sites to commercially available columns, in an effort to produce a stable ion chromatography column. These permanent modifications include covalent attachment of iminodiacetic acid[48,49] or lysine[50] to bare silica and electrostatic attachment of latex particles to bare silica.[24,32] These permanent ion-exchange sites, however, cannot be removed to allow the column to be used in its original form, or with a different coating. Surfactant coatings, on the other hand, allow the user to refine the ion-exchange capacity and selectivity of a column so as to optimize a given separation.

However, a limitation of surfactant coatings has been the perception of their lack of stability. The exponential decay trend of analyte retention on surfactant-coated columns is an important finding for researchers who are interested in combining the high efficiency of silica-based columns with ion-chromatographic separations. After an initial period of surfactant desorption, which can be overcome by flushing with ~900 column volumes of eluent, the retention times of the analytes stabilize and the efficiency of the separations remains constant. Thus making surfactant-coated columns a viable means of performing routine separations.

3.5 References

(1) Connolly, D.; Paull, B., *J. Chromatogr. A* **2002**, *953*, 299-303.

(2) Hatsis, P.; Lucy, C. A., *Anal. Chem.* **2003**, *75*, 995-1001.

(3) Connolly, D.; Victory, D.; Paull, B., *J. Sep. Sci.* **2004**, *27*, 912-920.

(4) Fritz, J. S.; Yan, Z.; Haddad, P. R., *J. Chromatogr. A* **2003**, *997*, 21-31.

(5) Hu, W.; Haddad, P. R.; Cook, H.; Yamamoto, H.; Hasebe, K.; Tanaka, K.; Fritz, J. S., *J. Chromatogr. A* **2001**, *920*, 95-100.

(6) Xu, Q.; Tanaka, K.; Mori, M.; Helaleh, M. I. H.; Hu, W. Z.; Hasebe, K.; Toada, H., *J. Chromatogr. A* **2003**, *997*, 183-190.

(7) Riordain, C. O.; Nesterenko, P.; Paull, B., *J. Chromatogr. A* **2005**, *1070*, 71-78.

(8) Paull, B.; Riordain, C. O.; Nesterenko, P. N., *Chem. Commun.* **2005**, 215-217.

(9) Riordain, C. O.; Barron, L.; Nesterenko, E.; Nesterenko, P. N.; Paull, B., *J. Chromatogr. A* **2006**, *1109*, 111-119.

(10) Yan, Z.; Haddad, P. R.; Fritz, J. S., *J. Chromatogr. A* **2003**, *985*, 359-365.

(11) Xu, Q.; Mori, M.; Tanaka, K.; Ikedo, M.; Hu, W. Z.; Haddad, P. R., *J. Chromatogr. A* **2004**, *1041*, 95-99.

(12) Chambers, S. D.; Glenn, K. M.; Lucy, C. A., *J. Sep. Sci.* **2007**, *30*, 1628-1645.

(13) Li, J.; Zhu, Y.; Guo, Y. Y., *J. Chromatogr. A* **2006**, *1118*, 46-50.

(14) Pelletier, S.; Lucy, C. A., *J. Chromatogr. A* **2006**, *1118*, 12-18.

(15) Gillespie, E.; Macka, M.; Connolly, D.; Paull, B., *Analyst* **2006**, *131*, 886-888.

(16) O Riordain, C.; Gillespie, E.; Connolly, D.; Nesterenko, P. N.; Paull, B., *J. Chromatogr. A* **2007**, *1142*, 185-193.

(17) Ito, K.; Takayama, Y.; Makabe, N.; Mitsui, R.; Hirokawa, T., *J. Chromatogr. A* **2005**, *1083*, 63-67.

(18) Xu, Q.; Mori, M.; Tanaka, K.; Ikedo, M.; Hu, W. Z., *J. Chromatogr. A* **2004**, *1026*, 191-194.

(19) Hu, W. Z.; Yang, P. J.; Hasebe, K.; Haddad, P. R.; Tanaka, K., *J. Chromatogr. A* **2002**, *956*, 103-107.

(20) Paull, B.; Victory, D., *International Ion Chromatography Symposium, Trier, Germany* **2004**.

(21) Conder, J. R.; Young, C. L., *Physicochemical Measurement by Gas Chromatography*, John Wiley & Sons, Toronto, 1979.

(22) Hutchinson, J. P.; Hilder, E. F.; Shellie, R. A.; Smith, J. A.; Haddad, P. R., *Analyst* **2006**, *131*, 215-221.

(23) Hutchinson, J. P.; Zakaria, P.; Bowie, A. R.; Macka, M.; Avdalovic, N.; Haddad, P. R., *Anal. Chem.* **2005**, *77*, 407-416.

(24) Hutchinson, J. P.; Hilder, E. F.; Macka, M.; Avdalovic, N.; Haddad, P. R., *J. Chromatogr. A* **2006**, *1109*, 10-18.

(25) Pool, C. F., *The Essence of Chromatography*, Elsevier Science B.V., Amsterdam, 2003.

(26) Berthod, A.; Girard, I.; Gonnet, C., *Anal. Chem.* **1986**, *58*, 1362-1367.

(27) Bartha, A.; Billiet, H. A. H.; Degalan, L.; Vigh, G., *J. Chromatogr.* **1984**, *291*, 91-102.

(28) Berthod, A.; Girard, I.; Gonnet, C., *Anal. Chem.* **1986**, *58*, 1356-1358.

(29) Geoffry, C.; Stuart, M. A. C.; Wong, K.; Cabane, B.; Bergeron, V., *Langmuir* **2000**, *16*, 6422-6430.

(30) Levchenko, A. A.; Argo, B. P.; Vidu, R.; Talroze, R. V.; Stroeve, P., *Langmuir* **2002**, *18*, 8464-8471.

(31) Cassidy, R. M.; Elchuck, S., *J. Chromatogr. Sci.* **1983**, *21*, 454.

(32) Glenn, K. M.; Lucy, C. A.; Haddad, P. R., *J. Chromatogr. A* **2007**, *1155*, 8-14.

(33) Greibrokk, T.; Andersen, T., *J. Chromatogr. A* **2003**, *1000*, 743-755.

(34) Bowermaster, J.; McNair, H. M., *J. Chromatogr. Sci.* **1984**, *22*, 165-170.

(35) www.merck.de.

(36) Tiberg, F.; Jonsson, B.; Lindman, B., *Langmuir* **1994**, *10*, 3714-3722.

(37) Yassine, M. M.; Lucy, C. A., *Anal. Chem.* **2004**, *76*, 2983-2990.

(38) Gulcev, M. D.; Lucy, C. A., *Anal. Chem.* **2007**, *(submitted)*.

(39) Nagashima, H.; Okamoto, T., *J. Chromatogr. A* **1999**, *855*, 261-266.

(40) Chambers, S. D.; Lucy, C. A., *J. Chromatogr. A, submitted.*

(41) Mata, J.; Varade, D.; Bahadur, P., *Thermochim. Acta* **2005**, *428*, 147-155.

(42) Modaressi, A.; Sifaoui, H.; Grzesiak, B.; Solimando, R.; Domanska, U.; Rogalski, M., *Colloids Surf. A: Physicochem. Eng. Aspects* **2007**, *296*, 104-108.

(43) Paruchuri, V. K.; Nguyen, A. V.; Miller, J. D., *Colloids and Surfaces a-Physicochemical and Engineering Aspects* **2004**, *250*, 519-526.

(44) Miller, J. M., *Chromatography, Concepts and Contrasts*, 2 edn., Wiley Interscience, Hoboken, 2005.

(45) Wolcott, R. G.; Dolan, J. W., *LCGC* **1999**, *17*, 316-321.

(46) Nagae, N.; Enami, T.; Doshi, S., *LCGC* **2002**, *20*, 964-972.

(47) Chambers, S. D.; Lucy, C. A., *Personal Communication*.

(48) Sugrue, E.; Nesterenko, P.; Paull, B., *Analyst* **2003**, *128*, 417-420.

(49) Sugrue, E.; Nesterenko, P.; Paull, B., *J. Sep. Sci.* **2004**, *27*, 921-930.

(50) Sugrue, W.; Nesterenko, P. N.; Paull, B., *J. Chromatogr. A* **2005**, *1075*, 167-175.

CHAPTER 4: Summary and Future Work

This thesis focused on methods for introducing stable ion-exchange sites onto commercially available silica monoliths. In recent years, research has focused on ionic surfactant coatings on reversed-phase columns. However, the perception of the lack of stability of surfactant coatings has limited their use for routine separations. In Chapter 2, the performance of a surfactant-coated column was compared to a column permanently modified with latex particles in terms of selectivity, efficiency and stability. The permanent ion-exchange phase was prepared via electrostatic attachment of functionalized latex particles to a bare silica monolith. This method was found to be more stable and more efficient than a surfactant-coated reversed-phase column. However, unlike surfactant coatings, the permanent nature of the latex coating did not allow the column capacity to be refined to suit a desired separation.

Chapter 3 explored the possibility of a stable surfactant coating. By performing long-term stability studies of surfactant coatings, an important finding made surfactant-coated columns a viable choice for routine separations. The exponential decay trend observed for cetyltrimethylammonium coatings indicated that a stable surfactant coating can be obtained simply by flushing eluent through the column for ~900 column volumes. Not only did retention times remain stable after the initial break-in period, but the efficiency of separation remained unchanged for the duration of each experiment. In addition, traditional methods to control the ion-exchange capacity of surfactant-coated columns were examined in terms of the effect on the final capacity the column.

A limitation of the work presented in this thesis arises from the pH instability of silica. Because silica can degrade at pH > 8, traditional highly-alkaline IC eluents, such as hydroxide or carbonate/bicarbonate, cannot be used. However, recently the Waters Corporation introduced a series of hybrid inorganic/organic silica columns which claim to have higher pH stability (up to pH 12).[1] These X-Bridge columns are composed of particles prepared from tetraethoxysilane and bis(triethoxysilyl)-ethane. This combination of monomers incorporates an ethylene bridge into the silica structure which does not easily hydrolyze and thus should lend improved pH stability with the high efficiency of silica. Such columns would be of significant value in advancing the research presented in this thesis, as it would allow surfactant coated reversed-phase columns to be used with easily suppressed highly-alkaline eluents. As a small side-project to this thesis, X-Bridge columns were coated with surfactant and used with carbonate/bicarbonate eluents.

An X-Bridge C_{18} column (4.6 x 20 mm, 2.5 μm particles) was coated with 1 mM cetylpyridinium chloride (CPC) in 10% ACN to give a capacity of ~45 μeq/column, according to the surfactant breakthrough time. Figure 4.1 shows two separations on the column using an alkaline eluent (6.8 mM sodium carbonate / 5.4 mM sodium bicarbonate, pH 10.4) at 1 mL/min. Chromatogram A of Figure 4.1 shows the first separation obtained on the column using a fresh coating of CPC. Separations were carried out throughout the day on the column with this original coating, and it was found that the retention time of nitrate decreased on average by about 7% per hour, owing to the surfactant leaching from the column and/or the possible dissolution of silica. With the hope of restoring the original capacity, a fresh

coating was applied to the column. Chromatogram B of Figure 4.1 shows a separation on the same column (freshly-coated with CPC again) after ~8 hours of flushing the highly alkaline eluent through the column at 1 mL/min. The efficiency of the column had been so drastically affected by the high pH that it was no longer usable for separations.

As an attempt to improve the stability of the CPC-coated X-Bridge column, the damaged column was placed in front of the injector to be used as a pre-column which saturated the mobile phase with CPC and dissolved silica. The analytical column used was another X-Bridge column (4.6 x 20 mm, 2.5 μm particles). Both columns were coated with 1 mM CPC in 10% ACN, giving the analytical column a capacity of ~40 μeq/column. A mobile phase of 6.3 mM Na_2CO_3 / 4.4 mM $NaHCO_3$ (pH 10.4) was flushed through the column at 1.00 mL/min. The columns were periodically re-coated and the efficiency monitored. Separations obtained on the same day with the same coating showed that the retention time of nitrate decreased on average by 1.6% per hour, a slower decrease than before due to the effects of the pre-column. With the pre-column, the X-Bridge column had a much longer lifetime than without the pre-column. Peak fronting began to occur after about 90 hours, with a 55-60% decrease in efficiency over the 90 hour period. However, this is still much too short a life-time to consider these columns to be used for routine IC separations with carbonate/bicarbonate eluents. If a 10% decrease in efficiency were considered acceptable, one column, which costs \$600-700[1], would last only about 15 hours at 1 mL/min with carbonate/bicarbonate eluents.

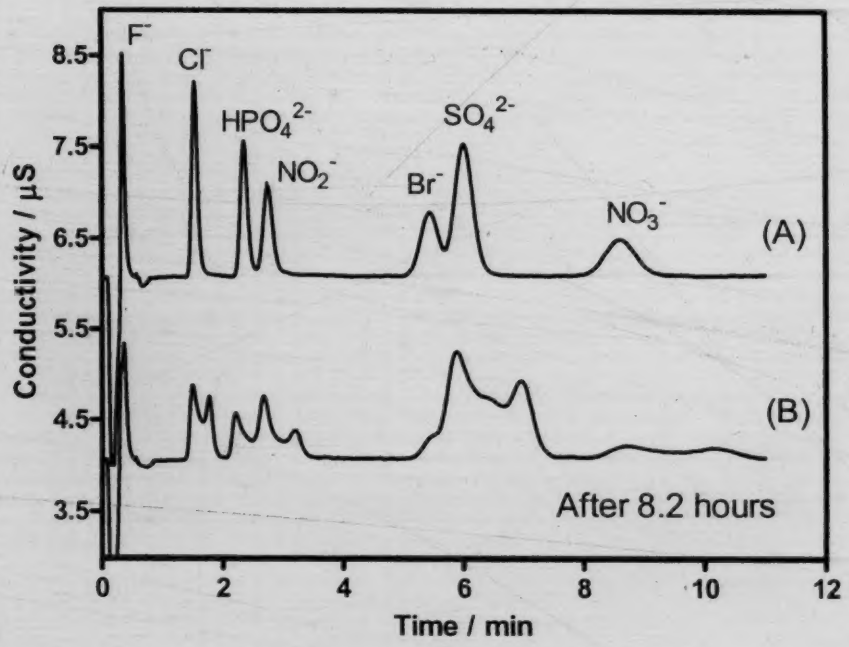

Figure 4.1. Anion separations on X-Bridge C_{18} column (4.6 x 20 mm, 2.5 µm particles) coated with 1 mM CPC in 10% ACN (capacity ~ 45 µeq/column). 0.05 mM analyte ions, 20 µL injection volume, eluent: 6.8 mM CO_3^{2-} / 5.4 mM HCO_3^- (pH 10.4) at 1.0 mL/min. Suppressed conductivity detection at 56 mA.

The above experiments used sodium carbonate / sodium bicarbonate eluents. Evidence in the literature suggests that organic eluents, especially those containing amines, are much more compatible with silica at high pH [2,3]. It is thought that the nitrogenous portion of these molecules sorbs to the silica surface, protecting it from dissolution. Thus, it may be worthwhile to try an ammonium carbonate / ammonium bicarbonate eluent as an attempt to enhance the lifetime of a silica-based column at high pH.

Alternatively, pH-stable stationary phases could be used with surfactant coatings, such as graphitic carbon or carbon-clad zirconia. The pH stability of such phases would allow traditional IC eluents to be used, resulting in faster separations and lower detection limits. Graphitic carbon, having a hydrophobic surface, could be coated with surfactant in much the same way as a reversed-phase silica column. Or, ion-exchange sites could be covalently bound to the carbon surface for a permanent ion-exchange column.

With regard to surfactant coatings in general, future work could involve the analysis of real-life samples. This would further prove the viability of surfactant coated columns with weak-acid eluents for use in routine IC separations in industrial settings.

It would be advantageous to chromatographers wishing to select the best surfactant for their application, or deciding which commercial IC column to buy, to know what physical properties govern retention in IC. Possible future studies could examine existing commercially available IC columns, and/or surfactant-coated columns, in terms of linear solvation energy relationships (LSER) [4] to understand the

properties that govern analyte retention in IC. LSER relationships are often used to compare retention using different stationary and mobile phases. Such a model already exists for reversed phases (i.e., Snyder's hydrophobic subtractive model [5]). Abraham and Zhao recently determined solvation descriptors for ionic species.[6] By examining the retention of several types of ionic analytes with varying polarizability, acidity and basicity, with various eluents and stationary phases, hypothetically a model could be devised for IC. Ultimately, the model would help to predict the selectivity differences of various types of IC phases. This would aid the chromatographer in selecting a stationary phase for their particular IC application.

References

(1) www.waters.com.

(2) Kirkland, J. J.; Henderson, J. W.; DeStefano, J. J.; van Straten, M. A.; Claessens, H. A., *J. Chromatogr. A* **1997**, *762*, 97-112.

(3) Kirkland, J. J.; van Straten, M. A.; Claessens, H. A., *J. Chromatogr. A* **1998**, *797*, 111-120.

(4) Vitha, M.; Carr, P. W., *J. Chromatogr. A* **2006**, *1126*, 143-194.

(5) Snyder, L. R.; Dolan, J. W.; Carr, P. W., *J. Chromatogr. A* **2004**, *1060*, 77-116.

(6) Abraham, M. H.; Zhao, Y. H., *J. Org. Chem.* **2004**, *69*, 4677-4685.